



Universidade de Aveiro

2021

**EDGAR MAURICIO  
VARGAS SOLANO**

**PRODUÇÃO DE BIODIESEL USANDO MATERIAIS  
RESIDUAIS**

**BIODIESEL PRODUCTION USING RESIDUAL  
MATERIALS**





Universidade de Aveiro

2021

**EDGAR MAURICIO  
VARGAS SOLANO**

**PRODUÇÃO DE BIODIESEL USANDO MATERIAIS  
RESIDUAIS**

**BIODIESEL PRODUCTION USING RESIDUAL  
MATERIALS**

Tese apresentada à Universidade de Aveiro para cumprimento dos requisitos necessários à obtenção do grau de Doutor em Engenharia Química, realizada sob a orientação científica da Doutora Maria Isabel da Silva Nunes, Professora Auxiliar do Departamento de Ambiente e Ordenamento da Universidade de Aveiro

Financial support from: Direction of Investigation, Creation and Extension of Jorge Tadeo Lozano University, FCT/MCTES for the financial support to CESAM (UIDP/50017/2020 & UIDB/50017/2020) and FCT, I.P. for the research contract CEECIND/00383/2017 under the CEEC Individual 2017.



I dedicate this doctoral thesis to my parents (Anita and Eliseo) who are in heaven and who have always been an example for my life.



## **o júri**

Presidente

**Professor Doutor João Manuel Nunes Torrão**  
Professor Catedrático, Universidade de Aveiro

**Professor Doutor Abel Gomes Martins Ferreira**  
Professor Auxiliar, Universidade de Coimbra

**Doutora Ana Sofia Ramos Brásio**  
Responsável pelo Desenvolvimento de Processos da Prio Energy

**Professor Doutor Luís António da Cruz Tarelho**  
Professor Associado, Universidade de Aveiro

**Professora Doutora Nídia de Sá Caetano**  
Professora Coordenadora, Instituto Superior de Engenharia do Porto

**Professora Doutora Maria Isabel da Silva Nunes**  
Professora Auxiliar, Universidade de Aveiro  
(orientadora)





## **acknowledgements**

The execution of this study only became reality thanks to people and organizations I have to thank:

First, to the professor Dra. Maria Isabel da Silva Nunes, who gave me a great learning experience, a great person and an exceptional professional.

To professor Doctor Luís António Tarelho (Associate Professor of the Department of Environment and Planning of the University of Aveiro), to professor Doctor João Manuel Coutinho (Full Professor at the Chemistry Department of University of Aveiro) and Dra. Márcia Carvalho Neves (PhD), auxiliary researcher (CICECO and Department of Chemistry, University of Aveiro).

To the Direction of Research, Creation and Extension of the Jorge Tadeo Lozano University, CESAM, CICECO, Department of Environment and Planning and Department of Chemistry.

I thank my family, who were present at every moment and especially my wife Adriana, my son Daniel Felipe and my daughter Maria Paula.

To my friends, both the ones I have (Alis, Yineth, Jorge, Andres, Ingrid, Sebastian, Laura, Duvan, Lizeth, Isaac ...) and the ones I did during my doctorate (Joaquim-Kim, Daniel, Ivonne), you are part of this work.

Finally, I thank everyone who encouraged and supported me throughout this journey.



## palavras-chave

Materiais residuais, FAME, catalisador sólido, catalisadores bifuncionais, óleo de cozinha residual, óleo de palma refinado, otimização de processos.

## resumo

A energia é um requisito básico para a existência humana e seu consumo aumenta a cada ano. Atualmente, a maior parte das necessidades energéticas é suprida pelos convencionais recursos de origem fóssil, tais como a gasolina, o gás liquefeito de petróleo, o petrodiesel e o gás natural. No entanto, o uso de combustíveis fósseis tem associados sérios problemas ambientais. Uma das fontes de energia alternativa (renovável) mais promissora é o biodiesel. Normalmente a produção de biodiesel é um processo catalisado, no qual são utilizados catalisadores alcalinos ou ácidos, para a conversão de triglicerídeos (reação de transesterificação) e ácidos gordos livres (reação de esterificação) em ésteres metílicos de ácidos gordos (FAME), utilizando metanol. Neste contexto, recentemente os catalisadores heterogêneos têm chamado a atenção dos investigadores pelas suas vantagens relativamente aos catalisadores homogêneos, nomeadamente em termos de maior rendimento de biodiesel, maior pureza do glicerol, separação mais fácil do catalisador (filtração simples), menos corrosivos e ambientalmente “mais amigáveis”. O presente trabalho teve como objetivo preparar um catalisador sólido bifuncional eficiente (i.e., capaz de catalisar simultaneamente as reações de transesterificação e esterificação), a partir de materiais residuais, com vista à produção de FAME a partir de misturas de óleos vegetais de baixo custo (óleo alimentar usado (OAU) e óleo de palma refinado (OPR)), e metanol. Também constituiu um objetivo de trabalho a otimização do processo de produção tanto num reator descontínuo como num reator de leito fixo contínuo. A cinza volante de biomassa (FAD) foi selecionada, de entre outros materiais residuais (rocha dolomítica natural, casca de ovo de galinha e tereftalato de polietileno - PET) estudados, por ter exibido melhor desempenho na produção de FAME, e também deter um caráter bifuncional. O rendimento máximo de FAME alcançado (processo não otimizado), na etapa de seleção dos materiais, foi cerca de 96 % (m/m), a 60 °C, 9:1 (mol/mol) razão metanol/óleo, 10 % (m/m) de carga de FAD, durante 180 min em reator descontínuo. Na etapa de otimização da produção em reator descontínuo, usando FAD, o rendimento máximo de FAME registado foi de 73.8 % para as condições operacionais: 13.6 % (m/m) de carga de catalisador, 6.7 de razão molar metanol / óleo, 72 % (m/m) de OAU/OPR e 55 °C. Observou-se que catalisador pode ser usado pelo menos até três ciclos consecutivos sem perda de atividade catalítica. Na otimização da produção de FAME em reator de leito fixo contínuo, com a FAD peletizada, a concentração máxima de FAME registada foi de 89.7 %, nas seguintes condições operacionais: 124 min de tempo de residência, 74.6 % (m/m) de OAU/OPR, 12:1 razão molar metanol/óleo e 60 °C. O catalisador manteve-se estável ao longo de 32 h de operação contínua, sem desativação perceptível. O presente trabalho dá um contributo para tornar o processo de produção de biodiesel mais alinhado com os princípios da economia circular, através da integração de resíduos, quer com uma função catalítica (FAD), quer como matéria-prima (OAU). Selecionou-se um material residual (cinza volante de biomassa) que necessita de um tratamento físico muito simples (secagem), para ser utilizado num processo descontínuo de produção de FAME. Além disso, este material na forma peletizada, continua a exibir excelentes propriedades catalíticas, permitindo assim a produção de FAME em contínuo. Os resultados deste trabalho são muito promissores, sobretudo quando se perspetiva uma futura aplicação industrial.





**keywords**

Waste materials, FAME, solid catalyst, bifunctional catalysts, waste cooking oil, refined palm oil, process optimization.

**abstract**

Energy is a basic requirement for human existence and its consumption increases every year. Currently, most of the energy needs come from conventional fossil fuels, such as gasoline, liquefied petroleum gas, petrodiesel and natural gas. However, the use of fossil fuels has serious environmental problems associated with it. One of the most promising alternative (renewable) energy sources is biodiesel. Usually the production of biodiesel is a catalyzed process, in which alkaline or acid catalysts are used, for the conversion of triglycerides (transesterification reaction) and free fatty acids (esterification reaction) into fatty acid methyl esters (FAME), using methanol. In this context, heterogeneous catalysts have recently attracted the attention of researchers due to their advantages over the homogeneous ones in terms of higher biodiesel yield, higher glycerol purity, easier catalyst separation (simple filtration), less corrosive and more environmentally "friendly". The present work aimed to prepare an efficient bifunctional solid catalyst (capable of simultaneously catalyzing the transesterification and esterification reactions), from residual materials, to produce FAME from low-cost vegetable oil mixtures (waste cooking oil (WCO) and refined palm oil (RPO)) and methanol. The optimization of the production process in both a batch reactor and a continuous fixed-bed reactor is also an objective of the work. The biomass fly ash (FAD) was selected from among other studied residual raw materials (natural dolomite rock, chicken eggshells and polyethylene terephthalate - PET), for exhibiting the best performance in the production of FAME, and also for having a bifunctional character.

The maximum yield of FAME reached (non-optimized process), in the raw materials selection stage, was about 96 wt%, at 60 °C, 9:1 (mol/mol) methanol/oil ratio, 10 wt% FAD loading, for 180 min in a batch reactor. In the production optimization stage in a batch reactor, using FAD, the maximum FAME yield reached was 73.8 % for the operating conditions: 13.57 wt% of catalyst loading, 6.7 of methanol/oil molar ratio, 72 wt% of WCO/RPO at 55 °C. It was observed that the catalyst could be used in up to three consecutive cycles without loss of catalytic activity. For the optimization in the continuous fixed bed reactor, with the pelletized FAD, the maximum concentration of FAME reached was 89.7 %, under the following operating conditions: 124 min residence time, 74.6 wt% of WCO/RPO, 12:1 methanol/oil molar ratio at 60 °C. The catalyst was stable during the 32 hours of continuous operation, without significant deactivation.

The present work contributes to the biodiesel production process being more aligned with the principles established by circular economy, by integrating waste, either with a catalytic function (FAD) or as a raw material (WCO). A residual material that needs a very simple physical treatment (drying) was selected to be used (biomass fly ash) in a discontinuous process for the production of FAME. Furthermore, this material in granulated form continues to exhibit excellent catalytic properties, thus allowing continuous production of FAME. The results of this work are very promising, especially when looking towards a future industrial application.

## Palabras clave

Materiales de desecho, FAME, catalizador sólido, catalizadores bifuncionales, aceite de cocina usado, aceite de palma refinado, optimización de procesos.

## resumen

La energía es un requisito básico para la existencia humana y su consumo aumenta cada año. Actualmente, la mayor parte de las necesidades energéticas proviene de combustibles fósiles convencionales, como la gasolina, el gas licuado del petróleo, el petrodiesel y el gas natural. Sin embargo, el uso de combustibles fósiles tiene asociados serios problemas ambientales. Una de las fuentes de energía alternativa (renovable) más prometedoras es el biodiesel. Normalmente la producción de biodiesel es un proceso catalizado, en el cual son utilizados catalizadores alcalinos o ácidos, para la conversión de triglicéridos (reacción de transesterificación) y ácidos grasos libres (reacción de esterificación) en ésteres metílicos de ácidos grasos (FAME), utilizando metanol. En este contexto, recientemente los catalizadores heterogéneos han llamado la atención de los investigadores por sus ventajas frente a los homogéneos en términos de mayor rendimiento de biodiesel, mayor pureza de glicerol, separación más fácil del catalizador (filtración simple), menos corrosivos y ambientalmente "más amigables". El presente trabajo tuvo como objetivo preparar un catalizador sólido bifuncional eficiente (es decir, capaz de catalizar simultáneamente las reacciones de transesterificación y esterificación), a partir de materiales residuales, para producir FAME a partir de mezclas de aceites vegetales de bajo costo (aceite de cocina residual (ACU) y aceite de palma refinado (APR)) y metanol. También constituye un objetivo del trabajo la optimización del proceso de producción tanto en un reactor discontinuo como en un reactor continuo de lecho fijo. Las cenizas volantes de biomasa (FAD) fueron seleccionadas de entre otras materias primas residuales (roca de dolomita natural, cáscaras de huevo de gallina y tereftalato de polietileno - PET) estudiadas, por haber exhibido el mejor desempeño en la producción de FAME, y también por tener un carácter bifuncional.

El rendimiento máximo de FAME alcanzado (proceso no optimizado), en la etapa de selección de las materias primas fue cerca del 96 % (m/m), a 60 °C, 9:1 (mol/mol) relación metanol/aceite, 10 % (m/m) de carga de FAD, durante 180 min en reactor discontinuo. En la etapa de optimización de la producción en un reactor discontinuo, usando FAD, el rendimiento máximo de FAME alcanzado fue del 73.8 % para las condiciones de operación: 13.57 % (m/m) de carga de catalizador, 6.7 de relación molar metanol/aceite, 72 % (m/m) de WCO/RPO a 55 °C. Se observó que el catalizador pudo ser usado hasta tres ciclos consecutivos sin pérdida de actividad catalítica. Para la optimización en el reactor de lecho fijo continuo, con el FAD peletizado, la concentración máxima de FAME alcanzada fue del 89.7 %, en las siguientes condiciones de operación: 124 min de tiempo de residencia, 74.6 % (m/m) de WCO/RPO, 12:1 relación molar metanol/aceite y 60 °C. El catalizador se mantuvo estable durante las 32 h de funcionamiento continuo, sin una desactivación apreciable.

El presente trabajo contribuye a que el proceso de producción de biodiésel esté más alineado con los principios de la economía circular, mediante la integración de residuos, ya sea con función catalítica (FAD) o como materia prima (ACU). Se seleccionó un material residual (cenizas volantes de biomasa) que necesita un tratamiento físico muy simple (secado), para ser utilizado en un proceso discontinuo de producción de FAME. Además, este material en forma granulada, continúa exhibiendo excelentes propiedades catalíticas, permitiendo así la producción de FAME en continuo. Los resultados de este trabajo son muy prometedores, especialmente cuando se mira hacia una futura aplicación industrial.





# Table of contents

Table of contents .....	xvii
List of figures .....	xxi
List of tables.....	xxiii
Notation.....	xxv
<b>SECTION A - The study proposal.....</b>	<b>1</b>
1 Presentation of the thesis .....	3
1.1 Introduction .....	3
1.2 Thesis objectives and structure .....	10
1.3 Scientific production within the scope of the thesis .....	13
1.3.1 Articles published in scientific journals .....	13
1.3.2 Articles published in scientific conferences .....	13
1.3.3 Participation in scientific events.....	14
References .....	16
<b>SECTION B – Bifunctional solid catalyst selection .....</b>	<b>19</b>
2 Solid catalysts obtained from wastes for FAME production using mixtures of refined palm oil and waste cooking oils.....	21
2.1 Introduction .....	22
2.2 Materials and Methods.....	23
2.2.1 Materials.....	24
2.2.2 Oil mixtures (RPO and WCO) characterization .....	24
2.2.3 Catalysts preparation and characterization .....	25
2.2.4 FAME synthesis.....	26
2.3 Results and discussion .....	28
2.3.1 Oil mixtures characterization .....	28
2.3.2 Catalysts characterization .....	29
2.3.2.1 BET surface area and Hammett indicators analyses .....	29
2.3.2.2 SEM and EDX analyses .....	31

2.3.2.3	XRD analyses.....	34
2.3.2.4	FTIR analyses.....	37
2.3.2.5	Catalysts performance.....	40
2.4	Conclusions.....	45
	References.....	47
<b>SECTION C - Optimization of FAME production in batch mode operation .....</b>		<b>53</b>
3	Optimization of FAME production from blends of waste cooking oil and refined palm oil using biomass fly ash as a catalyst .....	55
3.1	Introduction.....	56
3.2	Materials and Methods .....	57
3.2.1	Materials.....	58
3.2.2	Oil mixtures characterization .....	58
3.2.3	Catalysts preparation and characterization .....	59
3.2.4	FAME synthesis and quantification.....	60
3.2.5	Experimental design and optimization of FAME production process.....	61
3.2.6	Catalyst reusability .....	63
3.3	Results and discussion .....	64
3.3.1	Oil mixtures characterization .....	64
3.3.2	Catalysts characterization .....	64
3.3.2.1	BET surface area and Hammett indicators analyses .....	65
3.3.2.2	SEM and EDX analyses.....	66
3.3.2.3	XRD analyses.....	67
3.3.2.4	FTIR analyses.....	68
3.3.3	Optimization of FAME production process: regression model and statistical analysis .....	68
3.3.4	Catalyst reusability: catalytic performance assessment.....	76
3.4	Conclusions.....	79
	References.....	81
<b>SECTION D - Optimization of FAME production in continuous fixed-bed reactor .....</b>		<b>85</b>
4	Pelletized biomass fly ash for FAME production: optimization of a continuous process .....	87
4.1	Introduction.....	88
4.2	Materials and Methods .....	90

---

4.2.1	Oil mixtures characterization .....	90
4.2.2	Catalysts preparation and characterization .....	90
4.2.3	Experimental setup.....	92
4.2.4	FAME content .....	94
4.2.5	Preliminary assays for steady state identification .....	95
4.2.6	Experimental design for optimization of the FAME production .....	97
4.3	Results and discussion .....	99
4.3.1	Oil mixtures characterization .....	99
4.3.2	Catalysts characterization .....	100
4.3.2.1	XRD analysis .....	100
4.3.2.2	Hammett indicators and BET surface area analyses .....	101
4.3.2.3	SEM analysis.....	102
4.3.2.4	FTIR analysis .....	102
4.3.2.5	XPS analysis.....	103
4.3.3	Optimization of FAME production process: regression model and statistical analysis	104
4.3.4	Catalytic stability of the pelletized biomass ash .....	112
4.4	Conclusions .....	113
	References .....	115
	<b>SECTION E – Final remarks .....</b>	<b>121</b>
5	Final remarks .....	123
5.1	General conclusions.....	123
5.2	Future works .....	126
	Annexes .....	A1



## List of figures

Figure 1.1 - Simplified process flow chart of alkali-catalyzed biodiesel production (adapted from Leung et al. (2010)).	4
Figure 1.2 - Global transesterification reaction.	5
Figure 1.3 - Esterification reaction.	5
Figure 1.4 - Two-step conventional catalysis versus bifunctional catalyst process.	7
Figure 1.5 - Structure of the thesis in five sections.	15
Figure 2.1 - FAD catalyst: SEM (a) and EDX (b and c); FAC catalyst: SEM (e) and EDX (d and f).	32
Figure 2.2 - Dolomite C: SEM (a); Dolomite CSC: SEM (b) and EDX (c).	33
Figure 2.3 - CaO-SiO <sub>2</sub> : SEM (a); CaO-S-SiO <sub>2</sub> : EDX (b) and (c).	33
Figure 2.4 - SEM images of CA-PET (a) and CA-PET-S (b) catalysts.	34
Figure 2.5 - XRD patterns of catalysts: FAD and FAC (a), Dolomite C and Dolomite CSC (b), CaO-SiO <sub>2</sub> and CaO-S-SiO <sub>2</sub> (c), and CA-PET and CA-PET-S (d). (• SiO <sub>2</sub> , ■ CaCO <sub>3</sub> , ◆ CaO, ▲ CaSO <sub>4</sub> , ■ CaCO <sub>3</sub> , ▼ Ca(OH) <sub>2</sub> , ◆ CaO, □ Ca <sub>2</sub> SiO <sub>4</sub> and ★ MgO).	36
Figure 2.6 - FTIR spectra of catalysts: FAD and FAC (a), Dolomite C and Dolomite CSC (b), CaO-SiO <sub>2</sub> and CaO-S-SiO <sub>2</sub> (c), and CA-PET and CA-PET-S (d).	38
Figure 2.7 - Performance in terms of FAME yield and FFA conversion of catalysts: FAD and FAC (a) and (b), Dolomite C and Dolomite CSC (c) and (d), CaO-SiO <sub>2</sub> and CaO-S-SiO <sub>2</sub> (e) and (f), and CA-PET and CA-PET-S(g) and (h), for several RPO:WCO mixtures.	42
Figure 3.1 - Adsorption and desorption isotherms for the FAD catalyst.	65
Figure 3.2 - FAD catalyst characterization by: SEM (a and b) and EDX (c).	66
Figure 3.3 - XRD patterns of FAD catalyst.	67
Figure 3.4 - FTIR spectrum of FAD catalyst.	68
Figure 3.5 - (a) Residual normal probability plot, (b) Residual versus predicted response plot, (c) Predicted versus actual values plot.	73

Figure 3.6 - Response surface plots of FAME yield as a function of: (a) RPO/WCO ratio and catalyst loading at 50 °C and methanol/oil = 6 mol/mol; (b) RPO/WCO ratio and methanol/oil at 50 °C and catalyst loading = 10 wt%; (c) RPO/WCO ratio and temperature for catalyst loading = 10 wt% and methanol/oil = 6 mol/mol; (d) temperature and methanol/oil ratio for catalyst loading = 10 wt% and RPO/WCO = 50 wt%; (e) temperature (°C) and catalyst loading (wt%) for methanol/oil = 6 mol/mol and RPO/WCO = 50 wt%; (f) methanol/oil ratio and catalyst loading (wt%) at 50 °C and RPO/WCO = 50 wt%. ..... 74

Figure 3.7 - Reusability studies of the FAD catalyst under the optimal operating conditions. 77

Figure 3.8 - XRD patterns of FAD catalyst for the different reuse cycles..... 78

Figure 4.1- Biomass fly ash catalyst: (a) powder (before pelletization), (b) pelletized. .... 91

Figure 4.2 - Experimental setup diagram used in this work (1. Feed zone, 2. Reaction zone, 3. Separation zone). ..... 93

Figure 4.3 - Assembly of the fixed bed reaction system for continuous FAME production. .... 94

Figure 4.4 - Preliminary assays to identify the steady state of the continuous fixed bed reactor. .... 97

Figure 4.5 - XRD Diffractogram of biomass fly ash catalyst (• SiO<sub>2</sub>, ■ CaCO<sub>3</sub>, ▲ KCl, ★ Ca (OH)<sub>2</sub>). ..... 100

Figure 4.6 - Absorption and desorption isotherms of biomass fly ash. .... 101

Figure 4.7 - SEM images of biomass fly ash using a magnification of 500X (a) and 5000X (b). ..... 102

Figure 4.8 - FTIR spectrum of biomass fly ash catalyst. .... 103

Figure 4.9 - The XPS wide energy spectrum of biomass fly ash catalyst. .... 104

Figure 4.10 - (a) Residual normal probability plot, (b) Residual versus predicted response plot, (c) Predicted versus experimental values plot. .... 109

Figure 4.11 - FAME concentration response surface graphics based on: (a) Residence time and WCO/RPO ratio (wt%) at molar methanol/oil ratio of 9 mol/mol; (b) Time of residence and molar methanol/oil ratio at WCO/RPO ratio of 50 wt%; (c) Molar methanol/oil ratio and WCO/RPO ratio (wt%) at time of residence of 120 min. 110

Figure 4.12 - FAME concentration of the catalyst over 32 h of continuous operation. .... 113

---

## List of tables

Table 2.1 - Solid catalysts preparation procedures.....	25
Table 2.2 - Properties of the oil mixtures used. ....	28
Table 2.3 - Textural properties of the catalysts prepared in this work.....	29
Table 3.1 - Range and factor levels of operating variables used in the Box – Behnken experimental design. ....	62
Table 3.2 - Properties of the oil mixtures used in this work. ....	64
Table 3.3 - Experimental design and predicted results of RSM. ....	69
Table 3.4 - ANOVA results of the response surface quadratic model without interactions.....	70
Table 3.5 - ANOVA results for the coefficients of the variables in the quadratic regression model without interactions. ....	71
Table 3.6 - Textural properties and acid/basic strength of the FAD catalyst used in three FAME synthesis cycles. ....	78
Table 4.1 - Operating conditions of continuous flow reactors to produce FAME. ....	96
Table 4.2 - Factor and levels of process variables used in the Box – Behnken experimental design.....	98
Table 4.3 - Properties of the oil mixtures used. ....	99
Table 4.4 - Summary of XPS analysis done on the surface of biomass fly ash catalyst. ....	104
Table 4.5 - Experimental and predicted results of RSM.....	105
Table 4.6 - ANOVA table of the regression model. ....	106
Table 4.7 - Regression coefficients (coded factors) for the fitting quadratic polynomial model. .....	107
Table 4.8 - Experimental data on optimal operating conditions.....	112





## Notation

### *List of abbreviations*

ASTM	American Society for Testing and Materials
B10	10 % biodiesel and 90 % diesel
B20	20 % biodiesel and 80 % diesel
BET	Brunauer, Emmett y Teller
CA	Activated Carbon
CA-PET	Activated Carbon of Polyethylene Terephthalate
CA-PET-S	Activated Carbon of Polyethylene Terephthalate Sulfonation
CESAM	Center for Environmental and Marine Studies
CFBR	Continuous Fixed Bed Reactor
Dolomite C	Calcined Dolomite (catalyst)
Dolomite CSC	Calcined Sulfonated Calcined Dolomite
EDX	Energy Dispersive X-ray Spectroscopy
FAC	Biomass fly ash (calcined)
FAD	Biomass fly ash (dried)
FAME	Fatty Acid Methyl Esters
FFA	Free Fatty Acids
FTIR	Fourier Transform Infrared
ICONTEC	Colombian Institute of Technical Standards and Certification
NTC	Colombian technical standard

PAH	Polycyclic Aromatic Hydrocarbons
PET	Polyethylene Terephthalate
RPO	Refined Palm Oil
RSM	Response Surface Methodology
RT	Residence Time
SEM	Scanning Electron Microscope
SN	Saponification Number
WCO	Waste Cooking Oils
XPS	X-ray photoelectron spectroscopy
XRD	X-ray diffraction

## ***Nomenclature***

### *Roman Letters*

$A$	total peak areas of the methyl ester	
$A_{EI}$	the peak area of methyl heptadecanoate	
$AV$	acid value	(mg KOH/g)
$AV_i$	acid value of the initial oil mixture	(mg KOH/g)
$AV_f$	acid value of the final oil mixture	(mg KOH/g)
$\beta_i$	linear terms of polynomial equation	
$\beta_{ii}$	quadratic terms of polynomial equation	

$\beta_{ij}$	interaction terms of polynomial equation	
$\beta_0$	intercept coefficient (offset)	
$C$	concentration of FAME	
<i>C.V.</i>	coefficient of variation	
$M$	mixtures of WCO and RPO	
MW	molecular weight	(g/mol)
pKa	acidity measure	
pKb	basicity measure	
$R$	coefficient statistics of fit	
<i>S.D.</i>	standard deviation	
$T$	temperature	(K) or (°C)
$W$	the mass of the sample for analysis	(mg)
$W_{EI}$	the mass of methyl heptadecanoate	(mg)
$x_i$	independent variable	
$x_j$	independent variable	
$Y$	predicted response	

*Greek letters*

$\varepsilon$  measurement error

$\lambda$  wavelength (Å)

$\theta$  angle of incidence

---

## **SECTION A - The study proposal**

In Section A the subject of the study is introduced, which includes the motivation and the relevance of the work carried out. The general and specific objectives are also established as well as the thesis structure. The purpose of Section A is to show the reader the importance of biodiesel production from waste materials which is fully aligned with the principles of circular economy, and how the work is organized to achieve the proposed objectives.



# 1 Presentation of the thesis

## 1.1 Introduction

Energy is a basic requirement for human existence and its consumption increases all years. In the current situation, the foremost amount of primary and useful energy is supplied by the conventional fossil fuel resources, such as gasoline, liquefied petroleum gas, diesel fuel, and natural gas. However, the use of fossil fuels has several influences on the environment, such as large amount of greenhouse gas emissions, acid rain, resources depletion, etc. In addition to serious environmental issues, dwindling reserves of crude oil, fluctuating petroleum fuel prices, have made today's need to find alternative "green" sources of energy, which are sustainable, environmentally compatible, economically competitive, and easily available.

One of the most promising sources is biodiesel, an alternative diesel fuel derived from renewable sources with high quality, which allows the replacement of fossil diesel oil (Leung et al. 2010). Its advantages over petroleum diesel cannot be overemphasized: it is safe, renewable, non-toxic, biodegradable, sulfur free, and good lubricating properties. In addition, its use engenders numerous societal benefits, namely rural revitalization, creation of new jobs, and reduced global warming.

Biodiesel has significant influences in reducing engine emissions such as unburned hydrocarbons (68 %), particulate matter (40 %), carbon monoxide (44 %), sulfur oxide (100 %), and polycyclic aromatic hydrocarbons (PAH) (80–90 %) (Kiss et al. 2008).

Most of the biodiesel is produced by the alkali-catalyzed process. Figure 1.1 shows a simplified flow diagram of the alkaline catalyst process. Feedstock with high free fatty acids will undesirably react with the alkaline catalyst to form soap. The maximum amount of free fatty acids acceptable in an alkali catalyzed system is less than 2.5 wt%. If the oil or fat feedstock

has a FFA content greater than 2.5 wt%, a pretreatment step is necessary before the transesterification process.

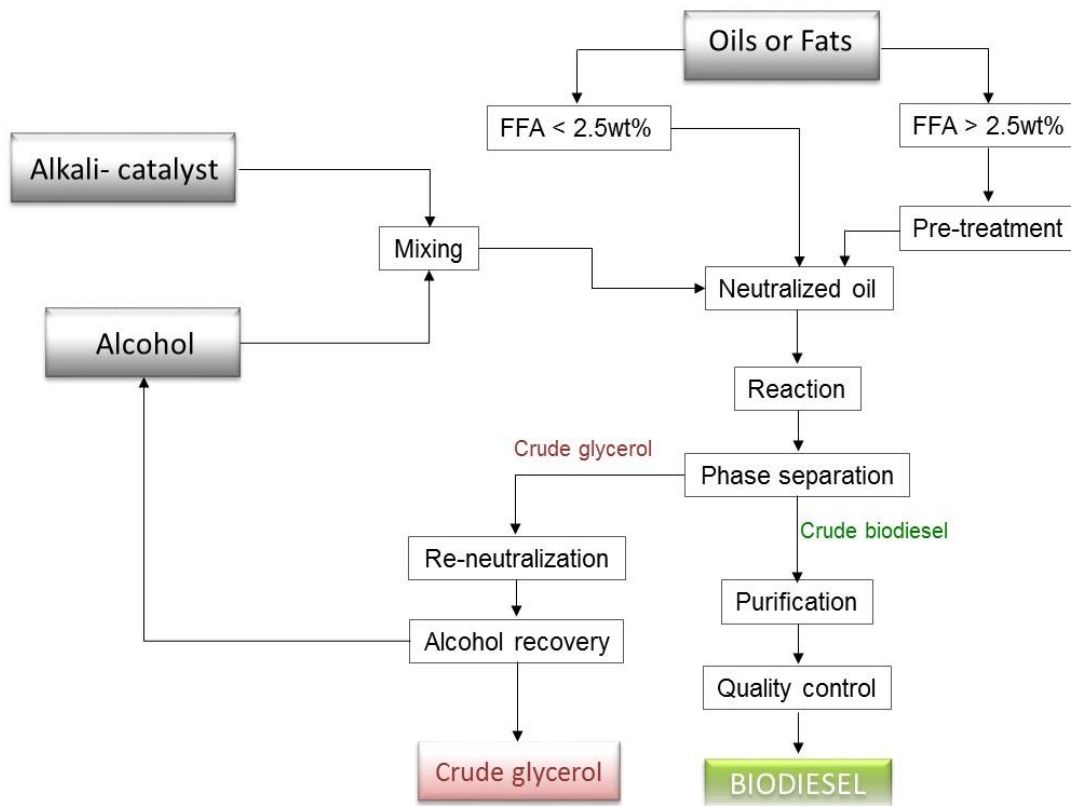


**Figure 1.1** - Simplified process flow chart of alkali-catalyzed biodiesel production (adapted from Leung et al. (2010)).

Usually the biodiesel production is a catalyzed process where alkali or acid compounds are used for the conversion of triglycerides and free fatty acids (FFA) into fatty acid methyl esters (FAME), when methanol is used in the synthesis, as shown in Figure 1.2 and Figure 1.3, respectively. The use of homogeneous alkaline catalyst such as NaOH and KOH for the transesterification of waste cooking oil to biodiesel posed serious separation problem. This is mainly due to the high FFA content in waste cooking oil that reacts, in the presence of water, with the alkaline catalyst to form soap. The formation of soap will cause serious difficulty in the separation of biodiesel and the glycerin (a reaction product) and, consequently the amount of water needed for washing the FAME will be higher, resulting in decreased yield to FAME; all



of these incur in high production costs and high volume of wastewater to be treated (Lam et al. 2009). Another alternative method (implemented in two-steps) is to use homogeneous acid catalyst such as  $\text{H}_2\text{SO}_4$  and  $\text{HCl}$  to initially reduce the FFA content through esterification reaction (first stage) and only then followed by the use of other homogeneous alkaline catalyst ( $\text{NaOH}$  or  $\text{KOH}$ ) for transesterification reaction (second stage). Although this method can utilize unrefined or waste oils for biodiesel production, the process requires multiple reactions, washing and separation stages. The strong acidic or alkaline catalysts used are highly corrosive (specially metallurgical), and must be removed from the biodiesel product by multiple washing steps (Yan et al. 2009). Thus, a significant amount of wastewater is generated, together with a loss of catalyst.

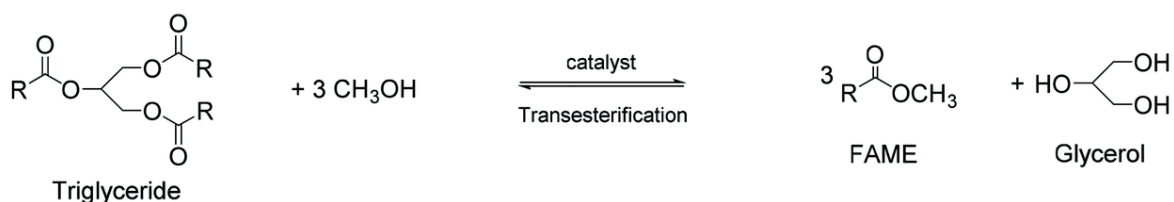


**Figure 1.2** - Global transesterification reaction.

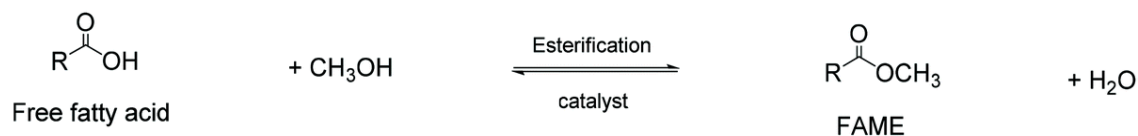


**Figure 1.3** - Esterification reaction.

In this regard, recently the heterogeneous catalysts have caught researchers' attention because of their advantages over homogenous catalysts in terms of higher biodiesel yield, higher glycerol purity, easier catalyst separation (simple filtration), lower corrosively and recoverability, price, safety, more environmentally friendly, and not requiring a washing step for the crude ester (Agarwal et al. 2012; Wen et al. 2010). Moreover, heterogeneous catalysts are preferred over homogenous catalysts in biodiesel production from waste cooking oil (WCO) because saponification reaction is eliminated (Wan Omar et al. 2011). However, it is worth mentioning that the activity of heterogeneous catalysts is largely reliant on their nature,

active sites, structural morphology, porosity, and thermal stability. Heterogeneous catalysts induce slower reaction rate but the limitation can be resolved by increasing the reaction temperature and the concentration of reactants (Avhad and Marchetti 2015). Similar to the homogeneous catalysts, the heterogeneous catalysts are also of two types, namely, acid and alkaline. Examples of heterogeneous acid catalysts are sulphated metal oxide, heteropolyacids, acidic ion exchange resin, and sulphonated amorphous catalysts (Sakai et al. 2009). Additional examples of heterogeneous alkaline catalysts include zinc oxide (ZnO), calcium oxide (CaO), strontium oxide (SrO) (Liu et al. 2007), and titanium oxide (TiO) (Chouhan and Sarma 2011).

Aiming to overcome the drawbacks/limitations of acid and alkaline catalysts stated before, the trends of the research in the catalysis technologies for biodiesel production is the development of solid materials able to simultaneously catalyze the esterification and transesterification reactions, and the possibility to be re-used. These types of heterogeneous catalysts are called “bifunctional”, since they act simultaneously as acid and alkaline catalysts. In other words, with bifunctional catalyst esterification and transesterification are carried out in one single reaction step and not in two-steps (first esterification and second transesterification) (Farooq et al. 2013; Kondamudi et al. 2011). As stated previously, due to high FFA content in low cost feedstock, the alkali catalyzed transesterification reaction to produce biodiesel gives low biodiesel yield because FFA reacts with alkali to form soap, resulting in serious emulsification and separation problems. To solve this problem, it is possible to produce biodiesel by a two-steps catalytic process. The process involved the esterification reaction (FFA conversion to FAME) followed by transesterification (triglycerides conversion to FAME). However, the two-steps method also faces the problem of catalyst removal in both steps (Enweremadu and Mbarawa 2009). The heterogeneous bifunctional catalyst would not only eliminate the long two-steps process but will also reduce the need of high cost equipment; consequently, minimizing the capital cost of the processing technology for biodiesel production (Alhassan et al. 2015). Figure 1.4 shows the two types of processes, i.e, the conventional catalysts (two-step) versus bifunctional catalyst.

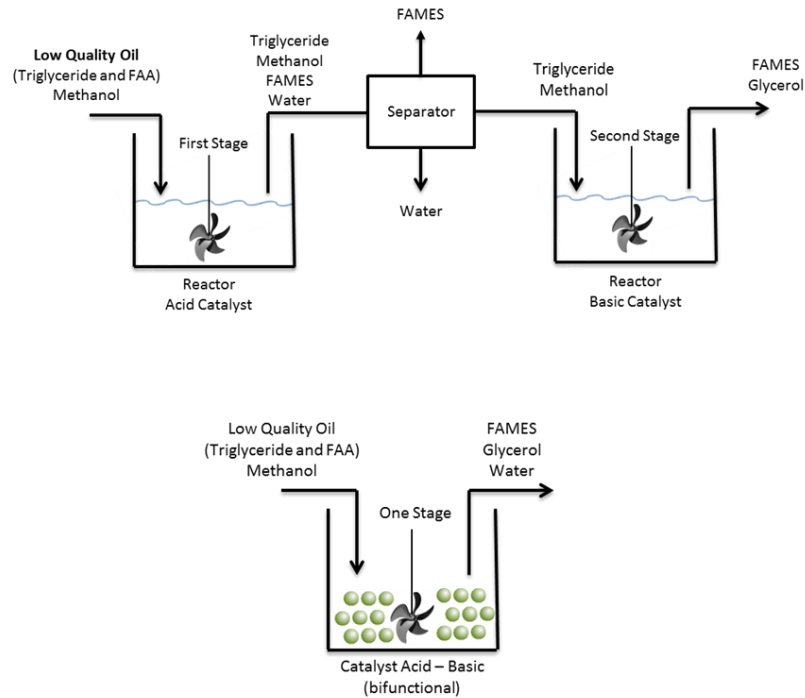


**Figure 1.4** - Two-step conventional catalysis versus bifunctional catalyst process.

In line with the circular economy principles, the development of solid catalysts from waste sources could be a promising way for reducing the environmental burdens of the process and the production costs. Some research works (e.g., Boey et al. 2009; Farooq et al. 2015) have focused on the exploitation of waste materials (e.g. shells, ashes, rocks and bones), due to their abundance and low cost, for solid catalysts preparation. The exploitation of such waste materials has become very attractive. For example, calcium oxide derived from mollusk shells (waste mud crab shells) has been proven to be a potential heterogeneous catalyst for biodiesel production (Viriyempikul et al. 2010). Chicken and quail eggshells calcined were found to be a reliable source of CaO, consisting of 85–95 % of calcium carbonate and 15–5 % other components (MgCO<sub>3</sub>, phosphate, organic matter and a small amount of metals) in dry eggshells (Chojnacka 2005). Another potential catalyst with high carbonate originating naturally and low cost are dolomite (CaMg(CO<sub>3</sub>)<sub>2</sub>). The dolomite is a rock that consists of 23.5 % Ca, 12.1 % Mg, 63 % CO<sub>3</sub> and 1.4 % other components (Fe, SiO<sub>2</sub>, PO<sub>2</sub>, SO<sub>4</sub>) (Zhao et al. 2019). Fly ashes are fine particulates that are obtained from the flue gas treatment systems (e.g. electrostatic precipitators), downstream of the combustion process, in a power plant, using

fossil or renewable energetic vector (e.g. coal or wood bark). These ashes are usually rich in  $\text{SiO}_2$ ,  $\text{Al}_2\text{O}_3$ ,  $\text{CaO}$ ,  $\text{MgO}$  and other oxides, which are pointed out to have excellent catalytic properties for transesterification and esterification reactions (Ho et al. 2014; Sharma et al. 2012).

Globally, the cost of production has been the main barrier in commercializing biodiesel. In the literature, it is consensual that the oily feedstock is the major contributor, about 80 % (Mansir et al. 2018), for the total production costs. The use of edible oils sparks concern in terms of food security while the non-edible oils need additional pretreatment steps. On the other hand, the wide availability of edible oils guarantees the supply while the alternative of non-edible oils is subject to an intermittent supply due to difficulties in its collection (Nurfitri et al. 2013).

The waste cooking oils (WCO) are some vegetable oils that have been previously used for frying or cooking and can constitute an additional source of raw material for biodiesel production. This feedstock can be two to three times cheaper than virgin vegetable oils (Demirbas 2009) and it is important to emphasize that the use of WCO can reduce biodiesel production costs by 60–90 % (Zhang et al. 2003). The WCO has many advantages, such as: (i) abundant supply, (ii) relatively inexpensive, and (iii) environmental benefits (e.g., recovery of hard management waste).

In many countries the waste vegetable oils are abundant; they can be readily collected from households and HORECA sector (hotels restaurants and catering). Nurfitri et al. (2013) reported that, annually, U.S recorded 0.7–1.0 million tons of collected waste oil, Turkey 350.000 tons, Canada 120.000 tons and Bogotá about 4000 tons. In addition, there are unknown amounts of uncollected oils which are discarded through sinks, regular garbage and eventually seeps into the soil and water sources. Furthermore, it is generally accepted that reusing used cooking oil for human consumption is harmful to health (Wei See et al. 2006).

The main factors affecting the yield in FAME production, must be chosen judiciously, namely (Leung et al. 2010; Ni and Meunier 2007): alcohol type, molar ratio of alcohol to oil, catalyst loading, reaction temperature, reaction time and type of reactor. Therefore, to find the

relationship between the operating conditions (levels of the factors evaluated) and the best yield to FAME requires specialized optimization methods. Response Surface Methodology (RSM) based on a Box–Behnken experimental design is an option, that corresponds to a set of mathematical and statistical techniques employed for designing experiments, creating correlations (regression model), evaluating the effects of several factors, and their interaction effects for desirable responses (Liu et al. 2014; Salamatinia et al. 2010). There is commercial software (e.g. Design – Expert) to assist this statistical data processing and analysis.

It is known that the catalytic behavior depends on the morphological characteristics of the solid material, because the catalytic process takes place on its surface (outer and inner). The most utilized techniques to characterize materials' morphology are BET, SEM and EDX. In terms of physical properties, the surface area is the place of catalytic activity, but only a part is utilized in the catalytic reaction (active center or site). In basic and acid catalysts, the active sites not only occupy a little fraction of the surface, but also differ in basic and acid strength and sometimes in nature. Hammett indicators are often used to determine the acid and basic strengths of a material. FTIR is useful to identify the main chemical functional groups present on the surface of solid materials. For bulk properties X-ray diffraction (XRD) is used to find: (i) the crystalline phases, (ii) crystalline degree and (iii) crystallite size and superficial elemental atomic concentration by means of X-ray photoelectronic spectroscopy (XPS). This technique is frequently used to assist the interpretation of the catalytic activity of one material.

Colombia has the fourth largest production of palm oil worldwide with 1.309.586 tons per year with 550.200 hectares of palm plantation, ranking the third in production of biodiesel (518.745 tons per year) in South America, followed by Argentina and Brazil. It is noteworthy that all biodiesel production in Colombia is from palm oil (edible feedstock). This sparks concern in terms of food security in addition to the misuse of fertile lands, water footprint and deforestation. So far, the costs of refined palm oil (RPO) feedstock and chemicals (methanol + NaOH) involved in biodiesel production reaches 88 % of the selling price of this biofuel in Colombia; therefore the government must subsidize this industry (80 million dollars per year) (Acevedo et al. 2015). That is why using the exploration of feedstock and catalysts from waste

should be intensified in order to make the biodiesel production process low cost, affordable and sustainable.

During the last years, the Colombian government has promoted the production and use of biofuels as a part of a strategy to reduce the petroleum dependence and to support the rural development. Colombian fuels must contain a percent of bioethanol and biodiesel blended with gasoline and diesel, respectively. Particularly, for biodiesel and according to the policy act 2629 of 2007, B10 blends (10 % biodiesel and 90 % diesel) must be implemented since 2010 and B20 since 2012. Nevertheless, these blending targets were not reached in these years. However, the market growth in Colombia implicates the expansion on biodiesel demand from B10 to B20 blend for 2020 (Rincón et al. 2015). In addition, the efforts to employ waste need to receive the support of governments, for instance, in terms of tax relief/reduction. Most importantly, the government can play a serious role in introducing regulations to enforce the use of waste substances. In this way, it is no longer a choice but a must to include the intake materials from waste products in many more processes.

## **1.2 Thesis objectives and structure**

This research work aims to prepare efficient bifunctional solid catalysts, from waste materials, to produce FAME from mixtures of low cost vegetable oils (WCO and RPO) with methanol, for later implementation in both optimized batch and continuous production processes. Thus, through the use of waste materials it could be possible a reduction the production costs of biodiesel and simultaneously extend the life-cycle of the materials in the economy, i.e., promoting a circular economy.

Besides that main objective, this proposal also comprises the following specific objectives:

- Prepare and characterize feedstocks (mixtures of oils – WCO and RPO), in terms of some physical chemical properties.

- Prepare and characterize solid catalysts from waste, using preparation procedures and instrumental analytical techniques, respectively.
- Assess the activity and stability of the solid catalysts prepared, using the yield to FAME and the conversion of the FFA as dependent target variables.
- Optimize the production of FAME using the Response Surface Methodology (RSM) based on a Box–Behnken experimental design for most efficient bifunctional catalyst (using the main factors affecting yield to FAME) and evaluating in both batch reactor and in continuous fixed bed reactor.

The novelty of this work is the successful use of a residual materials (either catalyst or feedstock) in the FAME production, carrying out the transesterification and esterification reactions simultaneously in only one stage, innovating over the conventional production process that requires two stages.

For better organization and understanding, the thesis was structured in five sections, as shown in Figure 1.5. Section A presents the study, introducing to the topic, which includes the motivation, the relevance of the study, the objectives and the structure of the thesis.

In sections B to D (in scientific article format), the studies carried out to achieve the objectives of the work are presented. It started with the selection of a catalyst with a bifunctional character, prepared with residual materials. The catalytic performance in the FAME production was assessed and one catalyst (out of eight) was selected. Then, an optimization study was carried out in batch process for FAME production, using the catalyst selected in the previous study. A third study was conducted, this time to produce FAME in a continuous process with the selected catalyst. Both optimization studies made it possible to identify the most significant (in the tested range) operating variables. Each of these experimental works provided results that allowed progressively to advance in the achievement of the objectives defined for this thesis.

Therefore, Section B presents the study to evaluate and choose an efficient bifunctional solid catalyst from waste materials (biomass fly ash, dolomite, egg shells and polyethylene

terephthalate (PET) from waste plastic containers) for production of FAME with methanol, using mixtures of refined palm oil (RPO) and used cooking oil (WCO) in different mass ratios. This study was carried out in a batch reactor due to the ease of operation and control of the process variables. More, the batch reactor allows to carry out the tests of catalytic activity in a reliable and efficient way.

Section C presents the study of optimization of the FAME production process with methanol, using mixtures of WCO and RPO and the catalyst (powder) selected in the previous work (section B). The Response Surface Methodology (RSM) based on a Box–Behnken experimental design was used to test four operating variables (in a batch reactor), namely: catalyst loading, methanol/oil molar ratio, RPO/WCO mass ratio and reaction temperature. Additionally, it was carried out a study of reusability of the catalyst aiming to assess its performance and catalytic stability over several cycles of utilization in the FAME synthesis process. The optimal operating conditions found by the regression model were used in this assay.

Section D presents the design, construction of a continuous fixed bed reactor (novel and simple reaction system to produce FAME with solid catalyst) and optimization study. The RSM based on a Box–Behnken experimental design was used to test the influence of three operating variables, namely: methanol/oil molar ratio, RPO/WCO mass ratio and residence time. It is important to mention that the biomass fly ash catalyst is a very fine powder and to be evaluated in a continuous fixed-bed reactor it was necessary to pelletize it. Additionally, the catalytic stability of the pelletized biomass fly ash was evaluated through an assay during 32 h of operation in the continuous fixed bed reactor. The optimal operating conditions found by the regression model were used in this assay.

Finally, in Section E, final remarks are made about results obtained throughout the study, and proposals for future studies are presented.



### 1.3 Scientific production within the scope of the thesis

The global information of the studies presented in Sections B to D of this thesis were published or submitted in scientific journals with peer review or at conferences, as mentioned in the next subchapters.

#### 1.3.1 Articles published in scientific journals

- E. M. Vargas, M. C. Neves, L. A. C. Tarelho, and M. I. Nunes, “Solid catalysts obtained from wastes for FAME production using mixtures of refined palm oil and waste cooking oils,” *Renew. Energy*, vol. 136, pp. 873–883, 2019, doi: 10.1016/j.renene.2019.01.048.
- E. M. Vargas, J. L. Ospina, L. A. C. Tarelho, and M. I. Nunes, “FAME production from residual materials: Optimization of the process by Box–Behnken model,” *Energy Reports*, vol. 6, pp. 347–352, 2019, doi: 10.1016/j.egyr.2019.08.071.
- E. M. Vargas, J. L. Ospina, M. C. Neves, L. A. C. Tarelho, and M. I. Nunes, “Optimization of FAME production from blends of waste cooking oil and refined palm oil using biomass fly ash as a catalyst”, *Renew. Energy*, vol. 163, pp. 1637–1647, 2021, doi: <https://doi.org/10.1016/j.renene.2020.10.030>.
- E. M. Vargas, Duvan O. Villamizar, M. C. Neves, and M. I. Nunes, “Pelletized biomass fly ash for FAME production: optimization of a continuous process”, *Fuel*, vol. 293, pp. 120425, 2021, doi: <https://doi.org/10.1016/j.fuel.2021.120425>.

#### 1.3.2 Articles published in scientific conferences

- E. M. Vargas, M. C. Neves, L. A. C. Tarelho, and M. I. Nunes, “Produção de biodiesel usando materiais residuais”, conferência nacional: Green Business Week, 15 a 17 de março de 2017 Lisboa, Portugal.
- E. M. Vargas, M. C. Neves, L. A. C. Tarelho, and M. I. Nunes, “Biodiesel production using residual materials”, conferência internacional: 4th international conference, Wastes Solutions Treatments Opportunities, 25 e 26 de setembro de 2017 Porto, Portugal.

- E. M. Vargas, M. C. Neves, L. A. C. Tarelho, and M. I. Nunes, “Produção de biodiesel a partir de materiais residuais”, TechDays, workshops e conferência, 12 a 14 de outubro de 2017 Aveiro, Portugal.
- E. M. Vargas, J. L. Ospina, L. A. C. Tarelho, and M. I. Nunes, “FAME production from residual materials: Optimization of the process by Box–Behnken model,” 6th International Conference on Energy and Environment Research, ICEER 2019, 22-25 July, University of Aveiro, Portugal.

### **1.3.3 Participation in scientific events**

- Perspectivas del post-conflicto: una mirada desde la ingeniería, Bogotá. Título do trabalho: Biodiesel production using residual materials: an alternative for Colombia. 9 e 10 outubro de 2017, Bogotá Colombia.
- 4to encuentro de semilleros de investigación, ciencia, arte e innovación. Título do trabalho: Producción de biodiésel a partir de mezclas de aceite de palma (RBD) con aceites usados de cocina (AUC), utilizando como catalizador CaO-SiO<sub>2</sub>. 2 e 3 de novembro de 2017, Bogotá Colombia.
- UA Open Campus, Aveiro. Título do trabalho: Produção de biodiesel a partir de materiais residuais. 22 a 24 de março de 2018.
- 4to encuentro de semilleros de investigación, ciencia, arte e innovación. Título do trabalho: Producción de biodiésel a partir de mezclas de aceite de palma (RBD) con aceites usados de cocina (AUC), utilizando como catalizador CaO-SiO<sub>2</sub>. 2 e 3 de novembro de 2017, Bogotá Colombia.
- Perspectivas del post-conflicto: una mirada desde la ingeniería. Título do trabalho: Biodiesel production using residual materials: an alternative for Colombia. 9 e 10 outubro de 2017, Bogotá Colombia.



**Figure 1.5** - Structure of the thesis in five sections.

## References

- Acevedo, Juan C, Jorge a Hernández, Carlos F Valdés, and Samir Kumar Khanal. 2015. "Analysis of Operating Costs for Producing Biodiesel from Palm Oil at Pilot-Scale in Colombia." *Bioresource technology* 188: 117–23. <http://www.ncbi.nlm.nih.gov/pubmed/25660089> (April 8, 2015).
- Agarwal, Madhu, Garima Chauhan, S. P. Chaurasia, and Kailash Singh. 2012. "Study of Catalytic Behavior of KOH as Homogeneous and Heterogeneous Catalyst for Biodiesel Production." *Journal of the Taiwan Institute of Chemical Engineers* 43(1): 89–94. <http://dx.doi.org/10.1016/j.jtice.2011.06.003>.
- Alhassan, Fatah H., Umer Rashid, and Y.H. Taufiq-Yap. 2015. "Synthesis of Waste Cooking Oil-Based Biodiesel via Effectual Recyclable Bi-Functional Fe<sub>2</sub>O<sub>3</sub>MnOSO<sub>4</sub>2-/ZrO<sub>2</sub> Nanoparticle Solid Catalyst." *Fuel* 142: 38–45. <http://linkinghub.elsevier.com/retrieve/pii/S0016236114010333> (April 9, 2015).
- Avhad, M. R., and J. M. Marchetti. 2015. "A Review on Recent Advancement in Catalytic Materials for Biodiesel Production." *Renewable and Sustainable Energy Reviews* 50: 696–718. <http://dx.doi.org/10.1016/j.rser.2015.05.038>.
- Boey, Peng Lim, Gaanty Pragas Maniam, and Shafida Abd Hamid. 2009. "Biodiesel Production via Transesterification of Palm Olein Using Waste Mud Crab (*Scylla Serrata*) Shell as a Heterogeneous Catalyst." *Bioresource Technology* 100(24): 6362–68. <http://dx.doi.org/10.1016/j.biortech.2009.07.036>.
- Chojnacka, Katarzyna. 2005. "Biosorption of Cr(III) Ions by Eggshells." *Journal of Hazardous Materials* 121(1–3): 167–73.
- Chouhan, a.P. Singh, and a.K. Sarma. 2011. "Modern Heterogeneous Catalysts for Biodiesel Production: A Comprehensive Review." *Renewable and Sustainable Energy Reviews* 15(9): 4378–99. <http://linkinghub.elsevier.com/retrieve/pii/S1364032111003595> (July 16, 2014).
- Demirbas, Ayhan. 2009. "Biodiesel from Waste Cooking Oil via Base-Catalytic and Supercritical Methanol Transesterification." *Energy Conversion and Management* 50(4): 923–27. <http://dx.doi.org/10.1016/j.enconman.2008.12.023>.
- Enweremadu, C. C., and M. M. Mbarawa. 2009. "Technical Aspects of Production and Analysis of Biodiesel from Used Cooking Oil-A Review." *Renewable and Sustainable Energy Reviews* 13(9): 2205–24.
- Farooq, Muhammad, and Anita Ramli. 2015. "Biodiesel Production from Low FFA Waste Cooking Oil Using Heterogeneous Catalyst Derived from Chicken Bones." *Renewable Energy* 76: 362–68. <http://dx.doi.org/10.1016/j.renene.2014.11.042>.
- Farooq, Muhammad, Anita Ramli, and Duvvuri Subbarao. 2013. "Biodiesel Production from Waste Cooking Oil Using Bifunctional Heterogeneous Solid Catalysts." *Journal of Cleaner Production* 59: 131–40. <http://linkinghub.elsevier.com/retrieve/pii/S095965261300396X> (May 14, 2015).

- Ho, Wilson Wei Sheng, Hoon Kiat Ng, Suyin Gan, and Sang Huey Tan. 2014. "Evaluation of Palm Oil Mill Fly Ash Supported Calcium Oxide as a Heterogeneous Base Catalyst in Biodiesel Synthesis from Crude Palm Oil." *Energy Conversion and Management* 88: 1167–78. <http://linkinghub.elsevier.com/retrieve/pii/S0196890414002623> (March 7, 2015).
- Kiss, Anton A., Alexandre C. Dimian, and Gadi Rothenberg. 2008. "Biodiesel by Catalytic Reactive Distillation Powered by Metal Oxides." *Energy and Fuels* 22(1): 598–604.
- Kondamudi, Narasimharao, Susanta K. Mohapatra, and Mano Misra. 2011. "Quintinite as a Bifunctional Heterogeneous Catalyst for Biodiesel Synthesis." *Applied Catalysis A: General* 393(1–2): 36–43. <http://linkinghub.elsevier.com/retrieve/pii/S0926860X10007799> (July 1, 2015).
- Lam, Man Kee, Keat Teong Lee, and Abdul Rahman Mohamed. 2009. "Sulfated Tin Oxide as Solid Superacid Catalyst for Transesterification of Waste Cooking Oil: An Optimization Study." *Applied Catalysis B: Environmental* 93(1–2): 134–39.
- Leung, Dennis Y C, Xuan Wu, and M. K H Leung. 2010. "A Review on Biodiesel Production Using Catalyzed Transesterification." *Applied Energy* 87(4): 1083–95. <http://linkinghub.elsevier.com/retrieve/pii/S0306261909004346> (July 10, 2014).
- Liu, Wei, Ping Yin, Xiguang Liu, and Rongjun Qu. 2014. "Design of an Effective Bifunctional Catalyst Organotriphosphonic Acid-Functionalized Ferric Alginate (ATMP-FA) and Optimization by Box-Behnken Model for Biodiesel Esterification Synthesis of Oleic Acid over ATMP-FA." *Bioresource Technology* 173: 266–71. <http://dx.doi.org/10.1016/j.biortech.2014.09.087>.
- Liu, Xuejun, Huayang He, Yujun Wang, and Shenlin Zhu. 2007. "Transesterification of Soybean Oil to Biodiesel Using SrO as a Solid Base Catalyst." *Catalysis Communications* 8(7): 1107–11.
- Mansir, Nasar et al. 2018. "Modified Waste Egg Shell Derived Bifunctional Catalyst for Biodiesel Production from High FFA Waste Cooking Oil. A Review." *Renewable and Sustainable Energy Reviews* 82(November 2016): 3645–55.
- Ni, J., and F. C. Meunier. 2007. "Esterification of Free Fatty Acids in Sunflower Oil over Solid Acid Catalysts Using Batch and Fixed Bed-Reactors." *Applied Catalysis A: General* 333(1): 122–30.
- Nurfitri, Irma et al. 2013. "Potential of Feedstock and Catalysts from Waste in Biodiesel Preparation: A Review." *Energy Conversion and Management* 74: 395–402. <http://linkinghub.elsevier.com/retrieve/pii/S0196890413002586> (March 13, 2015).
- Rincón, Luis E. et al. 2015. "Optimization of the Colombian Biodiesel Supply Chain from Oil Palm Crop Based on Techno-Economical and Environmental Criteria." *Energy Economics* 47: 154–67. <http://linkinghub.elsevier.com/retrieve/pii/S0140988314002631> (February 3, 2015).

- Sakai, Tsutomu, Ayato Kawashima, and Tetsuya Koshikawa. 2009. "Economic Assessment of Batch Biodiesel Production Processes Using Homogeneous and Heterogeneous Alkali Catalysts." *Bioresource Technology* 100(13): 3268–76.  
<http://dx.doi.org/10.1016/j.biortech.2009.02.010>.
- Salamatinia, Babak, Hamed Mootabadi, Subhash Bhatia, and Ahmad Zuhairi Abdullah. 2010. "Optimization of Ultrasonic-Assisted Heterogeneous Biodiesel Production from Palm Oil: A Response Surface Methodology Approach." *Fuel Processing Technology* 91(5): 441–48.
- Sharma, Meeta, Arif Ali Khan, S. K. Puri, and D. K. Tuli. 2012. "Wood Ash as a Potential Heterogeneous Catalyst for Biodiesel Synthesis." *Biomass and Bioenergy* 41: 94–106.  
<http://dx.doi.org/10.1016/j.biombioe.2012.02.017>.
- Viriya-empikul, N. et al. 2010. "Waste Shells of Mollusk and Egg as Biodiesel Production Catalysts." *Bioresource Technology* 101(10): 3765–67.  
<http://dx.doi.org/10.1016/j.biortech.2009.12.079>.
- Wan Omar, Wan Nor Nadyaini, and Nor Aishah Saidina Amin. 2011. "Optimization of Heterogeneous Biodiesel Production from Waste Cooking Palm Oil via Response Surface Methodology." *Biomass and Bioenergy* 35(3): 1329–38.  
<http://linkinghub.elsevier.com/retrieve/pii/S0961953410005076> (May 29, 2015).
- Wei See, Siao, Sathrugnan Karthikeyan, and Rajasekhar Balasubramanian. 2006. "Health Risk Assessment of Occupational Exposure to Particulate-Phase Polycyclic Aromatic Hydrocarbons Associated with Chinese, Malay and Indian Cooking." *Journal of Environmental Monitoring* 8(3): 369–76.
- Wen, Zhenzhong et al. 2010. "Biodiesel Production from Waste Cooking Oil Catalyzed by TiO<sub>2</sub>-MgO Mixed Oxides." *Bioresource Technology* 101(24): 9570–76.  
<http://dx.doi.org/10.1016/j.biortech.2010.07.066>.
- Yan, Shuli, Steven O. Salley, and K. Y. Simon Ng. 2009. "Simultaneous Transesterification and Esterification of Unrefined or Waste Oils over ZnO-La<sub>2</sub>O<sub>3</sub> Catalysts." *Applied Catalysis A: General* 353(2): 203–12.
- Zhang, Y, M.a Dubé, D.D McLean, and M Kates. 2003. "Biodiesel Production from Waste Cooking Oil: 2. Economic Assessment and Sensitivity Analysis." *Bioresource Technology* 90(3): 229–40. <http://linkinghub.elsevier.com/retrieve/pii/S0960852403001500> (December 26, 2014).
- Zhao, Shuang et al. 2019. "Experimental Investigation on Biodiesel Production through Transesterification Promoted by the La-Dolomite Catalyst." *Fuel* 257(July): 116092.  
<https://doi.org/10.1016/j.fuel.2019.116092>.

---

## SECTION B – Bifunctional solid catalyst selection

This section aims to develop an efficient bifunctional solid catalyst that would be able to catalyze the esterification and transesterification reactions simultaneously (single reaction step). These reactions were performed in batch regime using methanol, mixtures of waste cooking oil and refined palm oil and solid catalysts. The solid catalysts were prepared from waste feedstocks (biomass fly ashes, natural dolomite rock, chicken eggshells and polyethylene terephthalate - PET of waste plastic packaging) and characterized by SEM, EDX, XRD, BET, FT-IR and Hammett indicators. Eight potential solid catalysts were prepared and tested. Their performance in the esterification and transesterification catalysis was assessed by the FFA conversion and the yield to FAME (for both reactions), respectively.

The information presented in this section was adapted from the following published article:

- E. M. Vargas, M. C. Neves, L. A. C. Tarelho, and M. I. Nunes, “Solid catalysts obtained from wastes for FAME production using mixtures of refined palm oil and waste cooking oils,” *Renew. Energy*, vol. 136, pp. 873–883, 2019, doi: 10.1016/j.renene.2019.01.048.





## 2 Solid catalysts obtained from wastes for FAME production using mixtures of refined palm oil and waste cooking oils

**Abstract:** More than 95 % of biodiesel production feedstocks come from edible oils, however it may cause some problems such as the competition for land use for food production and biodiesel production. The waste cooking oils (WCO) are an alternative feedstock for biodiesel production; its usage reduces significantly the cost of biodiesel production and has environmental benefits, e.g., a waste recovery instead of its elimination. This work aims to produce a low-cost efficient solid catalyst for fatty acid methyl esters (FAME) production using mixtures of RPO and WCO (M1 (100 % RPO), M2 (75 % RPO, 25 % WCO), M3 (50 % RPO, 50 % WCO), M4 (25 % RPO, 75 % WCO) and M5 (100 % WCO)). Four low cost catalysts were prepared (biomass fly ashes, natural dolomite rock, chicken eggshells and polyethylene terephthalate - PET) and their derivatives, characterized (by SEM, EDX, XRD, BET, FT-IR and Hammett indicators) and tested regarding their performance in FAME production. The maximum yield of FAME achieved was around 96 wt% for biomass fly ashes catalyst at 60 °C, 9:1 (mol/mol) of methanol to oil mixture, 10 wt% catalyst to oil mixture, 600 rpm, over 180 min in batch reactor. The results point out for promising bifunctional catalysts able to yield also conversion of free fatty acids up to 100 % using mixtures of RPO and WCO.

**Keywords:** Waste materials; FAME; solid catalyst; bifunctional catalysts; waste cooking oil; refined palm oil.

## 2.1 Introduction

Energy is a basic requirement for human existence and its demand grows every year. In the current situation, the foremost amount of primary and useful energy is supplied by the conventional fossil fuel resources, such as gasoline, liquefied petroleum gas, diesel fuel, and natural gas. However, the use of fossil fuels has several influences on the environment, such as large greenhouse gas emissions, acid rain, resources depletion, etc. In addition to serious environmental issues, dwindling reserves of crude oil, fluctuating petroleum fuel prices, have made today's need to find alternative “green” sources of energy, which are sustainable, environmentally compatible, economically competitive, and easily available. One of the most promising sources is biodiesel, an alternative diesel fuel derived from renewable sources with high quality, which allows the replacement of fossil diesel oil (Leung et al. 2010). Usually the biodiesel production is a catalyzed process where alkali or acid compounds are used, respectively, for the conversion of triglycerides (transesterification reaction) and free fatty acids – FFA (esterification reaction) into fatty acid methyl esters (FAME), when methanol is used in the synthesis. In line with the circular economy principles, the development of solid catalysts from waste sources could be a promising way for reducing the environmental burdens of the process and the production costs. Some research works (Boey et al. 2009; Farooq et al. 2015) have focused on the exploitation of waste materials (e.g. shells, ashes, rocks and bones), due to their abundance and low cost, for solid catalysts preparation.

Globally, the cost of production has been the main barrier in commercializing biodiesel. In the literature, it is consensual that the oily feedstock is the major contributor, about 80 % (Mansir et al. 2018), for the total production costs. The use of edible oils sparks concern in terms of food security while the non-edible oils need additional pre-treatment steps. On the other hand, the wide availability of edible oils guarantees the supply while the alternative of non-edible oils is subject to an intermittent supply (Nurfitri et al. 2013).

The waste cooking oils (WCO) are some vegetable oils that have been previously used for frying or cooking and can constitute an additional source of raw material for biodiesel production. This feedstock can be two to three times cheaper than virgin vegetable oils (Demirbas 2009). Furthermore, it is generally accepted that reusing used cooking oil for human consumption is harmful to health (Chen et al. 2012) and the WCO is difficult to manage.

In the research that focuses on the biodiesel production process there is a new trend of bifunctional heterogeneous catalysts that, if used properly, can catalyze both transesterification and esterification reactions simultaneously. This ability is due to the presence of both basic and acidic sites on the same catalysts. Additionally, this kind of catalysts can be modified to introduce/improve certain physicochemical properties needed to handle with low grade feedstocks (e.g. some WCO). Usually these raw-materials have high FFA and/or water contents, which are undesirable for transesterification reaction (Farooq et al. 2013).

This work aims to produce an efficient solid bifunctional catalyst from residual materials for FAME production using mixtures of refined palm oil (RPO) and WCO in different ratios. Thus, this work tackles two current environmental concerns giving an alternative for recovering some important wastes fluxes (WCO, fly ashes, dolomite, eggshells and polyethylene terephthalate (PET) plastic garbage containers), aligned with the principles of circular economy, and for reducing the dependence of fossil fuel, through the production of biofuel mainly from waste materials feedstocks.

## **2.2 Materials and Methods**

Solid catalysts were prepared and characterized in terms of some of their chemical, physical and structural properties. The raw-material for FAME synthesis consisted of a mixtures of WCO and RPO in different ratios. The adopted procedures are described in next sections. The experimental plan for assessing the performance of the catalysts in the FAME production will be presented later as well as the analytical methods used.

### 2.2.1 Materials

Waste cooking oil for FAME production was provided by a local collecting company (Bioils) in Bogotá, Colombia. The WCO was pre-treated by filtration and heating (at 110 °C for 1 h) to remove suspended particles and traces of water, respectively. The RPO was purchased at a local store in Bogotá. The solid waste materials for catalyst preparation were obtained from the following sources:

- Biomass fly ashes – collected at the electrostatic precipitator of a thermal power-plant using residual forest biomass (derived from eucalyptus) as fuel, located in the Centre Region of Portugal;
- Natural dolomite rock- the mining industry in Colombia;
- Eggshells- several restaurants of Bogotá;
- PET- plastic bottles picked from garbage containers at the University Jorge Tadeo Lozano, Bogotá.

All the chemicals used were of analytical grade except n-hexane (GC grade) and methyl heptadecanoate (analytical standard) from Sigma-Aldrich and Merck.

### 2.2.2 Oil mixtures (RPO and WCO) characterization

Five feedstocks were prepared using different mass ratios of RPO and WCO: M1 (100 % RPO), M2 (75 % RPO, 25 % WCO), M3 (50 % RPO, 50 % WCO), M4 (25 % RPO, 75 % WCO) and M5 (100 % WCO).

These mixtures were characterized in terms of: acid value (NTC 218 (ICONTEC 218 1999)), density (NTC 336 (ICONTEC 2011)), saponification number (NTC 335(ICONTEC 2011)), viscosity (ASTM D445) (ASTM 2010), and moisture content (Karl Fisher, Coulometer 831-Metrohm). The saponification number (*SN*) was used to calculate the molecular mass (*MW*) according to Equation 2.1 (Mansir et al. 2018).

$$MW = \frac{56,1 \times 1000 \times 3}{SN} \quad (2.1)$$

The FFA content was calculated from the acid value ( $AV$ , mg KOH/g) using Equation 2.2 (Mansir et al. 2018).

$$\text{FFA} = \frac{AV}{2} \quad (2.2)$$

### 2.2.3 Catalysts preparation and characterization

Eight catalysts were prepared using low cost feedstocks, implementing the procedures summarized in Table 2.1. The sulfonation or the addition of silicon to some catalysts aimed to enhance their acid strength.

**Table 2.1** - Solid catalysts preparation procedures.

Catalyst reference		Preparation procedure
Biomass fly ash	FAD	Dry at 120 °C for 5 h sieve 75 µm.
	FAC	Calcine FAD at 700 °C for 5 h sieve 75 µm.
Natural dolomite rock	Dolomite C	Mill and sieve at 45 µm and calcine at 800 °C for 2 h.
	Dolomite CSC	Impregnate dolomite C with H <sub>2</sub> SO <sub>4</sub> 2M for 6 h at room temperature. Then, filter and dry for 12 h at 110 °C. Finally, calcine at 500 °C for 4 h.
Eggshells	CaO-SiO <sub>2</sub>	Wash with water and dry at 120 °C for 3 h. Then, sieved at 63 µm and calcine at 800 °C for 4 h. Impregnate with Na <sub>2</sub> SiO <sub>3</sub> 0.4 M aqueous solution at room temperature for 4 h. Finally dry at 100 °C for 12 h and calcine at 800 °C for 4 h.
	CaO-S-SiO <sub>2</sub>	Impregnate CaO-SiO <sub>2</sub> with H <sub>2</sub> SO <sub>4</sub> 2 M for 6 h at room temperature, dry at 110 °C for 12 h and calcine at 500 °C for 3 h.
PET	CA-PET	Reduce (cut) the PET containers to small pieces (<1 cm <sup>2</sup> ) and heat 10 °C/min for 2 h from room temperature up to 450 °C under a nitrogen atmosphere. Impregnate the resulting product with H <sub>2</sub> SO <sub>4</sub> 98 % (1.5:1 v/w, H <sub>2</sub> SO <sub>4</sub> : PET) at 150 °C for 2 h. Then, wash with water and dry at 120°C for 6 h. Mill and sieve at 106 µm, and finally dry at 105 °C for 24 h.
	CA-PET-S	Impregnate CA-PET with fuming sulfuric acid (5:1 v/w, H <sub>2</sub> SO <sub>4</sub> :CA-PET) at 150 °C for 10 h under a nitrogen atmosphere. Wash with water (until no sulfate ions are detected, using turbidimetric method) and dry at 105 °C for 24 h.

The solid catalysts were characterized in terms of: (i) crystallographic structures, by powder X-ray (XRD, PAN analytical Empyrean X-ray diffractometer equipped with Cu-K $\alpha$  radiation source  $\lambda = 1.54178 \text{ \AA}$  at 45 kV/ 40 mA); (ii) surface area, pore size and pore volume, by Brunauer-Emmet-Teller sorption isotherm (BET, using N<sub>2</sub> at -196 °C in Micromeritics ASAP 2020); (iii) surface morphology and quantitative elemental composition analysis, by surface scanning electron microscopy (SEM, using FEG-SEM Hitachi S4100 microscope operated at 25 kV) and energy dispersive X-ray spectroscopy (EDX, using a HR-FESEM Hitachi SU-70 operated at 15 kV, equipped with a Bruker Quantax 400 EDS system); (iv) surface functional species by Fourier transform infrared (FTIR, Agilent CARY 630 with wave number range from 400 to 4000 cm<sup>-1</sup>); and (v) basic and acid strength by using Hammett indicators (indicators for basic strength: neutral red (pKa = 6.8), bromothymol blue (pKa = 7.2), phenolphthalein (pKa = 9.3), indigo carmine (pKa = 12.2) and 2,4-dinitroaniline (pKa = 15.0); indicators for acid strength: bromothymol blue (pKa = 7.2), neutral red (pKa = 6.8), bromocresol purple (pKa = 6.1), bromocresol green (pKa = 4.7) and bromophenol blue (pKa = 3.8)). The latter method was carried out by dispersing about 25 mg of the sample in 5.0 mL of a solution of Hammett indicators (0.5 mg of indicator in 10 mL of methanol for basic strength or 10 mL of benzene for acid strength), and left for 2 h in order to attain the equilibrium. After reaching equilibrium, the color on the catalyst and solution were identified.

#### **2.2.4 FAME synthesis**

The experiments for FAME production were carried out in batch reactor (in stainless steel, 1 L of capacity, equipped with temperature control and mechanical agitator) at 60 °C, 9:1 (mol/mol) of methanol to oil mixture, 10 wt% catalyst to oil mixture, 600 rpm and over 180 min. After the pre-defined reaction time, for each assay, the catalyst and methanol were separated from the reaction mixture by centrifugation and evaporation, respectively. Then, the supernatant was placed into a separating funnel over 12 h for phase separation. The upper layer was dried with anhydrous sodium sulfate (10 wt%) and weighed. The resulting mixture, hereafter is so-called purified final mixture, was analyzed by gas chromatography for FAME

determination and was titrated with a KOH solution for final acid value quantification (ICONTEC 218 1999).

The Shimadzu G-C 2014 chromatograph was equipped with a flame ionization detector and a capillary column SGE BP-20 60 m x 0.25 mm i.d. x 0.25  $\mu$ m film thickness with a stationary phase of polyethylene glycol; the carrier gas was helium with a flow rate of 16.7 mL/min and a pressure of 2.5 atm; the injector (AOC-20i) was operated at 200 °C and an injection volume of 2.0  $\mu$ L in Split mode. Methyl heptadecanoate was used as internal standard and hexane as the solvent. The content of methyl esters was calculated based on the standard method UNE-EN ISO 14103:2011 (AENOR-EN 14103 2011) and expressed as concentration of FAME using the Equation 2.3.

$$C = \frac{\sum A - A_{EI}}{A_{EI}} \times \frac{W_{EI}}{W} \quad (2.3)$$

Where  $C$  is the concentration of FAME in the purified final mixture (w/w),  $\sum A$  is the total peak areas of the methyl ester from  $C_{14}$  until  $C_{24:1}$ ,  $A_{EI}$  is the peak area corresponding to methyl heptadecanoate,  $W_{EI}$  is the mass (mg) of methyl heptadecanoate used and  $W$  is the mass (mg) of the sample used in the analysis.

The catalysts performance was expressed in terms of FAME yield, Equation 2.4, and FFA conversion, Equation 2.5 (Uprety et al. 2016; Wan Omar et al. 2011a).

$$\text{FAME yield (\%)} = \frac{C \times \text{Total mass of purified final mixture}}{\text{Mass of oil used in the experiment}} \times 100 \quad (2.4)$$

$$\text{FFA conversion (\%)} = \left(1 - \frac{AV_f}{AV_i}\right) \times 100 \quad (2.5)$$

Where  $AV_i$  and  $AV_f$  correspond to the acid value of the initial oil mixture and of the purified final mixture, respectively.

## 2.3 Results and discussion

### 2.3.1 Oil mixtures characterization

The results of the characterization of the oil mixtures prepared for this study are shown in Table 2.2.

**Table 2.2** - Properties of the oil mixtures used.

	Mixture reference				
	M1	M2	M3	M4	M5
	%WCO %RPO	0 100	25 75	50 50	75 25
Moisture (wt%)	0.067 ± 0.010	0.141 ± 0.017	0.170 ± 0.003	0.177 ± 0.013	0.197 ± 0.012
Density (g/mL)	0.908 ± 0.008	0.907 ± 0.004	0.913 ± 0.010	0.905 ± 0.007	0.906 ± 0.003
AV (mg KOH/g)	0.307 ± 0.004	1.249 ± 0.061	2.458 ± 0.082	3.873 ± 0.088	4.934 ± 0.252
FFA (wt%)	0.172 ± 0.0048	0.622 ± 0.0512	1.240 ± 0.012	1.917 ± 0.048	2.453 ± 0.056
MW (g/mol)	843.15 ± 9.52	875.17 ± 10.28	864.04 ± 9.21	855.50 ± 3.69	857.82 ± 4.01
Viscosity (mm <sup>2</sup> /s) @ 60 °C	14.902 ± 0.193	17.069 ± 0.137	17.122 ± 0.123	17.717 ± 0.150	19.185 ± 0.392

The properties of the mixture M1 (i.e., 100 % RPO) are similar to those reported by Kansedo et al. (2009) and by Singh and Dipti (2010). Concerning the waste cooking oils properties, they are quite dependent of the vegetable oil feedstocks and their frying practices and conditions. The WCO (M5) used in this work has properties similar to those reported by Wan Omar et al. (2011b) and Lam et al. (2010) and it can be categorized as yellow grease (FFA < 15 %) (Avhad and Marchetti 2015).

Regarding the mixtures prepared with RPO and WCO, one observes that the density and the molecular weight are not affected by the blending ratio. On the other hand, the properties



related to acidity of the mixtures (*AV* and *FFA*) rise significantly as the percentage of WCO increases in the blend. The water content and the viscosity are properties that increase slightly by increasing the WCO percentage in the blend.

### 2.3.2 Catalysts characterization

The solid catalysts prepared by the methods shown in Table 2.1 were characterized in terms of some textural properties such as surface area, crystalline structure, but also their basic and acid strength, etc. The results are shown and discussed below.

#### 2.3.2.1 BET surface area and Hammett indicators analyses

The BET surface area, pore volume, pore diameter, basic and acid strength of catalysts are shown in Table 2.3.

**Table 2.3** - Textural properties of the catalysts prepared in this work.

Catalyst	Specific surface area (m <sup>2</sup> /g)	Pore volume (cm <sup>3</sup> /g)	Pore diameter (Å)	Basic strength	Acid strength
FAD	9.0280	0.01055	77.188	9.3 ≤ pKa < 12.2	6.8 ≤ pKa < 7.2
FAC	5.1750	0.00791	101.849	9.3 ≤ pKa < 12.2	6.8 ≤ pKa < 7.2
Dolomite C	12.0113	0.04145	136.908	12.2 ≤ pKa < 15	6.8 ≤ pKa < 7.2
Dolomite CSC	15.2617	0.05291	113.689	9.3 ≤ pKa < 12.2	6.1 ≤ pKa < 6.8
CaO-SiO <sub>2</sub>	6.6112	0.01285	56.874	7.2 ≤ pKa < 9.3	3.8 ≤ pKa < 4.7
CaO-S-SiO <sub>2</sub>	12.6773	0.04330	109.925	9.3 ≤ pKa < 12.2	6.8 ≤ pKa < 7.2
CA-PET	1105.2	0.85871	14.983	ND	6.1 ≤ pKa < 6.8
CA-PET-S	624.3	0.54221	14.871	ND	3.8 ≤ pKa < 4.7

ND – not detected

The calcination of fly ashes seems to reduce the surface area (ca 40 %) and pore volume (ca 25 %), which can be due to sintering of the compounds on the solid matrix surface

(Maneerung et al. 2015). Nevertheless, this thermal treatment does not affect both basic and acid strength of this catalyst. Both ash based catalysts have an intermediate basic strength ( $9.3 \leq pK_a < 12.2$ ) and a low acid strength ( $6.8 \leq pK_a < 7.2$ ).

The sulfonation of Dolomite increases both surface area (*ca* 30 %) and pore volume (*ca* 30 %), but reduces the pore diameter (*ca* 20 %). These physical changes may have effects on the performance of these materials in the catalysis of FAME production reactions. On one hand, higher surface area and pore volume will have a positive effect on the catalysis, but on the other hand, a decrease of pore diameter increases the diffusion limitations especially for molecules having long alkyl chain (Lam et al. 2009). Jacobson et al. (2008) identified the pore structure as the primary requirement for an ideal solid catalyst in the biodiesel production (via transesterification) since a typical triglyceride molecule has a diameter of approximately 58 Å. As foreseen, sulfonating the Dolomite C increases its acid strength ( $6.8 \leq pK_a < 7.2$  to  $6.1 \leq pK_a < 6.8$ ) and decreases the basic strength ( $12.2 \leq pK_a < 15$  to  $9.3 \leq pK_a < 12.2$ ), values close to those found by Yoosuk et al. (2011). However, Dolomite CSC has both acid and basic strength which, a priori, gives it a bifunctional character.

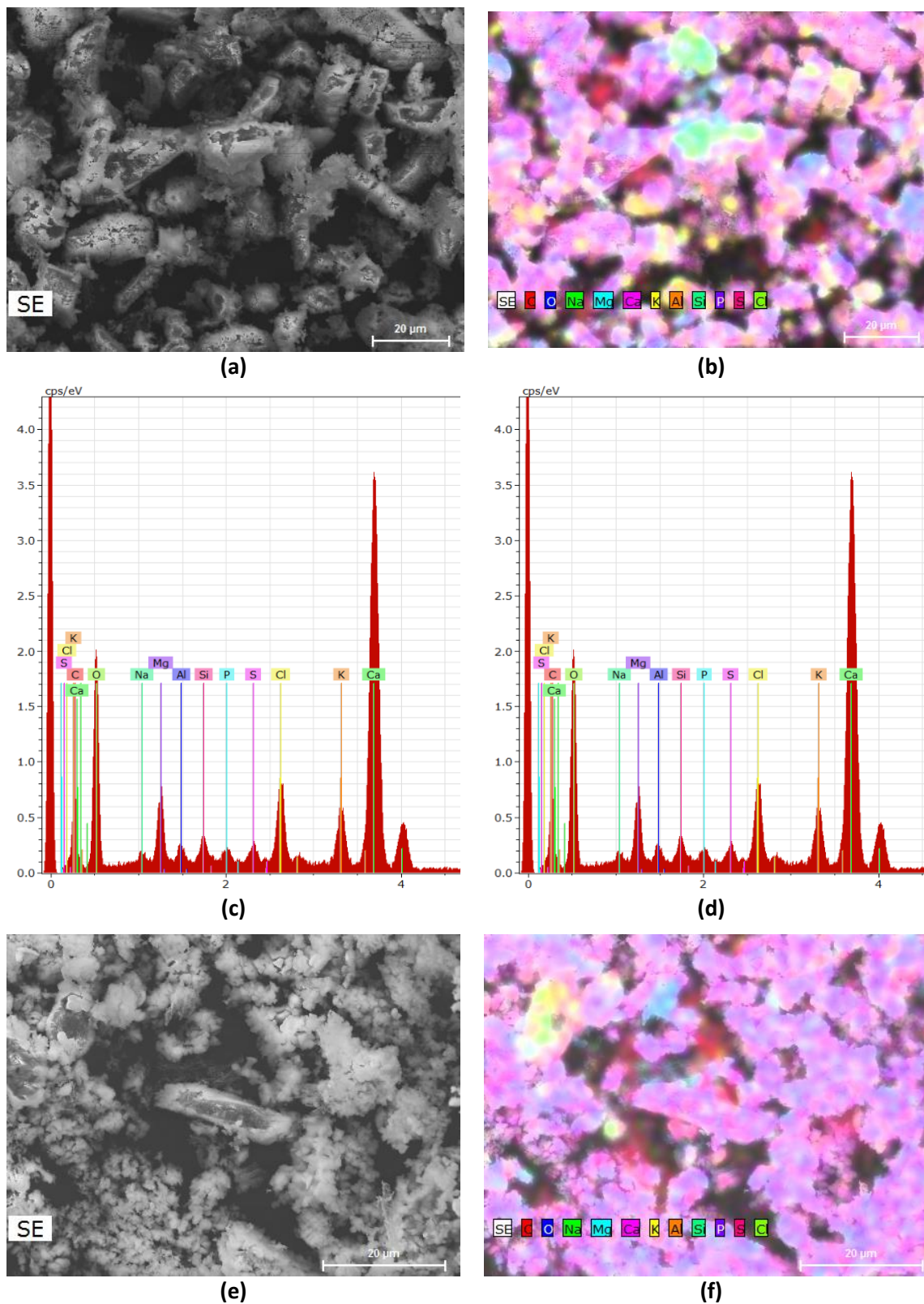
The sulfonation of CaO-SiO<sub>2</sub> catalyst enhances considerably the three textural properties: surface area, pore volume and pore diameter but decreases the acid strength ( $3.8 \leq pK_a < 4.7$  to  $6.8 \leq pK_a < 7.2$ ) and increases the basic strength ( $7.2 \leq pK_a < 9.3$  to  $9.3 \leq pK_a < 12.2$ ). The effect of sulfonation and calcination on these strengths could be due to the formation of new phases of basic character such as calcium sulfate and calcium silicate (Chen et al. 2015b).

In regard to the catalysts prepared from PET both have an acid character being CA-PET-S the strongest ( $3.8 \leq pK_a < 4.7$ ), and the basic strength was not detected in none. The acid character of this carbon catalyst may promote the esterification reaction of FFA but not the transesterification of triglycerides (Borges and Díaz 2012; Fadhil et al. 2016). The sulfonation treatment performed on the PET catalyst reduced its specific surface area (*ca* 44%) and pore volume (*ca* 37 %), which should be ascribed to the modification of a large number of –SO<sub>3</sub>H groups in the carbon framework.

In short, all catalysts prepared in this work could be classified as mesoporous catalysts since the pore diameters are within the intermediate range (20 – 500 Å) (Corma 1997), except for the carbonaceous catalysts (PET) which is microporous (< 20 Å). This feature may influence the catalysts' performance in the transesterification reaction since, as stated before, a typical triglyceride molecule has a diameter of around 58 Å. Hence, as larger are the porous the higher is the accessibility of those molecules to the inner pore structure network.

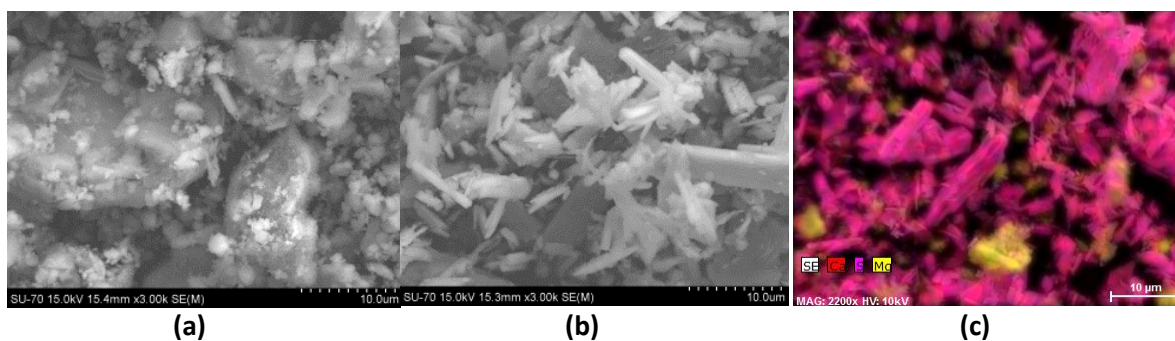
#### *2.3.2.2 SEM and EDX analyses*

The SEM images for characterizing the morphological characteristics and EDX for elemental analysis or chemical characterization of the catalysts were obtained. Figure 2.1 shows the morphological and the elemental composition of FAD and FAC catalysts. All particles of both ash catalysts have uniform distribution of agglomerates with irregular shapes, and the morphological sizes of the particles were reduced by the calcination treatment (Figure 2.1 a&e), possibly due to sintering processes, which decreases the surface area (Ho et al. 2014; Muthukumaran et al. 2015). The results of EDX show as predominant elements in these catalysts: Ca, Mg, Si, Al, O, K, S, Na, Cl and P. These elements remained on the solid surface after calcination, as shown in Figure 2.1 b&c and Figure 2.1 d&f for FAD and FAC, respectively.



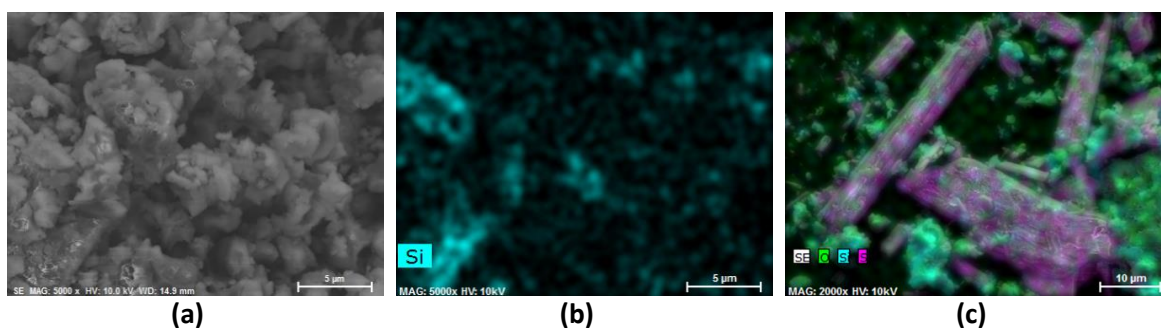
**Figure 2.1** - FAD catalyst: SEM (a) and EDX (b and c); FAC catalyst: SEM (e) and EDX (d and f).

Figure 2.2 displays the morphology of solid catalysts Dolomite C (Figure 2.2 a) and Dolomite CSC (Figure 2.2 b&c). The Dolomite C has a dense surface with heterogeneous distribution of particle sizes (i.e., irregular size) and smooth appearance, which should be derived from decarbonation process (calcination) of dolomite rock (Correia et al. 2015; Yoosuk et al. 2011). Sulfonation caused the elongation of the crystalline structures as fibers due to sulfur compounds formation, as depicted in Figure 2.2 b&c.



**Figure 2.2** - Dolomite C: SEM (a); Dolomite CSC: SEM (b) and EDX (c).

The catalyst prepared from eggshells  $\text{CaO-SiO}_2$  exhibits large and regular blocks particles (Figure 2.3 a). The same was observed in the  $\text{CaO-S-SiO}_2$  catalyst (image not shown) and one infers that this morphology could be owed to the coverage of Si compounds on the CaO surface (see Figure 2.3 b&c). More, the same effect was observed by Chen et al. (2015b). As in the dolomitic catalysts, the sulfonation of  $\text{CaO-SiO}_2$  solid also originated the formation of crystalline structures as flat elongated fibers (Figure 2.3 c) in this eggshells based material. This phenomenon was also observed by Embong et al. (2016).



**Figure 2.3** -  $\text{CaO-SiO}_2$ : SEM (a);  $\text{CaO-S-SiO}_2$ : EDX (b) and (c).

The images taken for catalysts prepared from PET are shown in Figure 2.4, where it can be seen irregular and flat surface with crevices.

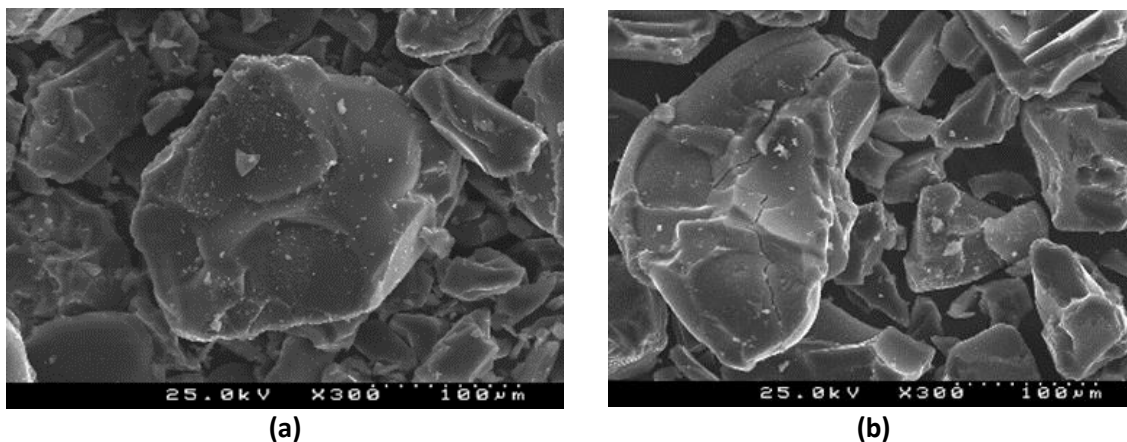


**Figure 2.4** - SEM images of CA-PET (a) and CA-PET-S (b) catalysts.

The sulfonation does not generate observable significant differences in the morphology of this material, since particles have similar shapes in both photos (a) and (b) of Figure 2.4. Similar behavior was observed in other studies (Dawodu et al. 2014; Fadhil et al. 2016; Hajamini et al. 2016).

### 2.3.2.3 XRD analyses

The XRD diffractograms of the fly ash catalysts are depicted in Figure 2.5 a. The structure and crystalline compounds of FAD and FAC are similar, being only their main differences the area and the intensity of the peaks after calcination. The XRD pattern for FAD catalyst shows clear diffraction peaks corresponding to calcium oxide (CaO) phase detected at  $2\theta=32.2^\circ$ ,  $37.4^\circ$ ,  $53.8^\circ$ ,  $65.2^\circ$ , and  $67.5^\circ$ , calcium carbonate ( $\text{CaCO}_3$ -major component) phase detected at  $2\theta=23.3^\circ$ ,  $29.6^\circ$ ,  $36.2^\circ$ ,  $39.7^\circ$ ,  $43.4^\circ$ ,  $47.8^\circ$ ,  $48.8^\circ$ ,  $56.9^\circ$ ,  $61.0^\circ$  and  $65.0^\circ$ , potassium chloride (KCl) phase detected at  $2\theta=28.5^\circ$ ,  $40.5^\circ$ , and silicon dioxide ( $\text{SiO}_2$ ) phase detected at  $2\theta=20.9^\circ$ ,  $26.7^\circ$ ,  $36.38^\circ$ ,  $39.46^\circ$ ,  $40.28^\circ$ ,  $50.2^\circ$ ,  $60.2^\circ$  and  $68.5^\circ$ , among other components. After the ash calcination, i.e. for FAC catalyst,  $\text{CaCO}_3$  was transformed into CaO (Chen et al. 2015a; Sharma

et al. 2012) and this is evident by the higher intensity of the corresponding peak. This latter is the major component in FAC followed by the silicon dioxide ( $\text{SiO}_2$ ).

Figure 2.5 b shows the XRD of Dolomite C and Dolomite CSC catalysts. The presence of both phases: CaO ( $2\theta=32.2^\circ$ ) and MgO ( $2\theta=42.7^\circ$ ) in the Dolomite C could promote the transesterification reaction.  $\text{Ca(OH)}_2$  ( $2\theta=34.1^\circ$ ) is part of the chemical composition of these catalysts, its formation occurs readily upon an exposure of CaO to humidity of ambient, resulting in a significant loss of the transesterification activity (Correia et al. 2015; Jaiyen et al. 2014). It seems that calcination time of dolomite rock was sufficient to decompose  $\text{MgCO}_3$  in to MgO, but not enough to convert completely the  $\text{CaCO}_3$  in to CaO, since  $\text{CaCO}_3$  is present ( $2\theta=29.3^\circ$ ) in this catalyst after that thermal treatment; similar result was observed by Ngamcharussrivichai et al. (2010). The sulfonation of Dolomite C originated new peaks in the diffractogram (of Dolomite CSC), corresponding to calcium sulfate ( $\text{CaSO}_4$ -major component) at  $2\theta=25.6^\circ$ ,  $31.3^\circ$ ,  $38.6^\circ$ ,  $40.9^\circ$ ,  $48.6^\circ$ ,  $52.2^\circ$ ,  $55.8^\circ$ , and  $65.0^\circ$ . As discussed previously, this treatment had also effects on the basic and acid strengths of the solid catalyst due to the replacement of calcium carbonate by calcium sulfate, which in turn could affect its catalytic activity.

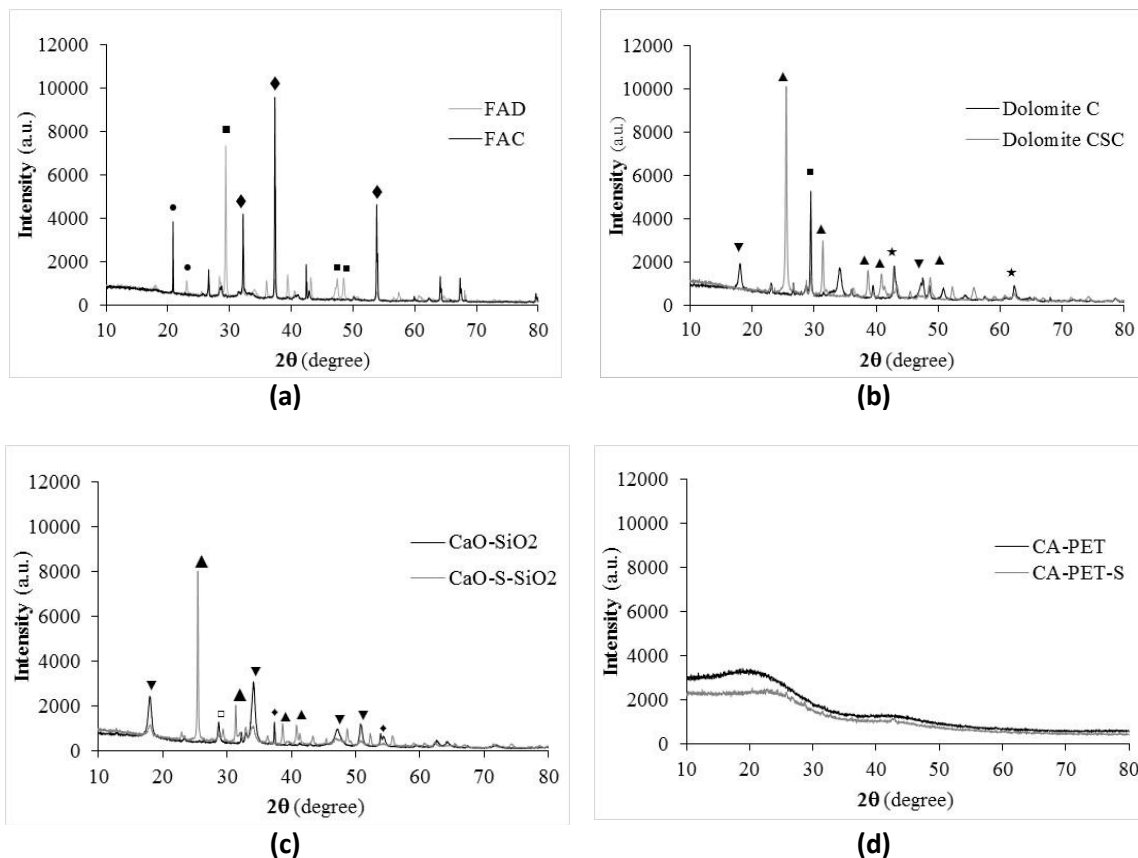


**Figure 2.5** - XRD patterns of catalysts: FAD and FAC (a), Dolomite C and Dolomite CSC (b), CaO-SiO<sub>2</sub> and CaO-S-SiO<sub>2</sub> (c), and CA-PET and CA-PET-S (d). (• SiO<sub>2</sub>, ■ CaCO<sub>3</sub>, ◆ CaO, ▲ CaSO<sub>4</sub>, ■ CaCO<sub>3</sub>, ▼ Ca(OH)<sub>2</sub>, ◆ CaO, □ Ca<sub>2</sub>SiO<sub>4</sub> and ★ MgO).

The XRD patterns of the catalysts produced from eggshells are shown in Figure 2.5 c. For CaO-SiO<sub>2</sub> catalyst the peaks at  $2\theta = 37.2^\circ$ ,  $64.2^\circ$ ,  $76.1^\circ$  and  $2\theta = 20.2^\circ$ ,  $33.4^\circ$ ,  $39.7^\circ$ ,  $55.3^\circ$ ,  $59.8^\circ$  correspond to CaO and Ca(OH)<sub>2</sub>, respectively. Besides, calcium silicate compounds (Ca<sub>2</sub>SiO<sub>4</sub>) peaks appear at  $2\theta = 23.3^\circ$ ,  $26.2^\circ$ ,  $28.0^\circ$ ,  $32.9^\circ$ ,  $35.1^\circ$ ,  $41.2^\circ$  due to the reaction of Na<sub>2</sub>SiO<sub>3</sub> with CaO and Ca(OH)<sub>2</sub> during the catalyst preparation process (Leite et al. 2017). For the CaO-S-SiO<sub>2</sub> catalyst new peaks have arose at  $2\theta = 25.6^\circ$ ,  $31.3^\circ$ ,  $48.6^\circ$  and at  $2\theta = 29.3^\circ$ , corresponding to CaSO<sub>4</sub> and CaCO<sub>3</sub>, respectively (Nur Syazwani et al. 2017). There are the three main compounds that can be identified in the CaO-SiO<sub>2</sub> catalyst, namely: CaO, Ca(OH)<sub>2</sub> and Ca<sub>2</sub>SiO<sub>4</sub>. The latter two are the most abundant, which means that part of the calcium existing in the eggshells has reacted with Na<sub>2</sub>SiO<sub>3</sub> to form calcium silicate (Leite et al. 2017). After CaO-SiO<sub>2</sub>



sulfonation, the hydroxides and silicates of calcium were mainly converted into  $\text{CaSO}_4$ , the predominant compound in this catalyst.

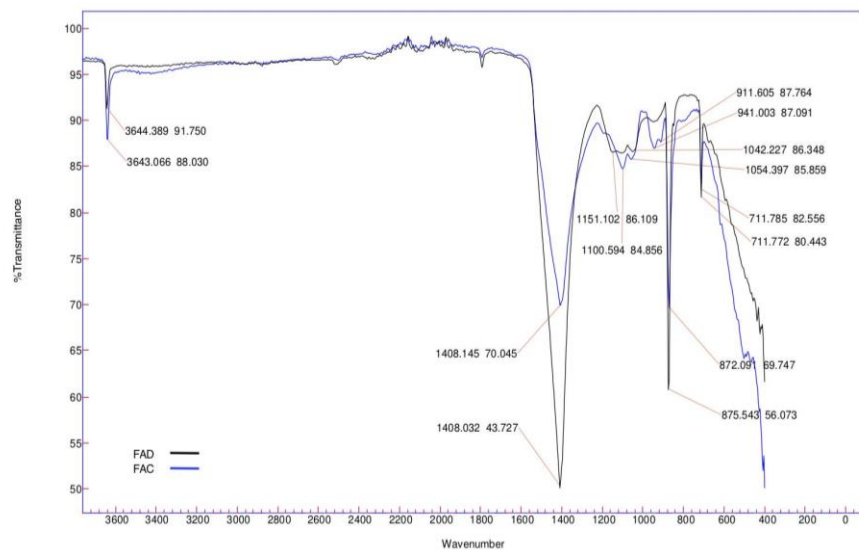
Finally, the XRD diffractograms of catalysts prepared from PET are depicted in Figure 2.5 d. Both diffractograms exhibit a broad diffraction peaks indicating an amorphous carbons, C(002) and C(101), which is composed of the oriented random fashion of carbon sheets. Therefore, both samples are composed of high non-graphitic carbon content. Fadhil et al. (2016) and Chang et al. (2015) observed that these kind of carbons have oriented random fashion sheets. In short, both catalysts prepared from PET have high content of non-graphitic carbon.

#### 2.3.2.4 FTIR analyses

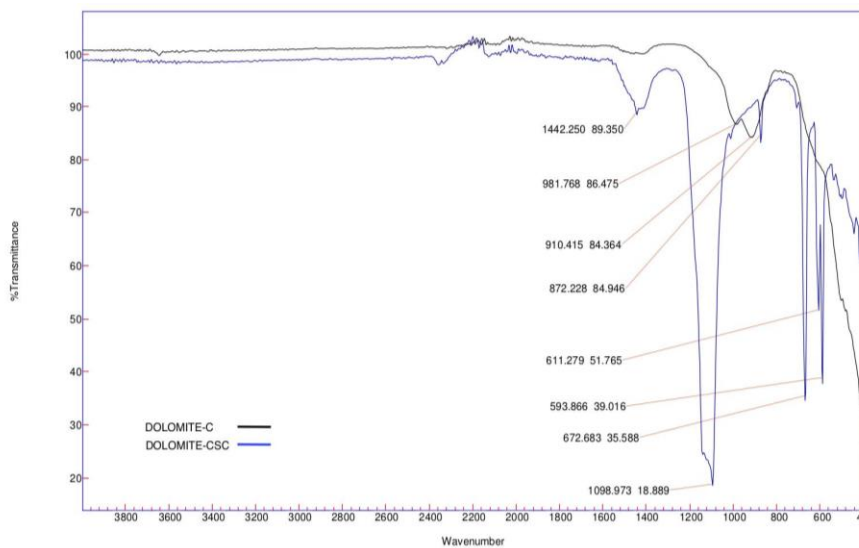
The FTIR spectra of all catalysts prepared in this work are shown in Figure 2.6. The FTIR spectrum of FAD (Figure 2.6 a) shows the major absorption broad band at  $1408.1\text{ cm}^{-1}$  and minor absorption bands at  $875.5$  and  $711.2\text{ cm}^{-1}$ , which correspond to the asymmetric stretching and to out-of-plane band and in-plane band vibration modes of carbonate ( $\text{CO}_3^{2-}$ ) group, respectively. This result confirms the presence of  $\text{CaCO}_3$  in FAD, detected by XRD.  $\text{PO}_4^{3-}$  and Si-O components (silica phosphates) show broad bands in the region between  $1100.5$  and  $911.6\text{ cm}^{-1}$ ; the same was observed by Maneerung et al. (2015) and Sharma et al. (2012) but using bottom ash waste arising from woody biomass gasification and wood ash from the *Acacia nilotica* (babul), respectively. Moreover, the absorption sharp band at  $3643\text{ cm}^{-1}$ , which is attributed to -OH band, was observed for both catalysts (calcined and uncalcined). This band is an evidence of water absorption on the CaO surface producing  $\text{Ca(OH)}_2$  (Boey et al. 2011).

The typical transmittance FTIR spectra of the Dolomite C and Dolomite CSC are shown in Figure 2.6 b. The bands at  $1442.2$  and  $1438\text{ cm}^{-1}$  can be assigned to the symmetric and asymmetric stretching vibrations of O-C-O bonds of unidentate carbonate at the surface of the calcium-magnesium oxide in both dolomitic catalysts (Algoufi et al. 2017). The band at  $872.2\text{ cm}^{-1}$  arises also from these carbonates groups. For the Dolomite CSC, the peaks at  $1098.9$ ,  $672.6$ ,  $611.2$

and  $593.8\text{ cm}^{-1}$  are attributed to the functional group  $\text{SO}_4^{2-}$  of calcium sulfate (major component) (Kong et al. 2012; Zhao et al. 2016).

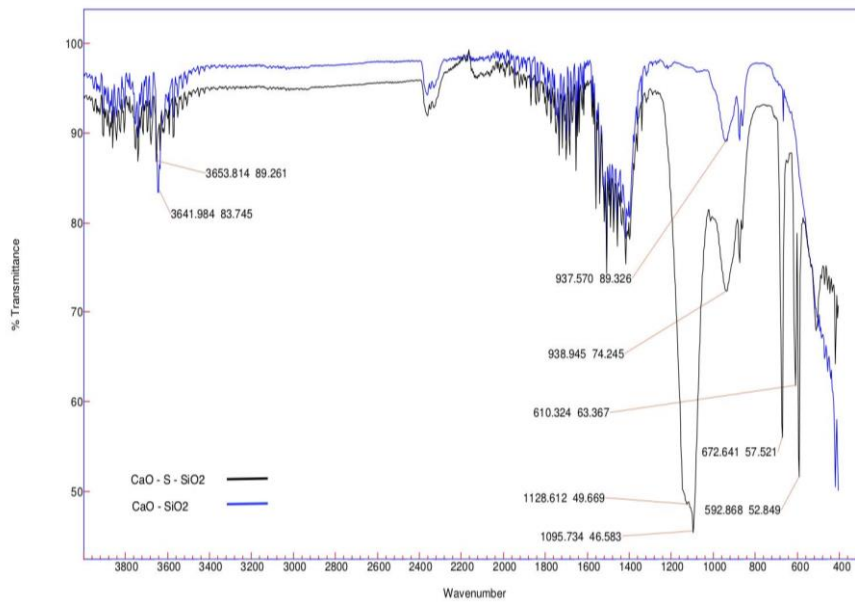


(a)

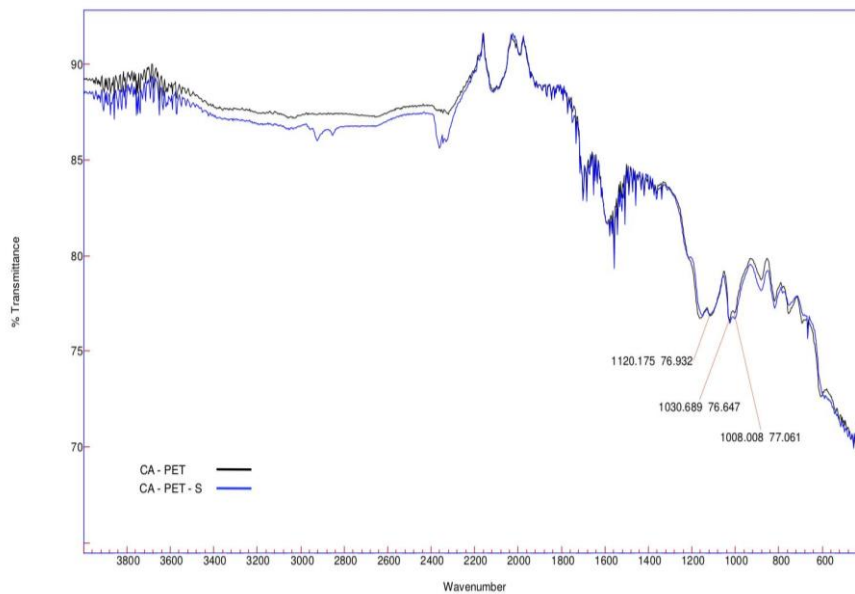


(b)

**Figure 2.6** - FTIR spectra of catalysts: FAD and FAC (a), Dolomite C and Dolomite CSC (b),  $\text{CaO-SiO}_2$  and  $\text{CaO-S-SiO}_2$  (c), and CA-PET and CA-PET-S (d).



(c)



(d)

**Figure 2.6 (cont.)**- FTIR spectra of catalysts: FAD and FAC (a), Dolomite C and Dolomite CSC (b), CaO-SiO<sub>2</sub> and CaO-S-SiO<sub>2</sub> (c), and CA-PET and CA-PET-S (d).

Regarding the FTIR spectra of CaO-SiO<sub>2</sub> and CaO-S-SiO<sub>2</sub> catalysts (Figure 2.6 c), one observes nearby absorption bands, such as at 3641.9 and 3653.8 cm<sup>-1</sup> that correspond to the stretching O-H due to physisorption of water on the solid surface. The spectra show matching bands namely at 937.5 and 938.9 cm<sup>-1</sup>, which belong to Si-O symmetric elongation vibrations and Si-O-Ca (Boro et al. 2011; Chen et al. 2015a). The absorption band at 1128.6 cm<sup>-1</sup> could be attributed to O-Si-O bond of silicate compounds (Amani et al. 2016). For CaO-S-SiO<sub>2</sub> catalyst, the bands at 1095.7, 672.6, 610.3 and 592.8 cm<sup>-1</sup> are attributed to the stretching vibrations of S=O on the group SO<sub>4</sub><sup>2-</sup> of calcium sulfate (Kong et al. 2012; Zhao et al. 2016).

Concerning the FTIR spectra of CA-PET and CA-PET-S catalysts (Figure 2.6 d), both are similar in respect to the position of their bands. The absorption bands observed at 1008, 1030 and 1120 cm<sup>-1</sup> are assigned to the symmetric stretching vibrations of S=O as result of inducing the SO<sub>3</sub>H group (Chang et al. 2015; Xing et al. 2007). These evidences indicate a successful incorporation of SO<sub>3</sub>H functional groups in the carbon framework.

#### 2.3.2.5 Catalysts performance

The performance of the catalysts prepared from waste materials was assessed through the esterification and transesterification reaction yields, in the conversion of RPO and WCO mixtures to FAME. The results are plotted in Figure 2.7 for FAME yield (Equation 2.4) and FFA conversion (Equation 2.5). As FAME are produced by both the esterification and the transesterification reaction, the FAME yield reflects the global conversion of these two reactions. However, in this work, the FFA content is low, so the contribution of the esterification reaction to the FAME yield will be much less than that of the transesterification reaction.

Regarding the results obtained in this work, as the WCO percentage in the reaction mixture increases two main conclusions are withdrawn by an overview of Figure 2.7, namely:

- A decrease of FAME yield for catalysts with moderate or high basic strength. This can be due to the neutralization of their basic catalyst sites, as stated by Kaur et al. (2011) and Kouzu et al. (2008);
- An increase (or maintenance, for FAD) of FFA conversion.

Thus, the presence of FFA in the reaction mixture favors their conversion to FAME but has a negative effect on transesterification reaction yield.

A more detailed analysis of each catalyst group shows that the fly ash catalysts (Figure 2.7 a&b) promoted the highest FAME yield for all oil blends tested. One of the best performances (of all catalysts) in FFA conversion is also related to one of these catalysts, the FAD, achieving values above 96 % for all mixtures. However, rising the WCO in the reaction mixture decreases the FAME yield in ca. 30 to 35 %, being the FAC performance the most affected.

Among the two ash based catalysts, the FAC is the one that has a worse performance in both FAME yield and FFA conversion. This evidence may be due to changes in surface morphology (sintering processes) and decrease of both crystalline phases and active functional groups on the surface for the calcined catalyst, as observed by XRD and FTIR. Additionally, the most abundant compound in FAD is  $\text{CaCO}_3$  and in FAC is  $\text{CaO}$ , which may be another reason for the observed differences in performance. However, as the amount of WCO in the blend increases these differences in performance of the catalyst decrease significantly.

Despite of the low acid strength of both catalysts ( $6.8 \leq \text{pKa} < 7.2$ ), the FAD roughly converts all FFA present in the initial reaction mixture and the FAC increases its performance as the WCO percentage rises, achieving ca. 86 % of conversion for 100 wt% of WCO (M5). Summing up, it is reasonable to conclude that these catalysts have a bifunctional character, especially the FAD which enables attaining FAME yield and FFA conversions around 95 % for WCO blends of 25 wt% (M2).

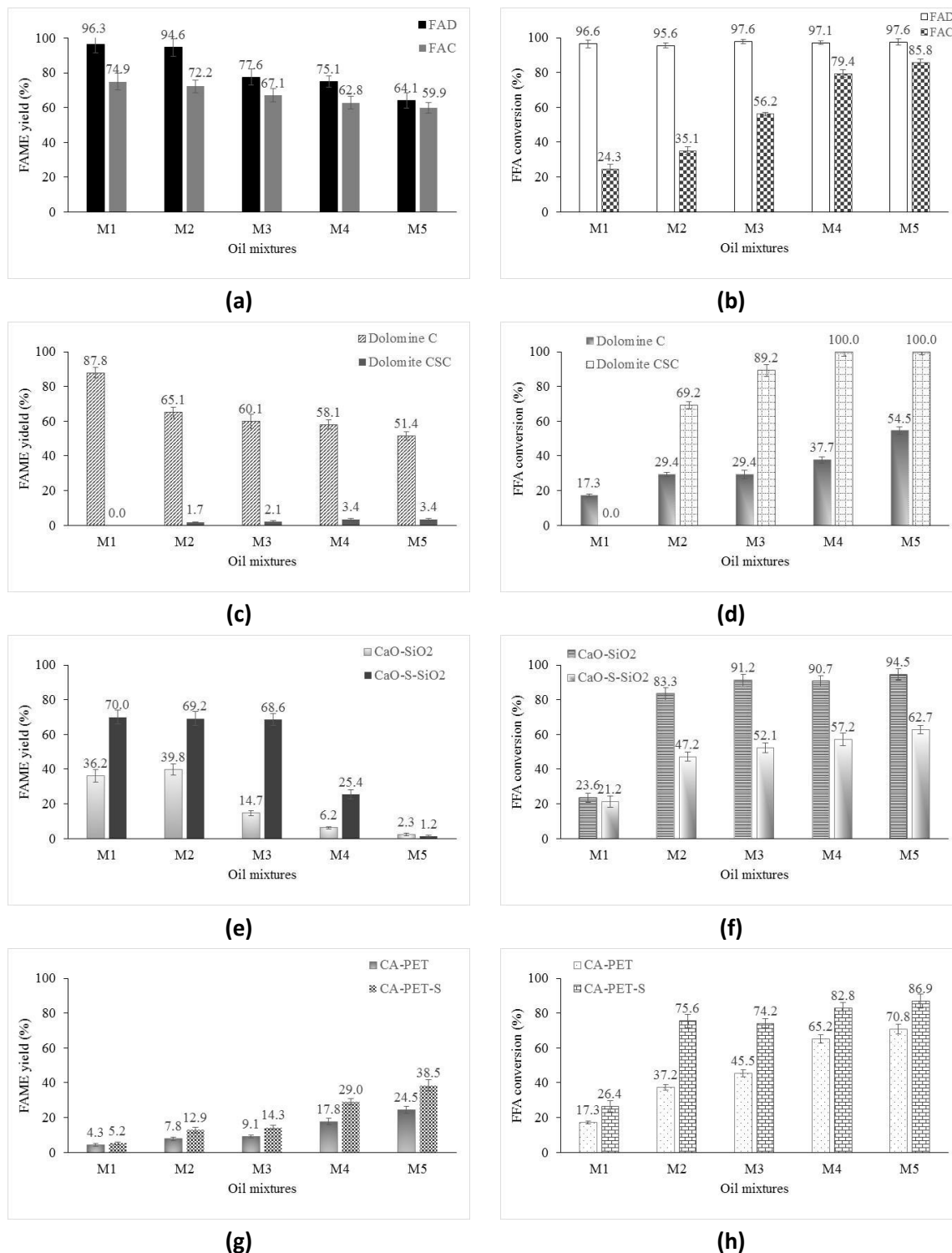


**Figure 2.7** - Performance in terms of FAME yield and FFA conversion of catalysts: FAD and FAC (a) and (b), Dolomite C and Dolomite CSC (c) and (d), CaO-SiO<sub>2</sub> and CaO-S-SiO<sub>2</sub> (e) and (f), and CA-PET and CA-PET-S (g) and (h), for several RPO:WCO mixtures.

The FAME yields and FFA conversions attained using Dolomite catalysts are summarized in the Figure 2.7 c and Figure 2.7 d, respectively. Dolomite C has the highest basic strength ( $12.2 \leq \text{pKa} < 15$ ), but this is not reflected in higher FAME yields. Furthermore, in comparison to ash catalysts, Dolomite C has higher surface area, pore volume and pore diameter, and all these features do not seem to be sufficient to give a better performance to this catalyst. Thus, chemical composition of the catalyst could have a stronger influence than those physical characteristics. The highest FAME yield achieved by this catalyst is ca. 88 % for M1, and decreases 37 % for the mixture with higher acid value (M5). With regard to FFA conversion, the values attained are consistent with the low acid strength exhibited by this catalyst, i.e., Dolomite C has a low acid strength and consequently is a weak catalyst of esterification reaction, so the FFA conversion values reached are one of the lowest registered (for each oil mixture).

The sulfonation and subsequent calcination of Dolomite C, giving rise to Dolomite CSC, has strongly affected its ability to catalyze the transesterification reaction, nearly annulling it. This could be due to the decrease of basic strength (by neutralization) and/or to the decrease of pore diameter, which in turn increases the diffusion limitations for long alkyl chain molecules (e.g., triglycerides). However, this treatment has improved the performance of this material for catalyzing the esterification reaction, reaching conversions of 100 % for oil mixtures with the highest acid values (M4 and M5) tested in this work. The moderate acid character of this catalyst ( $6.1 \leq \text{pKa} < 6.8$ ) and the functional groups on its surface (group  $\text{SO}_4^{2-}$ ) could be the driving force of its performance in converting FFA to FAME.

The data concerning the performance of eggshell catalysts ( $\text{CaO-SiO}_2$  and  $\text{CaO-S-SiO}_2$ ) are plotted in the Figure 2.7 e&f. The FAME yield are negatively affected by the initial acid value of the oil mixtures, achieving the lowest values (of all catalysts) for M5. The highest yield levels reached was 70 % for M1 in  $\text{CaO-S-SiO}_2$  catalyst and 40 % for M2 in  $\text{CaO-SiO}_2$ ; similar results were obtained by Chen et al. (2015b). The sulfonation and calcination of  $\text{Ca-SiO}_2$  material increases the FAME yield, possibly due to the formation of new active phases such as calcium

sulfate ( $\text{CaSO}_4$ ) and calcium carbonate formed from calcium hydroxide ( $\text{Ca}(\text{OH})_2$ ) and calcium silicate ( $\text{Ca}_2\text{SiO}_4$ ), as shown in the Figure 2.5 c, which have low activity towards the transesterification reaction. Relating to the performance of eggshells based catalysts to converting the FFA to FAME, one can say that as WCO percentage in the oil mixture increases the higher is the conversion, being the Ca-SiO<sub>2</sub> catalyst the best one. This finding is in agreement with the acid strength of that catalyst (Ca-SiO<sub>2</sub>), which is one of the highest ( $3.8 \leq \text{pKa} < 4.7$ ) observed in this work.

Compared to the several catalysts discussed above, those produced from PET exhibit an inverse trend over the FAME yield (Figure 2.7 g). It was registered an increase of yield as the amount of FFA in the oil mixtures rises, but the higher values attained were low, i.e., ca. 25 % and 39 % for M5 in CA-PET and CA-PET-S, respectively. This result can be explained considering the lack of basic strength in these catalysts (see Table 2.3). In fact, PET catalysts only have an acid character, being CA-PET-S the catalyst with the most acidic character produced in this work ( $3.8 \leq \text{pKa} < 4.7$ ). Though, they do not have the best performance in the esterification reaction catalysis. In Figure 2.7 h one observes that the FFA conversions increases as the acid value of oil mixture rises, achieving the maximum values of ca. 71 % and 87 % for M5 in CA-PET and CA-PET-S, respectively. Thus, although these catalysts have the largest specific surface area, the largest pore volume and one of the highest acidic strengths, this does not seem to be enough to make them the best catalysts for the esterification reaction. A plausible reason for this may lie in the fact that they have the smallest pore size observed among the catalyst developed in this work. In addition, among the two PET catalysts, CA-PET-S is the one that has a better performance in the catalysis of both esterification and transesterification reactions.



## 2.4 Conclusions

In the present study, efficient heterogeneous catalysts were successfully prepared from solid waste materials for biodiesel production by transesterification and esterification, using mixtures of refined palm oil and waste cooking oil in different ratios and methanol. The results demonstrate that all the catalysts evaluated have different catalytic performances. The better catalyst for catalyzing simultaneous both transesterification and esterification reactions, i.e., having a bifunctional character, was biomass fly ash dried (FAD), achieving yields and conversions above 95 % for a blend of up to 25 wt% of WCO.

The catalyst produced from dolomite rock did not have a strong bifunctional character. They showed good performances in catalyzing the transesterification and esterification reactions, but not simultaneously. Indeed, the sulfonation of Dolomite C was aimed at increasing its acidic strength so as to give it the potential to catalyze the esterification reaction. However, that treatment strongly affected that ability, practically canceling it. In further procedures, the sulfonation stage should be more lenient.

The sulfonation of material prepared from eggshells improved its ability for catalyzing the transesterification reaction, however the maximum values attained do not exceed 70 % of yields. On the other hand, this treatment worsened the performance of this catalyst in FFA conversion.

Regarding the catalysts produced from PET, the results showed that they are good candidates for catalyzing the esterification reaction of high acid value feedstocks.

In short, none of the catalysts produced in this work has both high basic and acidic strengths and the only one that has these two strengths balanced (on a moderate level) is the Dolomite CSC. However, the catalyst that exhibited a bifunctional character was undoubtedly FAD, which means this material can be directly and immediately used from the electrostatic precipitator

equipment located at the biomass thermal power-plant, as its moisture content is very low, with subsequent economic benefits.

By the exploitation of residual feedstocks (e.g., WCO) and the use of waste based catalysts, this work gives a contribution to make the biodiesel production a low cost, affordable and sustainable process, and simultaneously minimizing the environmental burdens traditionally inherent to the management of those wastes. Therefore, an awareness should be created so that any material that is deemed to be waste could be exploited for usage in this or other applications, thereby implementing the principles of circular economy.

### **Acknowledgments**

Edgar M. Vargas S. express his sincere gratitude to the Jorge Tadeo Lozano University of Colombia (Direction of Investigation, Creation and Extension) for the financial assistance of this work. The authors thanks for the financial support to CESAM (UID/AMB/50017 - POCI-01-0145-FEDER-007638), funded by national funds (FCT/MCTES) through PIDDAC and co-funded by the FEDER, within the PT2020 Partnership Agreement and Compete 2020.

## References

- AENOR-EN 14103. 2011. *Productos Derivados de Aceites y Grasas. Ésteres Metílicos de Ácidos Grasos (FAME). Determinación de Los Contenidos de Éster y de Éster Metílico Del Ácido Linolénico*. España. [www.agilent.com/chem](http://www.agilent.com/chem). (February 15, 2019).
- Algoufi, Y. T., G. Kabir, and B. H. Hameed. 2017. "Synthesis of Glycerol Carbonate from Biodiesel By-Product Glycerol over Calcined Dolomite." *Journal of the Taiwan Institute of Chemical Engineers* 70: 179–87. <http://dx.doi.org/10.1016/j.jtice.2016.10.039>.
- Amani, H., M. Asif, and B. H. Hameed. 2016. "Transesterification of Waste Cooking Palm Oil and Palm Oil to Fatty Acid Methyl Ester Using Cesium-Modified Silica Catalyst." *Journal of the Taiwan Institute of Chemical Engineers* 58: 226–34.
- ASTM. 2010. "Standard Test Method for Kinematic Viscosity of Transparent and Opaque Liquids (and Calculation of Dynamic Viscosity)." *Annual Book of ASTM Standards*: 1–10.
- Avhad, M. R., and J. M. Marchetti. 2015. "A Review on Recent Advancement in Catalytic Materials for Biodiesel Production." *Renewable and Sustainable Energy Reviews* 50: 696–718. <http://dx.doi.org/10.1016/j.rser.2015.05.038>.
- Boey, Peng-Lim, Gaanty Pragas Maniam, and Shafida Abd Hamid. 2009. "Biodiesel Production via Transesterification of Palm Olein Using Waste Mud Crab (*Scylla Serrata*) Shell as a Heterogeneous Catalyst." *Bioresource technology* 100(24): 6362–68. <http://www.ncbi.nlm.nih.gov/pubmed/19666218> (May 5, 2015).
- Boey, Peng Lim et al. 2011. "Utilization of BA (Boiler Ash) as Catalyst for Transesterification of Palm Olein." *Energy* 36(10): 5791–96. <http://dx.doi.org/10.1016/j.energy.2011.09.005>.
- Borges, M.E., and L. Díaz. 2012. "Recent Developments on Heterogeneous Catalysts for Biodiesel Production by Oil Esterification and Transesterification Reactions: A Review." *Renewable and Sustainable Energy Reviews* 16(5): 2839–49. <http://linkinghub.elsevier.com/retrieve/pii/S1364032112000834> (July 11, 2014).
- Boro, Jutika, Ashim J. Thakur, and Dhanapati Deka. 2011. "Solid Oxide Derived from Waste Shells of *Turbonilla Striatula* as a Renewable Catalyst for Biodiesel Production." *Fuel Processing Technology* 92(10): 2061–67. <http://dx.doi.org/10.1016/j.fuproc.2011.06.008>.
- Chang, Binbin et al. 2015. "Synthesis of Sulfonated Porous Carbon Nanospheres Solid Acid by a Facile Chemical Activation Route." *Journal of Solid State Chemistry* 221: 384–90. <http://dx.doi.org/10.1016/j.jssc.2014.10.029>.

- Chen, Guan Yi, Rui Shan, Jia Fu Shi, and Bei Bei Yan. 2015a. "Transesterification of Palm Oil to Biodiesel Using Rice Husk Ash-Based Catalysts." *Fuel Processing Technology* 133: 8–13. <http://dx.doi.org/10.1016/j.fuproc.2015.01.005>.
- Chen, Guanyi, Rui Shan, Shangyao Li, and Jiafu Shi. 2015b. "A Biomimetic Silicification Approach to Synthesize CaO-SiO<sub>2</sub> Catalyst for the Transesterification of Palm Oil into Biodiesel." *Fuel* 153: 48–55. <http://dx.doi.org/10.1016/j.fuel.2015.02.109>.
- Chen, Jein Wen et al. 2012. "Carcinogenic Potencies of Polycyclic Aromatic Hydrocarbons for Back-Door Neighbors of Restaurants with Cooking Emissions." *Science of the Total Environment* 417–418: 68–75. <http://dx.doi.org/10.1016/j.scitotenv.2011.12.012>.
- Corma, Avelino. 1997. "From Microporous to Mesoporous Molecular Sieve Materials and Their Use in Catalysis." *Chemical Reviews* 97(6): 2373–2420. <http://pubs.acs.org/doi/abs/10.1021/cr960406n>.
- Correia, Leandro Marques et al. 2015. "Characterization and Application of Dolomite as Catalytic Precursor for Canola and Sunflower Oils for Biodiesel Production." *Chemical Engineering Journal* 269: 35–43. <http://dx.doi.org/10.1016/j.cej.2015.01.097>.
- Dawodu, Folasegun A. et al. 2014. "Effective Conversion of Non-Edible Oil with High Free Fatty Acid into Biodiesel by Sulphonated Carbon Catalyst." *Applied Energy* 114: 819–26. <http://dx.doi.org/10.1016/j.apenergy.2013.10.004>.
- Demirbas, Ayhan. 2009. "Biodiesel from Waste Cooking Oil via Base-Catalytic and Supercritical Methanol Transesterification." *Energy Conversion and Management* 50(4): 923–27. <http://dx.doi.org/10.1016/j.enconman.2008.12.023>.
- Embong, Nurul Hajar et al. 2016. "Utilization of Palm Fatty Acid Distillate in Methyl Esters Preparation Using so 42-/TiO<sub>2</sub>-SiO<sub>2</sub> as a Solid Acid Catalyst." *Journal of Cleaner Production* 116: 244–48. <http://dx.doi.org/10.1016/j.jclepro.2015.12.108>.
- Fadhil, Abdelrahman B., Akram M. Aziz, and Marwa H. Al-Tamer. 2016. "Biodiesel Production from Silybum Marianum L. Seed Oil with High FFA Content Using Sulfonated Carbon Catalyst for Esterification and Base Catalyst for Transesterification." *Energy Conversion and Management* 108: 255–65.
- Farooq, Muhammad, Anita Ramli, and Abdul Naeem. 2015. "Biodiesel Production from Low FFA Waste Cooking Oil Using Heterogeneous Catalyst Derived from Chicken Bones." *Renewable Energy* 76: 362–68. <http://linkinghub.elsevier.com/retrieve/pii/S0960148114007575> (February 6, 2015).

- Farooq, Muhammad, Anita Ramli, and Duvvuri Subbarao. 2013. "Biodiesel Production from Waste Cooking Oil Using Bifunctional Heterogeneous Solid Catalysts." *Journal of Cleaner Production* 59: 131–40. <http://linkinghub.elsevier.com/retrieve/pii/S095965261300396X> (May 14, 2015).
- Hajamini, Zahra, Mohammad Amin Sobati, Shahrokh Shahhosseini, and Barat Ghobadian. 2016. "Waste Fish Oil (WFO) Esterification Catalyzed by Sulfonated Activated Carbon under Ultrasound Irradiation." *Applied Thermal Engineering* 94: 1–10. <http://dx.doi.org/10.1016/j.applthermaleng.2015.10.101>.
- Ho, Wilson Wei Sheng, Hoon Kiat Ng, Suyin Gan, and Sang Huey Tan. 2014. "Evaluation of Palm Oil Mill Fly Ash Supported Calcium Oxide as a Heterogeneous Base Catalyst in Biodiesel Synthesis from Crude Palm Oil." *Energy Conversion and Management* 88: 1167–78. <http://linkinghub.elsevier.com/retrieve/pii/S0196890414002623> (March 7, 2015).
- ICONTEC. 2011. NTC 218. Grasas y Aceites Vegetales y Animales. Determinación Del Índice de Acidez y de La Acidez. Colombia. <https://tienda.icontec.org/wp-content/uploads/pdfs/NTC218.pdf>.
- ICONTEC. 1999. NTC 218. "Grasas Y Aceites Vegetales Y Animales. Determinacion de Índice de Acidez." (571). Colombia. <https://tienda.icontec.org/wp-content/uploads/pdfs/NTC218.pdf>.
- Jacobson, Kathlene, Rajesh Gopinath, Lekha Charan Meher, and Ajay Kumar Dalai. 2008. "Solid Acid Catalyzed Biodiesel Production from Waste Cooking Oil." *Applied Catalysis B: Environmental* 85(1–2): 86–91.
- Jaiyen, Siyada, Thikumporn Naree, and Chawalit Ngamcharussrivichai. 2014. "Comparative Study of Natural Dolomitic Rock and Waste Mixed Seashells as Heterogeneous Catalysts for the Methanolysis of Palm Oil to Biodiesel." *Renewable Energy* 74: 433–40. <http://dx.doi.org/10.1016/j.renene.2014.08.050>.
- Kansedo, Jibrail, Keat Teong Lee, and Subhash Bhatia. 2009. "Cerbera Odollam (Sea Mango) Oil as a Promising Non-Edible Feedstock for Biodiesel Production." *Fuel* 88(6): 1148–50. <http://dx.doi.org/10.1016/j.fuel.2008.12.004>.
- Kaur, Mandeep, and Amjad Ali. 2011. "Lithium Ion Impregnated Calcium Oxide as Nano Catalyst for the Biodiesel Production from Karanja and Jatropha Oils." *Renewable Energy* 36(11): 2866–71. <http://dx.doi.org/10.1016/j.renene.2011.04.014>.

- Kong, Bao et al. 2012. "Synthesis of  $\alpha$ -Calcium Sulfate Hemihydrate Submicron-Rods in Water/n-Hexanol/CTAB Reverse Microemulsion." *Colloids and Surfaces A: Physicochemical and Engineering Aspects* 409: 88–93.  
<http://dx.doi.org/10.1016/j.colsurfa.2012.05.041>.
- Kouzu, Masato et al. 2008. "Calcium Oxide as a Solid Base Catalyst for Transesterification of Soybean Oil and Its Application to Biodiesel Production." *Fuel* 87(12): 2798–2806.
- Lam, Man Kee, and Keat Teong Lee. 2010. "Accelerating Transesterification Reaction with Biodiesel as Co-Solvent: A Case Study for Solid Acid Sulfated Tin Oxide Catalyst." *Fuel* 89(12): 3866–70. <http://dx.doi.org/10.1016/j.fuel.2010.07.005>.
- Lam, Man Kee, Keat Teong Lee, and Abdul Rahman Mohamed. 2009. "Sulfated Tin Oxide as Solid Superacid Catalyst for Transesterification of Waste Cooking Oil: An Optimization Study." *Applied Catalysis B: Environmental* 93(1–2): 134–39.
- Leite, F. H G, T. F. Almeida, R. T. Faria, and J. N F Holanda. 2017. "Synthesis and Characterization of Calcium Silicate Insulating Material Using Avian Eggshell Waste." *Ceramics International* 43(5): 4674–79.  
<http://dx.doi.org/10.1016/j.ceramint.2016.12.146>.
- Leung, Dennis Y C, Xuan Wu, and M. K H Leung. 2010. "A Review on Biodiesel Production Using Catalyzed Transesterification." *Applied Energy* 87(4): 1083–95.  
<http://linkinghub.elsevier.com/retrieve/pii/S0306261909004346> (July 10, 2014).
- Maneerung, Thawatchai, Sibudjing Kawi, and Chi Hwa Wang. 2015. "Biomass Gasification Bottom Ash as a Source of CaO Catalyst for Biodiesel Production via Transesterification of Palm Oil." *Energy Conversion and Management* 92: 234–43.  
<http://dx.doi.org/10.1016/j.enconman.2014.12.057>.
- Mansir, Nasar et al. 2018. "Modified Waste Egg Shell Derived Bifunctional Catalyst for Biodiesel Production from High FFA Waste Cooking Oil. A Review." *Renewable and Sustainable Energy Reviews* 82(May 2017): 3645–55.
- Muthukumar, N. et al. 2015. "Synthesis of Cracked Calophyllum Inophyllum Oil Using Fly Ash Catalyst for Diesel Engine Application." *Fuel* 155: 68–76.  
<http://dx.doi.org/10.1016/j.fuel.2015.04.014>.
- Ngamcharussrivichai, Chawalit, Pramwit Nunthasanti, Sithikorn Tanachai, and Kunchana Bunyakiat. 2010. "Biodiesel Production through Transesterification over Natural Calciums." *Fuel Processing Technology* 91(11): 1409–15.  
<http://dx.doi.org/10.1016/j.fuproc.2010.05.014>.

- Nur Syazwani, O. et al. 2017. "Esterification of High Free Fatty Acids in Supercritical Methanol Using Sulfated Angel Wing Shells as Catalyst." *Journal of Supercritical Fluids* 124: 1–9. <http://dx.doi.org/10.1016/j.supflu.2017.01.002>.
- Nurfitri, Irma et al. 2013. "Potential of Feedstock and Catalysts from Waste in Biodiesel Preparation: A Review." *Energy Conversion and Management* 74: 395–402. <http://linkinghub.elsevier.com/retrieve/pii/S0196890413002586> (March 13, 2015).
- Sharma, Meeta, Arif Ali Khan, S. K. Puri, and D. K. Tuli. 2012. "Wood Ash as a Potential Heterogeneous Catalyst for Biodiesel Synthesis." *Biomass and Bioenergy* 41: 94–106. <http://dx.doi.org/10.1016/j.biombioe.2012.02.017>.
- Singh, S. P., and Dipti Singh. 2010. "Biodiesel Production through the Use of Different Sources and Characterization of Oils and Their Esters as the Substitute of Diesel: A Review." *Renewable and Sustainable Energy Reviews* 14(1): 200–216.
- Uprety, Bijaya K., Wittavat Chaiwong, Chinomnso Ewelike, and Sudip K. Rakshit. 2016. "Biodiesel Production Using Heterogeneous Catalysts Including Wood Ash and the Importance of Enhancing Byproduct Glycerol Purity." *Energy Conversion and Management* 115: 191–99. <http://dx.doi.org/10.1016/j.enconman.2016.02.032>.
- Wan Omar, Wan Nor Nadyaini, and Nor Aishah Saidina Amin. 2011a. "Biodiesel Production from Waste Cooking Oil over Alkaline Modified Zirconia Catalyst." *Fuel Processing Technology* 92(12): 2397–2405. <http://linkinghub.elsevier.com/retrieve/pii/S0378382011003031> (January 2, 2015).
- Wan Omar, Wan Nor Nadyaini, and Nor Aishah Saidina Amin. 2011b. "Optimization of Heterogeneous Biodiesel Production from Waste Cooking Palm Oil via Response Surface Methodology." *Biomass and Bioenergy* 35(3): 1329–38. <http://linkinghub.elsevier.com/retrieve/pii/S0961953410005076> (May 29, 2015).
- Xing, Rong et al. 2007. "Active Solid Acid Catalysts Prepared by Sulfonation of Carbonization-Controlled Mesoporous Carbon Materials." *Microporous and Mesoporous Materials* 105(1–2): 41–48.
- Yoosuk, Boonyawan, Parncheewa Udomsap, and Buppa Puttasawat. 2011. "Hydration–Dehydration Technique for Property and Activity Improvement of Calcined Natural Dolomite in Heterogeneous Biodiesel Production: Structural Transformation Aspect." *Applied Catalysis A: General* 395(1–2): 87–94. <http://linkinghub.elsevier.com/retrieve/pii/S0926860X11000421> (May 29, 2015).
- Zhao, Yuzeng et al. 2016. "Inhibition of Calcium Sulfate Scale by Poly (Citric Acid)." *Desalination* 392: 1–7. <http://dx.doi.org/10.1016/j.desal.2016.04.010>.





---

## SECTION C - Optimization of FAME production in batch mode operation

Section C presents the optimization study of the FAME production process (in batch mode) with methanol, using mixtures of WCO and RPO and biomass fly ash as a catalyst (chosen in section B). The Box–Behnken experimental design and the Response Surface Methodology were used in the optimization, and four operating variables were tested, namely: catalyst loading, methanol/oil molar ratio, RPO/WCO mass ratio and reaction temperature. Furthermore, the catalyst was characterized by SEM, EDX, XRD, BET, FT-IR and Hammett indicators. Additionally, it was carried out a study of reusability of the catalyst aiming to assess its performance over several cycles of utilization in the FAME synthesis process. The optimal operating conditions found by the regression model were used in this set of assays and the catalyst was characterized after each reuse by XRD, BET and Hammett indicators.

The information presented in this section was adapted from the following published article:

- E. M. Vargas, J. L. Ospina, M. C. Neves, L. A. C. Tarelho, and M. I. Nunes, “Optimization of FAME production from blends of waste cooking oil and refined palm oil using biomass fly ash as a catalyst” *Renew. Energy*, vol. 163, pp. 1637-1647, 2020, doi: 10.1016/j.renene.2020.10.030.
- E. M. Vargas, J. L. Ospina, L. A. C. Tarelho, and M. I. Nunes, “FAME production from residual materials: Optimization of the process by Box–Behnken model,” *Energy Reports*, vol. 6, pp. 347–352, 2019, doi: 10.1016/j.egy.2019.08.071.



### **3 Optimization of FAME production from blends of waste cooking oil and refined palm oil using biomass fly ash as a catalyst**

**Abstract:** One of the problems associated with biomass combustion is the amount of fly ashes generated and its subsequent management. The search for ways of valorizing these ashes has been a challenge for the academic and industrial community. On the other hand, used cooking oils are wastes which management is quite difficult, by they have a very important energetic potential. The goal of this work was to optimize the Fatty Acid Methyl Esters (FAME) process, recovering two residual materials (waste cooking oils (WCO), and biomass fly flash (FAD)). The optimization of the process was achieved using the response surface methodology and a Box-Benhken experimental design applied to mixtures of WCO and refined palm oil (RPO), using FAD as catalyst. The influence on FAME yield of four variables (catalyst loading, methanol/oil molar ratio, RPO/WCO ratio and reaction temperature) was studied. The higher FAME yield achieved was 73.8 % for the following operating conditions: 13.57 wt% of catalyst loading, 6.7 of methanol/oil molar ratio, 28.04 wt% of RPO in the oil mixture with WCO and 55 °C for the reaction temperature. The reusability of the FAD catalyst in the process was also studied through three successive usage cycles finding no loss of catalytic activity.

**Keywords:** Biomass fly ash; FAME; optimization; refined palm oil; response surface methodology; waste cooking oil.

### 3.1 Introduction

The production of biodiesel has become a very important area of research due to the rapid depletion of energy reserves and the increase in oil prices along with environmental concerns (Liu et al. 2014). In the current situation, the foremost amount of energy is supplied by the conventional fossil fuel resources, such as gasoline, liquefied petroleum gas, diesel fuel, coal and natural gas. It is imperative to find alternative fuels to the petroleum based ones in order to, along with environmental issues, prolong the petroleum supply. One of the most promising biofuel is biodiesel, a “green fuel” alternative to diesel fuel, derived from renewable sources with high quality (Leung et al. 2010). The integration of wastes as a catalyst or as an (vegetable) oil feedstock into the biodiesel production process can be a promising way to reduce environmental burdens and the production costs, while also aligning with the principles of circular economy.

Globally, the cost of production has been the main barrier in commercializing biodiesel. In the literature, it is consensual that the oily feedstock is the major contributor, about 80 % (Mansir et al. 2018), for the total production costs. The waste cooking oils (WCO) are edible vegetable oils that have been previously used for frying or cooking and can constitute an additional source of raw material for biodiesel production. This feedstock can be two to three times cheaper than virgin vegetable oils (Demirbas 2009; Nurfitri et al. 2013). Furthermore, it is generally accepted that reusing WCO for human consumption is harmful to health and this waste is difficult to manage (Chen et al. 2012).

It is important to mention that the catalyst commonly used in the biodiesel production is the sodium or potassium hydroxide, which have been economically unfeasible to recover from the process. Aiming to tackle this hotspot of the process, some research (Boey et al. 2009; Chakraborty et al. 2010; Mendonça et al. 2019) have been focused on the exploitation of waste materials (e.g. shells, ashes, peels and bones), due to their abundance and low cost, for solid catalysts preparation. On the other hand, biomass fly ashes (FAD) are a residual materials whose disposal and management represent a significant challenge (Kotwal et al. 2009), given

its increasing production over the last two decades (Girón et al. 2015). The development of alternative solutions for FAD proper utilization/valorization with emphasis on finding new applications is currently a very important issue (Chatterjee et al. 2018). The use of FAD, as a (heterogeneous) catalyst, on the biodiesel production process has been proving to be a promising alternative to valorize this waste; it has been found that FAD have a potential for catalyzing the reactions for FAME (Fatty Acid Methyl Esters) production and have bifunctional characteristics (acid and basic) that allow catalyzing transesterification and esterification reactions simultaneously (Vargas et al. 2019).

The main objective of this work was to optimize the FAME production process using mixtures of WCO and refined palm oil, and FAD as catalyst. The effect on FAME yield of four operating variables was tested, namely: catalyst loading, methanol/oil molar ratio, RPO/WCO mass ratio and reaction temperature. Additionally, it was carried out a study of reusability of the catalyst aiming to assess its performance over several cycles of utilization in the FAME synthesis process.

### **3.2 Materials and Methods**

The Box-Benhken experimental design and Response Surface Methodology (RSM) were used to design the experiments to optimize the FAME production process and for the data treatment.

Previously, the solid catalyst (FAD) was prepared and characterized in terms of some of its chemical, physical and structural properties. The raw-material for FAME synthesis consisted of a blends of WCO and RPO in different ratios. The adopted procedures are described in the next sections as well as the analytical methods used.

### 3.2.1 Materials

Waste cooking oil for FAME production was provided by a local collecting company (Bioils) in Bogotá, Colombia. The WCO was pre-treated by filtration to remove suspended particles and heating (at 110 °C for 1 h) to eliminate traces of water. The RPO was purchased at a local store in Bogotá. The FAD came from a dedusting system (electrostatic precipitator) of a thermal power-plant using residual forest biomass (mainly derived from eucalyptus) sited in the Centre Region of Portugal.

All the chemicals used were analytical grade except n-hexane (GC grade) and methyl heptadecanoate (analytical standard) from Sigma-Aldrich and Merck.

### 3.2.2 Oil mixtures characterization

According to the experimental design presented in Section 3.2.5, three oily feedstock were prepared using different mass ratios of RPO/WCO: M1 (100 % RPO), M2 (50 % RPO, 50 % WCO) and M3 (0 % RPO). These mixtures were characterized in terms of: acid value (NTC 218)(ICONTEC 218 1999), density (NTC 336) (ICONTEC 1998), saponification number (NTC 335)(ICONTEC 1998), viscosity (ASTM D445)(ASTM 2010), and moisture content (Karl Fisher, Coulometer 831-Metrohm).

The saponification number (SN) was used to calculate the molecular mass ( $MW$ , g/mol) according to Equation 3.1 (Mansir et al. 2018).

$$MW = \frac{56,1 \times 1000 \times 3}{SN} \quad (3.1)$$

The FFA content was calculated from the acid value ( $AV$ , mg KOH/g) using Equation 3.2 (Demirbas 2009).

$$FFA = \frac{AV}{2} \quad (3.2)$$

### 3.2.3 Catalysts preparation and characterization

Usually the solid catalysts are characterized by different instrumental techniques in order to measure their morphology, physical properties and bulk properties. The catalytic behavior depends on the morphological characteristics of the solid material, because the catalytic process takes place at its surface (outer and inner). The most utilized techniques to characterize materials' morphology are BET and SEM. In terms of physical properties, the surface area is the place of catalytic activity, but only a part is utilized in the catalytic reaction (active center). In basic and acid catalysts, the active sites not only occupy a little fraction of the surface, but also differ in basic and acid strength and sometimes in nature. Hammett indicators are often used to determine the acid and basic strengths of a material. FTIR is useful to identify the main chemical functional groups present on the surface of solid materials. For bulk properties X-ray diffraction (XRD) is used to find: (i) the crystalline phases, (ii) crystalline degree and (iii) crystallite size (Leofanti et al. 1997), with which the catalytic activity can be interpreted.

In this work, the catalyst was prepared by drying the fly ash (FAD) for 2 h at 120 °C. Then, the resulting material was characterized in terms of: (i) crystallographic structures, by powder X-ray (XRD, PAN analytical Empyrean X-ray diffractometer equipped with Cu-K $\alpha$  radiation source  $\lambda = 1.54178 \text{ \AA}$  at 45 kV/ 40 mA); (ii) surface area (SBET) was estimated by the BET (Brunauer-Emmett-Teller) method, pore size and pore volume were determined by the BJH (Barrett-Joyner-Halenda) model. The specific surface area and pore structure characterization were determined by nitrogen adsorption at 77 K using a surface area analyzer Micromeritics Gemini V-2380. The samples were degassed overnight at 373 K before measurement; (iii) surface morphology and quantitative analysis of elemental composition, by surface scanning electron microscopy (SEM) and energy dispersive X-ray spectroscopy (EDX), using a HR-FESEM Hitachi SU-70 operated at 15 kV, equipped with a Bruker Quantax 400 EDS system; (iv) surface functional species by Fourier transform infrared (FTIR, Agilent CARY 630 with wave number range from 400 to 4000  $\text{cm}^{-1}$ ); (v) basic and acid strength by using Hammett indicators (for basic strength: neutral red, pKa = 6.8; bromothymol blue, pKa = 7.2; phenolphthalein, pKa = 9.3; indigo carmine, pKa = 12.2; and 2,4-dinitroaniline, pKa = 15.0; indicators for acid

strength: bromothymol blue, pKa = 7.2; neutral red, pKa = 6.8; bromocresol purple, pKa = 6.1; bromocresol green, pKa = 4.7; and bromophenol blue, pKa = 3.8). The latter method was carried out by dispersing about 25 mg of the sample (catalyst) in 5.0 mL of a solution of Hammett indicators (0.5 mg of indicator in 10 mL of methanol for basic strength or 10 mL of benzene for acid strength), and left for 2 h to reach the chemical equilibrium. Then, the color of the resulting solution was identified.

### 3.2.4 FAME synthesis and quantification

The experiments for FAME production were carried out in a batch reactor (in glass, 0.25 L of capacity, equipped with temperature control and magnetic agitator), using 2 h of reaction time at 600 rpm stirring speed.

At the end of each batch assay, the catalyst and methanol were separated from the reaction mixture by centrifugation and evaporation, respectively. Then, the supernatant was placed into a separating funnel over 12 h for phase separation. The water contained in the upper layer of the liquid mixture was removed with anhydrous sodium sulfate (10 wt%) and weighed. The resulting mixture, hereafter is so-called purified final mixture, was analyzed by gas chromatography for FAME determination and was titrated with a KOH solution for final acid value quantification (ICONTEC 218 1999).

The Shimadzu G-C 2014 chromatograph used for FAME determination was equipped with a flame ionization detector and a capillary column SGE BP-20 60 m x 0.25 mm i.d. x 0.25 µm film thickness with a stationary phase of polyethylene glycol; the carrier gas was helium with a flow rate of 16.7 mL/min and a pressure of 2.5 atm; the injector (AOC-20i) was operated at 200 °C and an injection volume of 2.0 µL in Split mode. Methyl heptadecanoate was used as internal standard and hexane the solvent. The content of methyl esters was calculated based on the standard method (UNE-EN ISO 14103) (AENOR-EN 14103 2011) and expressed as concentration of FAME using the Equation 3.3:

$$C = \frac{\sum A - A_{EI}}{A_{EI}} \times \frac{W_{EI}}{W} \quad (3.3)$$



Where  $C$  is the concentration of FAME in the purified final mixture (w/w),  $\sum A$  is the total peak areas of the methyl ester from  $C_{14}$  until  $C_{24:1}$ ,  $A_{EI}$  is the peak area corresponding to methyl heptadecanoate,  $W_{EI}$  is the mass (mg) of methyl heptadecanoate used and  $W$  is the mass (mg) of the sample used in the analysis.

The catalyst performance was assessed by the FAME yield and FFA conversion, calculated by Equation 3.4 and Equation 3.5, respectively (Uprety et al. 2016; Wan Omar and Amin 2011a).

$$\text{FAME yield (\%)} = \frac{C \times \text{Total mass of purified final mixture}}{\text{Mass of oil used in the experiment}} \times 100 \quad (3.4)$$

$$\text{FFA conversion (\%)} = \left(1 - \frac{AV_f}{AV_i}\right) \times 100 \quad (3.5)$$

Where  $AV_i$  and  $AV_f$  correspond to the acid value of the initial oil mixture and of the purified final mixture, respectively.

### 3.2.5 Experimental design and optimization of FAME production process

Response Surface Methodology (RSM) based on a Box–Behnken experimental design are a set of mathematical and statistical techniques employed for designing experiments, creating correlations, evaluating the effects of several factors, and their interaction effects for desirable responses. This method uses the minimum required data that give the best reaction condition for a desired response (Liu et al. 2014; Salamatina et al. 2010) and was applied to optimize and to investigate the relationship between operating conditions and the FAME yield. The effect of four independent variables - catalyst loading, methanol/oil, RPO/WCO and reaction temperature on the FAME yield was studied. The experimental range for each independent variable (*aka* factor) tested in this work is shown in Table 3.1.

**Table 3.1** - Range and factor levels of operating variables used in the Box – Behnken experimental design.

Real variables	Coded variables	Level		
		Low (-1)	Medium (0)	High (+1)
Catalyst loading (wt%)	A	5	10	15
Methanol/oil (molar ratio)	B	3	6	9
Temperature (°C)	C	45	50	55
RPO/WCO (wt%)	D	0 (M3)	50 (M2)	100 (M1)

Twenty nine experimental runs were required, including five replicates of the central point. The correlation in the form of a quadratic polynomial equation was developed for predicting the response (i.e., FAME yield) as a function of independent variables and their interactions according to Equation 3.6.

$$Y = \beta_0 + \sum_{i=1}^k \beta_i x_i + \sum_{i=1}^k \beta_{ii} x_i^2 + \sum_{i=1}^k \sum_{j=i+1}^k \beta_{ij} x_i x_j + \varepsilon \quad (3.6)$$

Where  $Y$  is the predicted response for the process, i.e., the dependent variable;  $\beta_0$  is the intercept coefficient (offset);  $\beta_i$  are the linear terms;  $\beta_{ii}$  are the quadratic terms;  $\beta_{ij}$  are the interaction terms;  $x_i$  and  $x_j$  are the independent variables; and  $\varepsilon$  is the error (Hajamini et al. 2016).

Simplified regression models of Equation 3.6 (e.g., without interaction terms) were also fitted to the experimental results. The best fit achieved with the simplest model was the one selected and presented in this work.

The inference on the regression model was performed through an analysis of variance (ANOVA), for a 95 % confidence level, where the statistically significant factors in the response variable were identified, and an analysis of the coefficients of determination of the model,  $R^2$  and adjusted  $R^2$  (“Adj  $R^2$ ”), was used to evaluate the adequacy of the regression model to the experimental data. In this step one used the sum of the squares of residuals, instead of the pure error.

Validation of the regression model assumptions (i.e., the assessment of the adequacy of the model) was performed through a residual analysis (normality and residual plots). This analysis was based on normalized/studentized residuals.

Once the best regression model was selected and validated, the optimal operating conditions were identified through the response surface. Then, for statistical validity purposes, three runs were performed using those optimal conditions, thus allowing to determine the deviations of the data predicted by the model and the real values obtained experimentally. The software Design – Expert 7.0.0 was used for the statistical data processing and analysis.

### **3.2.6 Catalyst reusability**

Recovery, stability and reuse are important aspects of a heterogeneous catalyst to be applied in biodiesel production. The reusability of FAD catalyst in esterification and transesterification reactions was investigated through 2 successive catalytic cycles (i.e., in total 3 cycles) using the optimal reaction conditions found in the optimization step. After each cycle, the solid catalyst was recovered and activated by simple centrifugation, washing with isopropyl alcohol for removing organic compounds eventually retained in the solid surface, calcined at 700 °C for 3 h and reused in the next catalytic cycle. At the end of each cycle, the catalyst was characterized by XRD, textural properties and Hammett indicator.

### 3.3 Results and discussion

#### 3.3.1 Oil mixtures characterization

The properties of the oil mixtures prepared for this study are shown in Table 3.2.

**Table 3.2** - Properties of the oil mixtures used in this work.

	<b>M1</b>	<b>M2</b>	<b>M3</b>
<b>%WCO</b>	<b>0</b>	<b>50</b>	<b>100</b>
<b>%RPO</b>	<b>100</b>	<b>50</b>	<b>0</b>
Moisture (wt%)	0.067±0.010	0.170 ± 0.003	0.197 ± 0.012
Density (g/mL)	0.908 ± 0.008	0.913 ± 0.010	0.906 ± 0.003
AV (mg KOH/g)	0.307 ± 0.004	3.958 ± 0.082	4.934 ± 0.252
FFA (wt%)	0.172 ± 0.005	1.979 ± 0.041	2.453 ± 0.056
MW (g/mol)	843.15 ± 9.52	886.34 ± 1.21	857.82 ± 4.01
Viscosity (mm <sup>2</sup> /s) @ 60 °C	14.902 ± 0.193	17.122 ± 0.123	19.185 ± 0.392

The properties of M1 (i.e., 100 % RPO) are similar to those reported by Kansedo et al. (2009) and by Metawea et al. (2018). Concerning the waste cooking oils properties, they are quite dependent of the vegetable oil feedstocks and their frying practices and conditions. The WCO (M3) used in this work has properties similar to those reported by Wan Omar et al. (2011b) and Lam and Keak (2010), and it can be categorized as yellow grease (FFA < 15 %) (Avhad and Marchetti 2015).

As the percentage of WCO increases in the blend (see Table 3.2) higher are the moisture and the FFA contents, the acid value and the viscosity, while the remaining properties values (density and molecular weight) are similar among the three blends.

#### 3.3.2 Catalysts characterization

The solid catalyst prepared was characterized for some textural properties such as specific surface area, crystalline structure, surface functional groups, but also their basic and acid strength, etc. The results are shown and discussed in the next sections.

### 3.3.2.1 BET surface area and Hammett indicators analyses

FAD used in this work has an intermediate basic strength ( $10.1 \leq \text{pKb} < 12.2$ ), due to the high basicity of the metal-oxygen groups (Lewis bases) present in the calcium compounds on its surface (see Sections 3.3.2.2 and 3.3.2.3) and a low acid strength ( $6.8 \leq \text{pKa} < 7.2$ ) (Maneerung et al. 2015). With regard to its textural properties, FAD has a low (BET) surface area ( $9.028 \text{ m}^2/\text{g}$ ), characteristic of this type of material, a pore volume of  $0.01055 \text{ cm}^3/\text{g}$ , and an average pore diameter ( $77.188 \text{ \AA}$ ), which shows some potential to the adsorption and desorption of molecules such as triglycerides, glycerin and FAME (Chakraborty et al. 2010; Jacobson et al. 2008).

The average pore size distribution could be estimated from the nitrogen adsorption-desorption isotherms. Figure 3.1 shows those isotherms for FAD catalyst, which behaves like a type IV(a) according to the classification of the International Union of Pure and Applied Chemistry. The initial part of this graph exhibits a behavior such as the type II isotherm, typical of monolayer adsorption. Subsequently, a hysteresis cycle associated with the characteristic capillary condensation of mesoporous solids is observed, which is observed for pore size ranges between  $20\text{-}500 \text{ \AA}$  (Thommes et al. 2015).

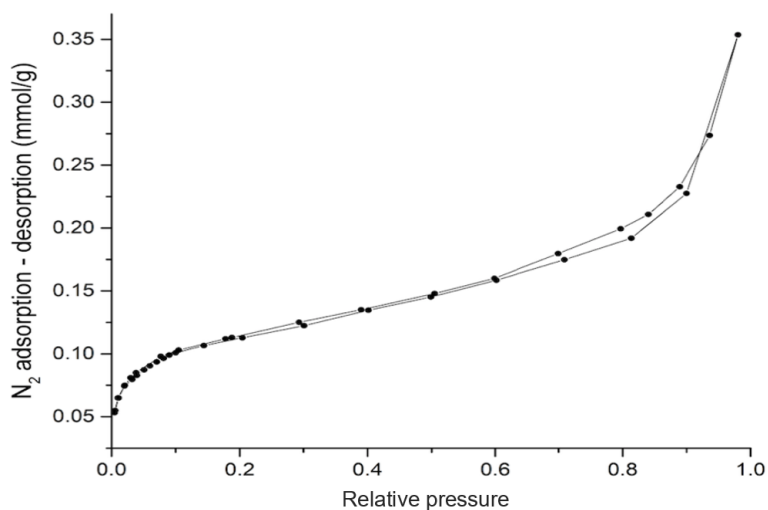


**Figure 3.1** - Adsorption and desorption isotherms for the FAD catalyst.

### 3.3.2.2 SEM and EDX analyses

The SEM images for characterizing the morphological characteristics and EDX for elemental analysis and chemical characterization of the catalysts were obtained. Figure 3.2 shows the morphological and the elemental composition of FAD catalyst. Ash particles have uniform distribution of agglomerates with irregular shapes and rough structure. The same characteristics were observed by Rajamma et al. (2009). In addition, the average particle size for the FAD catalyst was  $4.353 \mu\text{m}$  ( $\pm 1.07$ ) as determined using the ImageJ software. The results of EDX show as predominant elements: Ca, Mg, Si, Al, O, K, S, Na, Cl and P (Figure 3.2 c).

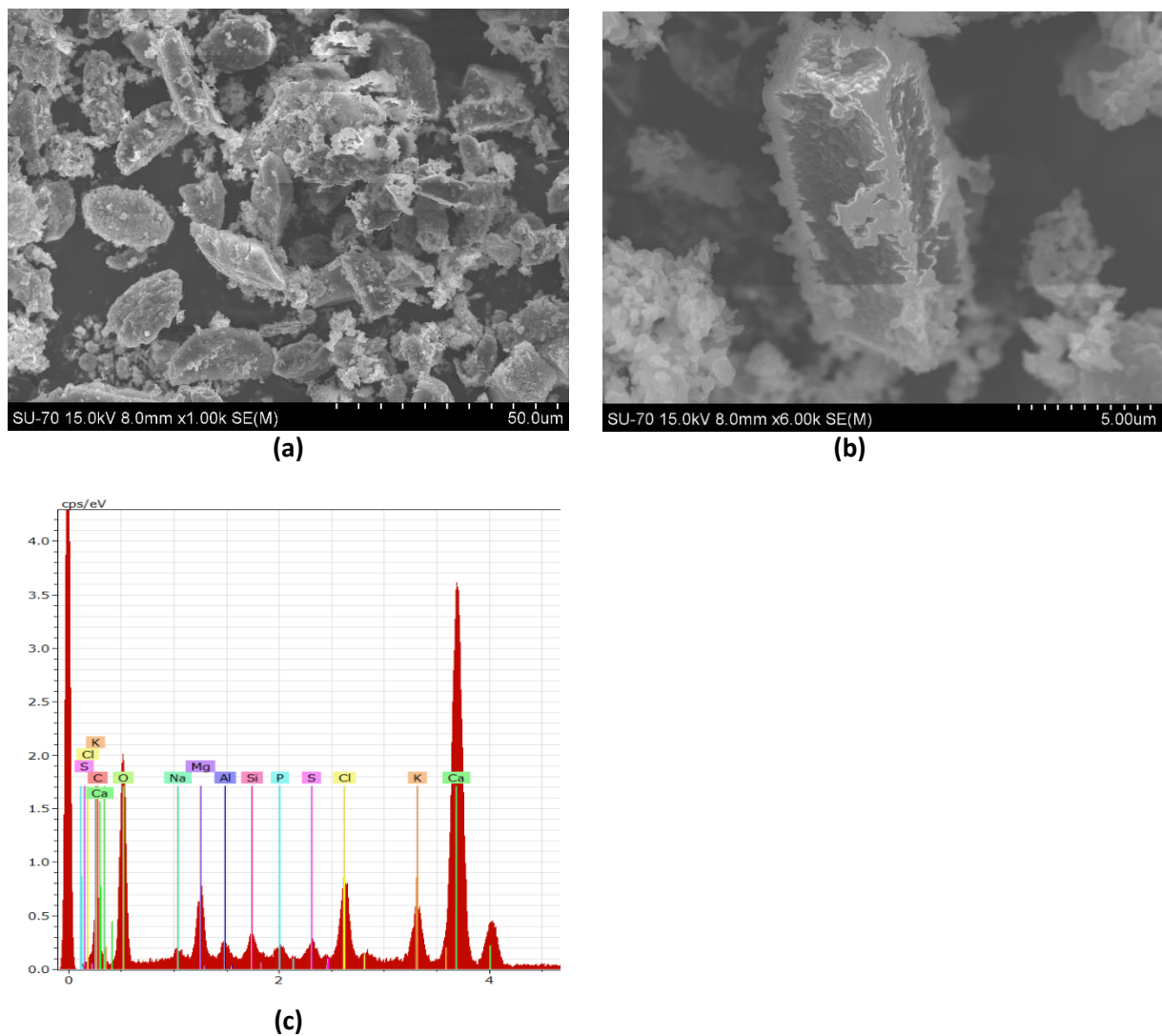


**Figure 3.2** - FAD catalyst characterization by: SEM (a and b) and EDX (c).

### 3.3.2.3 XRD analyses

The XRD diffractogram of the FAD catalyst is depicted in Figure 3.3. The XRD pattern shows clear diffraction peaks corresponding to calcium oxide (CaO) phase detected at  $2\theta=32.2^\circ$ ,  $37.4^\circ$ ,  $53.8^\circ$ ,  $65.2^\circ$ , and  $67.5^\circ$ , calcium carbonate (CaCO<sub>3</sub>-major component) phase detected at  $2\theta =23.3^\circ$ ,  $29.6^\circ$ ,  $36.2^\circ$ ,  $39.7^\circ$ ,  $43.4^\circ$ ,  $47.8^\circ$ ,  $48.8^\circ$ ,  $56.9^\circ$ ,  $61.0^\circ$  and  $65.0^\circ$ , potassium chloride (KCl) phase detected at  $2\theta =28.5^\circ$ ,  $40.5^\circ$ , and silicon dioxide (SiO<sub>2</sub>) phase detected at  $2\theta =20.9^\circ$ ,  $26.7^\circ$ ,  $36.38^\circ$ ,  $39.46^\circ$ ,  $40.28^\circ$ ,  $50.2^\circ$ ,  $60.2^\circ$  and  $68.5^\circ$ , among other components such as calcium hydroxide detected at  $2\theta=17.91^\circ$ ,  $28.51^\circ$ ,  $33.95^\circ$ ,  $47.41^\circ$ ,  $50.68^\circ$ ,  $64.60^\circ$ .

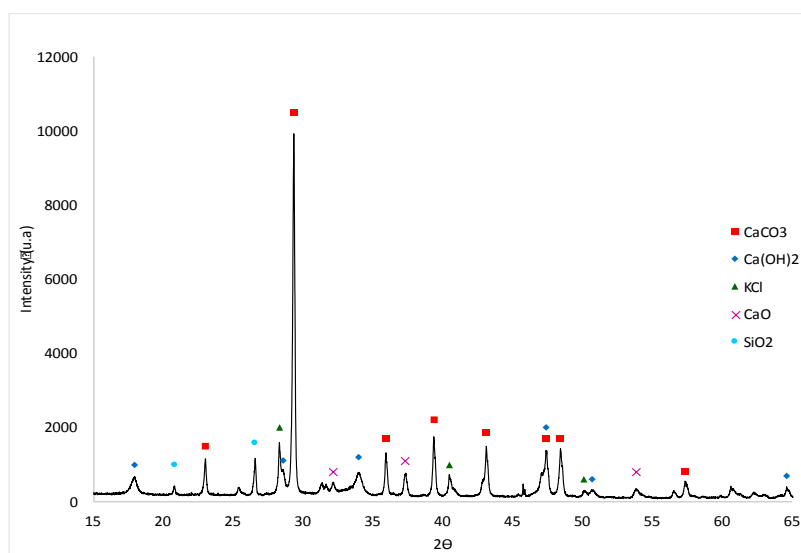


**Figure 3.3** - XRD patterns of FAD catalyst.

Regarding the semi-quantitative mass composition, a high content of calcium carbonate (71.0 %) was found, followed by calcium hydroxide (12.9 %), potassium chloride (7.1 %), calcium oxide (3.8 %), silicon dioxide (2.3 %) and other components in smaller proportion were identified (3.0 %); similar compounds were reported by Sharma et al. (2012) for wood ash and by Ho et al. (2014) for palm oil mill fly ash. The presence of calcium hydroxide may be due to the ambient humidity that reacts (after the combustion process) with calcium oxides presents on the surface of the solid; this phenomenon was also observed by Maneerung et al. (2015). The high calcium carbonate content results from the carbonation of calcium oxides and hydroxides since solid material was in contact with atmospheric carbon dioxide, after the combustion process.

### 3.3.2.4 FTIR analyses

The FTIR spectrum of FAD used in this work is shown in Figure 3.4. It shows the major absorption broad band at  $1408.1\text{ cm}^{-1}$  and minor absorption bands at  $872$  and  $712\text{ cm}^{-1}$ , which correspond to the asymmetric stretching and to out-of-plane band and in-plane band vibration modes of carbonate ( $\text{CO}_3^{2-}$ ) group, respectively. The small bands at  $2510$  and  $2320\text{ cm}^{-1}$  also correspond to the characteristic spectrum of this functional group. This result confirms the presence of  $\text{CaCO}_3$  in FAD, detected by XRD.

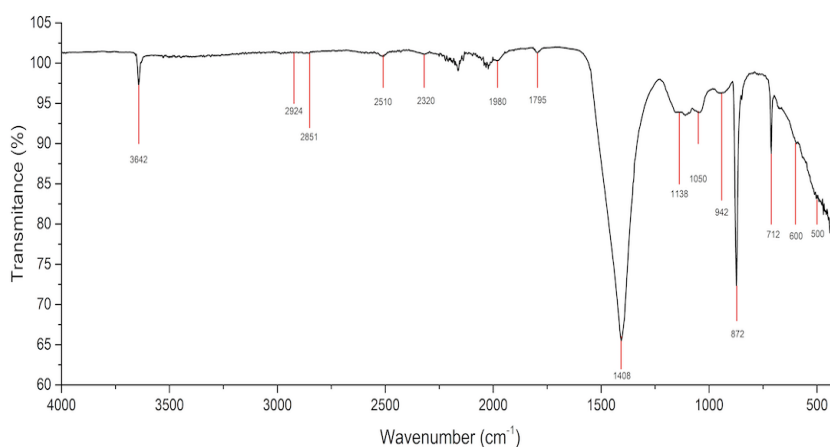


**Figure 3.4** - FTIR spectrum of FAD catalyst.

$\text{PO}_4^{3-}$  and Si-O components (silica phosphates) show broad bands in the region between  $1138$  and  $942\text{ cm}^{-1}$ ; the same was observed by Maneerung et al. (2015) and Sharma et al. (2012) in bottom ash waste from woody biomass gasification and wood ash from the combustion of *Acacia nilotica* (babul), respectively. Moreover, the absorption sharp band at  $3642\text{ cm}^{-1}$ , which is attributed to -OH band, was observed in the FAD catalyst, this band is in agreement with the presence of  $\text{Ca}(\text{OH})_2$  as determined by XRD, and an evidence of the possible water absorption on the CaO surface producing  $\text{Ca}(\text{OH})_2$  (Boey et al. 2011).

### 3.3.3 Optimization of FAME production process: regression model and statistical analysis

The experimental results obtained in the set of assays aiming at optimizing the FAME yield are shown in Table 3.3.



**Table 3.3** - Experimental design and predicted results of RSM.

Run	Real variables				FAME yield (wt%)	
	Catalyst loading	Methanol/oil	T	RPO/WCO	Experimental	Predicted*
	(wt%)	(mol/mol)	(°C)	(wt%)		
1	15	6	50	100	11.40	21.35
2	10	6	55	0	60.94	63.48
3	10	3	50	0	41.44	41.84
4	10	6	50	50	62.86	55.95
5	10	9	55	50	64.64	62.18
6	15	6	45	50	25.82	31.83
7	10	3	45	50	12.25	17.16
8	10	3	50	100	0.00	6.68
9	5	9	50	50	38.33	35.43
10	10	6	45	0	25.24	26.45
11	5	6	50	100	8.96	1.57
12	15	6	55	50	65.35	68.86
13	10	6	50	50	70.34	55.95
14	5	6	55	50	47.94	49.07
15	10	6	55	100	27.57	28.32
16	10	6	45	100	7.39	-8.70
17	15	3	50	50	52.83	47.22
18	10	9	45	50	33.25	25.16
19	10	9	50	100	8.57	14.68
20	5	3	50	50	28.34	27.43
21	5	6	45	50	0.00	12.05
22	10	9	50	0	40.32	49.83
23	15	6	50	0	68.20	56.51
24	10	6	50	50	38.63	55.95
25	10	3	55	50	59.65	54.18
26	10	6	50	50	45.84	55.95
27	15	9	50	50	57.38	55.21
28	5	6	50	0	38.70	36.73
29	10	6	50	50	62.08	55.95

\*Predicted by Equation 3.7

The regression model of Equation 3.6 fitted to the experimental results revealed that the interaction between the factors  $\beta_{ij}x_i x_j$  was not significant ( $p$ -value  $> 0.05$ ). Thus, the simplified model (i.e., quadratic model without interactions) was used and the goodness-of-fit was evaluated by the several parameters determined in the ANOVA. The results are shown in Table 3.4, where it can be seen that model has a good fit as  $R^2=0.8702$  and  $\text{Adj } R^2=0.8182$ . The  $R^2$  value indicates that 87.02 % of the variability in the data is predicted by the model.

**Table 3.4** - ANOVA results of the response surface quadratic model without interactions.

Source of variations	Sum of squares	Degrees of freedom	Mean square	F - value	p - value
Model	12028.36	8	1503.55	16.75	< 0.0001
Residual	1794.79	20	89.74		
Lack of fit	1100.2	16	68.76	0.936	0.9183
Pure error	694.59	4	173.65		
Total	13823.15	28			
	$R^2 = 0.8702$	Adj	Pred	C.V. <sup>a</sup> = 24.88%	S.D. <sup>b</sup> = 9.47
		$R^2 = 0.8182$	$R^2 = 0.7424$		

<sup>a</sup> C.V.= coefficient of variation.

<sup>b</sup> S.D.= standard deviation.

The low  $p$ -value ( $< 0.0001$ ) of the model means that it is statistically significant. On the other hand, the lack of fit  $F$ -value of 0.936 implies that is not significant relative to the pure error, i.e. the lack of fit of the model is statistically non-significant; there is a 91.83 % chance that this value could occur due to noise. The “Pred  $R^2$ ” of 0.7424 is in reasonable agreement with the “Adj  $R^2$ ” value of 0.8182. In short, the selected regression model satisfactorily predicts the effect of the four factors on FAME yield. Equation 3.7 represents the model developed:

$$Y = 55.95 + 9.89 x_A + 4.00 x_B + 18.51 x_C - 17.58 x_D - 6.92 x_A^2 - 7.70 x_B^2 - 8.57 x_C^2 - 19.98 x_D^2 \quad (3.7)$$

Where  $Y$  is the response variable (FAME yield, wt%),  $x_A$  (catalyst loading, wt%),  $x_B$  (methanol/oil, molar ratio),  $x_C$  (reaction temperature, °C) and  $x_D$  (RPO/WCO, wt%) are the studied factors. The positive sign of a coefficient term means synergistic effect while the

negative sign reveals the opposite effect, of the influencing variables on FAME yield (Liu et al. 2014). The FAME yield predicted by this regression model is shown in Table 3.3, for comparison with experimental results.

The statistical significance of each regression coefficient of the model on the response variable was evaluated using ANOVA testing and the results are shown in Table 3.5. The p-values indicate the significance of each regression coefficient. In general, smaller p-value ( $< 0.05$ ) indicates higher significance of the corresponding coefficient (Avramović et al. 2010). According to obtained results, three of the four linear factors were statistically significant ( $x_A$ ,  $x_C$ , and  $x_D$ ) and only one ( $x_B$ ) was not significant (for confidence level of 95 %). Besides that, the influence of square value of RPO/WCO ( $x_D^2$ ) with a negative effect of -19.98 (p-value  $< 0.0001$ ) was found to be the most significant term affecting the FAME yield; the quadratic term of the temperature was also significant (p-value = 0.0320).

**Table 3.5** - ANOVA results for the coefficients of the variables in the quadratic regression model without interactions.

Model parameters	Estimate coefficient	F - value	p - value
Intercept	55.95		
$x_A$	9.89	13.09	0.0017
$x_B$	4.00	2.14	0.1592
$x_C$	18.51	45.82	$< 0.0001$
$x_D$	-17.58	0.158	$< 0.0001$
$x_A^2$	-6.92	3.46	0.0775
$x_B^2$	-7.70	4.29	0.0515
$x_C^2$	-8.57	5.31	0.0320
$x_D^2$	-19.98	28.88	$< 0.0001$

In order to validate the assumptions of the simplified regression model (i.e., quadratic model without interactions), statistical graphical methods were used. A normal probability plot of residuals is shown in Figure 3.5 a, which corresponds to the difference between the

experimental and the predicted response. The data points are located approximately along a straight line, thus one can intuitively conclude that the residuals follow a normal distribution. Plot of residuals versus fitted response values (predicted) is depicted in Figure 3.5 b, which shows that the residuals are randomly distributed. Residuals are located in a horizontal line and the number of points that exist in the above and below of horizontal line is equal. Moreover, residual values are in the range  $\pm 3.00$ ; typically, a threshold of three standard deviations is employed as a definition of an outlier (Noshadi et al. 2012). The actual FAME yield versus the predicted values is plotted in Figure 3.5 c, which corroborates the goodness-of-fit of the regression model developed. In brief, this analysis confirms the accuracy and reliability of the proposed regression model.

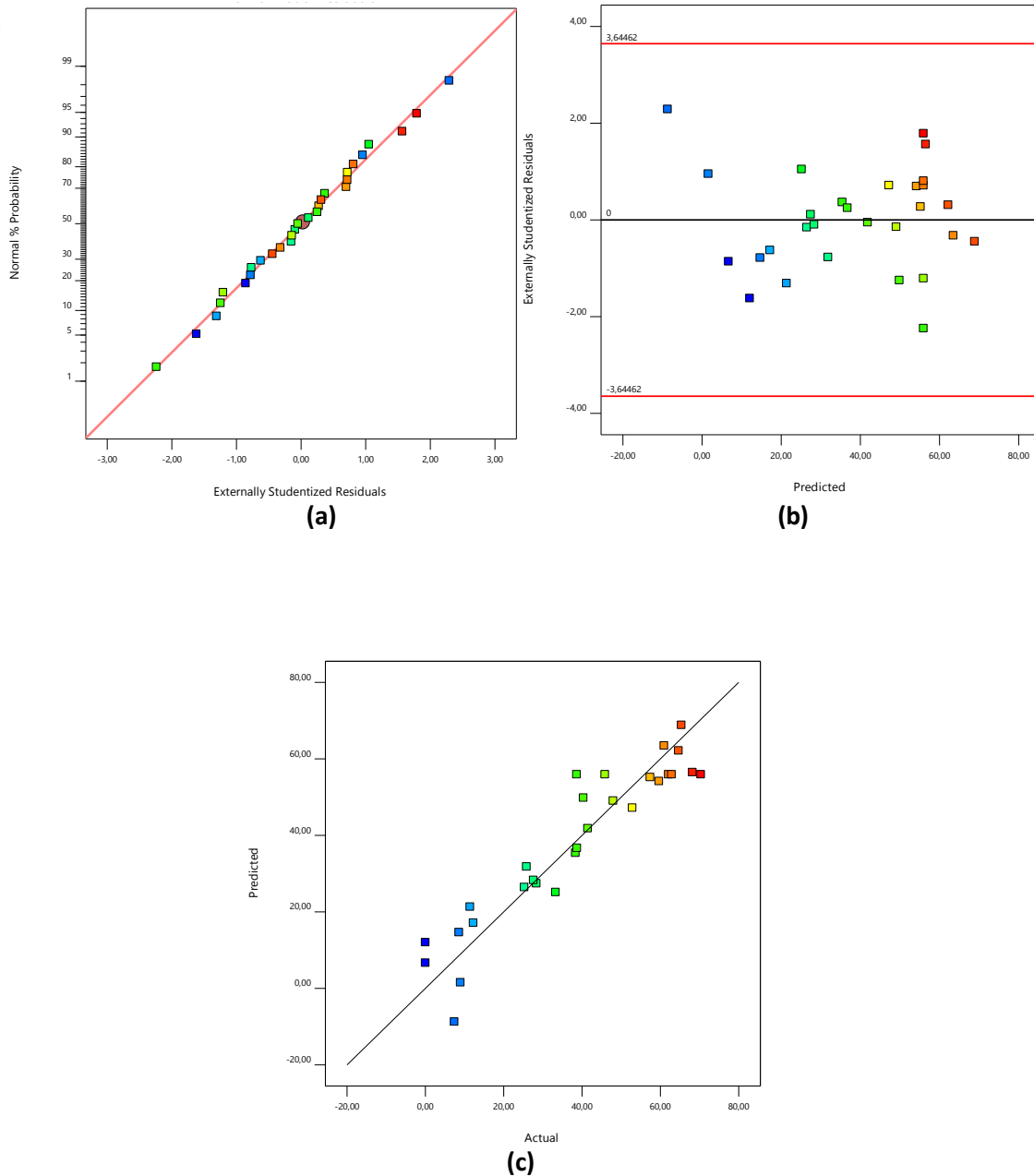


**Figure 3.5** - (a) Residual normal probability plot, (b) Residual versus predicted response plot, (c) Predicted versus actual values plot.

As stated before, in the range tested (Table 3.1), the factors studied in this work, except methanol/oil molar ratio, had a statistically significant influence on FAME yield; although some were more significant than others. This is shown as response surface plots in Figure 3.6.

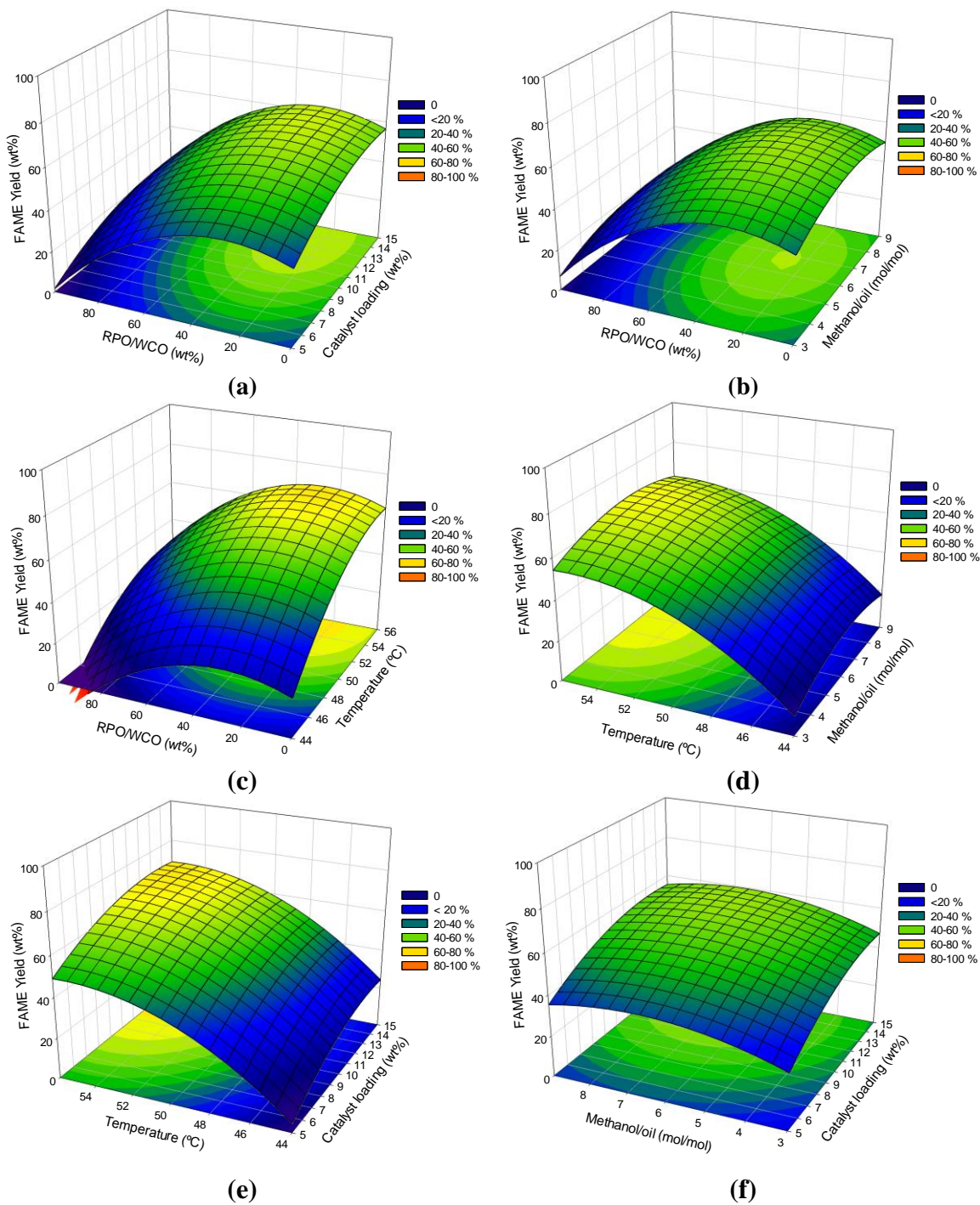


**Figure 3.6** - Response surface plots of FAME yield as a function of: (a) RPO/WCO ratio and catalyst loading at 50 °C and methanol/oil = 6 mol/mol; (b) RPO/WCO ratio and methanol/oil at 50 °C and catalyst loading = 10 wt%; (c) RPO/WCO ratio and temperature for catalyst loading = 10 wt% and methanol/oil = 6 mol/mol; (d) temperature and methanol/oil ratio for catalyst loading = 10 wt% and RPO/WCO = 50 wt%; (e) temperature (°C) and catalyst loading (wt%) for methanol/oil = 6 mol/mol and RPO/WCO = 50 wt%; (f) methanol/oil ratio and catalyst loading (wt%) at 50 °C and RPO/WCO = 50 wt%.

From Figure 3.6 a, higher yields of FAME (64 %) were achieved with high catalyst loading (13.2 wt%) and moderate (28.0 wt%) RPO/WCO mass ratio. For any fixed RPO/WCO mass ratio, as catalyst loading increased higher FAME yields were observed, which may be due to the higher number of active sites (of the catalyst) available in the reaction medium. On the other hand, RPO/WCO mass ratio higher than 28.0 wt% affected negatively the FAME yield for any catalyst loading tested. Thus, the low acid strength and intermediate basic strength of FAD seems to be suitable to catalyze oily mixtures with higher FFA contents, which, according to some authors (Rabiah et al. 2014; Wan Omar et al. 2011b), could be due to the balance of acid and basic catalyst sites. This is a promising result for the economic and environmental sustainability of the process. Concerning methanol/oil molar ratio, Figure 3.6 b shows the weak influence of this factor on the response variable; therefore, the methanol/oil molar ratio of 6.6 can be used to achieve the highest yields to FAME (64 %). Similar behavior was mentioned by Volli et al. (2019) for the same methanol/oil molar ratio but using bone impregnated fly ash as a catalyst. Figure 3.6 c shows the influence on FAME yield of the two most significant factors studied in this work: temperature and RPO/WCO mass ratio. Indeed, increasing the reaction temperature rose the FAME yield independently of the RPO/WCO mass ratio used. The higher yield was observed at 55 °C with 28.0 wt% of RPO/WCO mass ratio (loading = 10 wt% and methanol/oil = 6 mol/mol); Uprety et al. (2016) also found a very significant effect between 50 and 60 °C (reaction temperature) on the yield, using a catalyst of CaO and RPO as raw material. Figure 3.6 d shows once more the different relevance of the temperature and methanol/oil molar ratio on the response variable. Catalyst loading and reaction temperature had similar positive effects on the FAME yield (Figure 3.6 e), being the higher yields achieved (c.a. 74 %) at 55 °C and catalyst loading 13.2 wt% (for methanol/oil molar ratio of 6 and RPO/WCO mass ratio of 50 wt%). This high FAME yield achieved may be due to the crystalline phases (calcium hydroxide and calcium oxide), the functional groups (carbonate group) and pore diameter (average 77.188 Å) found in the solid catalyst.

Regarding the percentage of conversion of free fatty acids, similar results were obtained for the different experiments with values close to  $84.3 \% \pm 6.0 \%$ ; which may be due to the slightly acid character of the solid catalyst ( $6.8 \leq \text{pKa} < 7.2$ ). These conversion values point out to a

bifunctional character of the FAD catalyst, i.e., simultaneous catalysis of transesterification and esterification reactions, already found by Vargas et al. (2019).

### **Optimal operating condition**

An important objective of this study was to find optimal operating conditions to achieve maximum FAME yield, combining the several independent variables studied. The RMS suggested that the highest FAME yield was 73.8 %, which can be achieved by using 13.57 wt% of catalyst loading, 6.7 methanol/oil molar ratio, 28.04 wt% of RPO/WCO mass ratio and 55 °C for the reaction temperature. To validate the proposed operating conditions, three replicate experiments were conducted under them, over 2 h at 600 rpm stirring speed. The average experimental FAME yield was 78.8 % ( $\pm 1.7$  %), which is close to the predicted value (i.e., 73.8 %). So, the validity of the proposed correlation is confirmed again with an error of 6.8 % ( $\pm 0.05$  %). The FAME yield and the respective relative error between model predictions and experimental value were close to the obtained by Badday et al. (2013), using activated carbon-supported tungstophosphoric as catalyst on the *Jatropha* oil and a Central Composite Design (CCD) as experimental design method.

### **3.3.4 Catalyst reusability: catalytic performance assessment**

The reusability of a catalyst is very important for its commercial feasibility. In order to investigate the reusability of the FAD catalyst, the subsequent reaction cycles were carried out under the optimized reaction condition: 13.57 wt% of catalyst loading, 6.7 methanol/oil molar ratio, 28.04 wt% of RPO in the oil mixture and 55 °C for the reaction temperature, 2 h reaction time and 600 rpm stirring speed. Between each cycle the catalyst was regenerated, according to the procedure stated in Section 3.2.6. The FAME yields obtained from the reused catalyst in each cycle is shown in Figure 3.7, where a slight increase on FAME yield with the repeated usage of the catalyst is observed. However, a statistical analysis of the data (ANOVA for a confidence level of 95 %) showed that differences observed among the three assays were not statistically significant with  $p$ -value = 0.1258; therefore, the activity of the FAD catalyst could be considered roughly constant over three cycles of use. Similar catalytic stability were



reported by Chakraborty et al. (2010) and Maneerung et al. (2015) using fly ash from a thermal power plant with a combustion technology and bottom ash waste arising from woody biomass gasification, respectively.

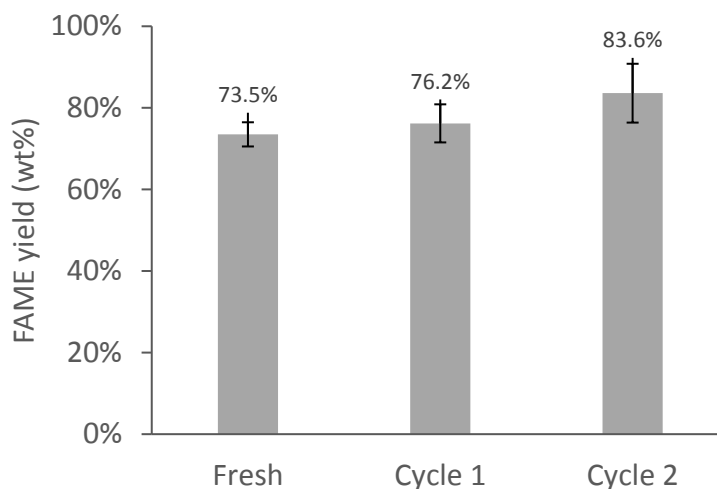


**Figure 3.7** - Reusability studies of the FAD catalyst under the optimal operating conditions.

The XRD patterns of the reused catalyst after each regeneration cycle are shown in Figure 3.8. It can be observed in the superimposed diffractograms that the majority phase was calcium carbonate ( $\text{CaCO}_3$ ), phase detected at  $2\theta=23.3^\circ$ ,  $29.6^\circ$ ,  $36.2^\circ$ ,  $39.7^\circ$ ,  $43.4^\circ$ ,  $47.8^\circ$ ,  $48.8^\circ$  and  $56.9^\circ$ , followed by calcium hydroxide ( $\text{Ca(OH)}_2$ ) detected at  $2\theta=17.91^\circ$ ,  $33.95^\circ$  and  $50.68^\circ$ , indicating that CaO was partially transformed into  $\text{Ca(OH)}_2$ , probably through the reaction of CaO ( $2\theta=32.2^\circ$ ,  $37.4^\circ$  and  $53.8^\circ$ ) with  $\text{H}_2\text{O}$  in small amount in the reactants and/or moisture during the repeated usage of catalyst (Maneerung et al. 2015). This may explain the observed slight increase of FAME yield over the reuse cycles of the FAD, as  $\text{Ca(OH)}_2$  has catalytic properties. A peak is also observed in  $2\theta=26.7^\circ$  due to the presence of the phase silicon dioxide ( $\text{SiO}_2$ ) that gives the catalyst a low acid strength (and thus a bifunctional). The KCl ( $2\theta=28.5^\circ$  and  $40.5^\circ$ ) found did not contribute to the catalytic activity of the FAD. This conclusion arose from three experimental tests performed with pure KCl as a catalyst and where no FAME yield was registered (results not shown).

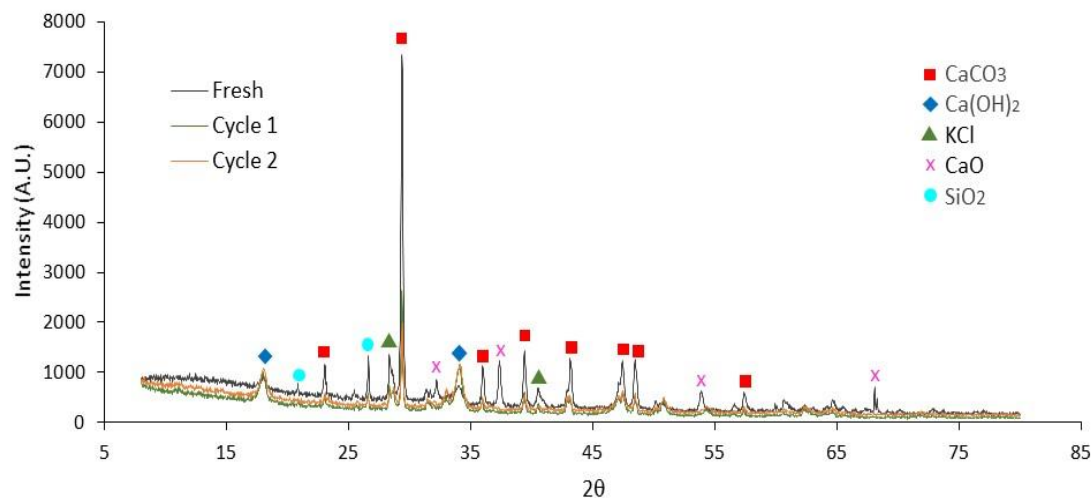


**Figure 3.8** - XRD patterns of FAD catalyst for the different reuse cycles.

The BET surface area, pore volume, pore diameter and basic and acid strength of reused catalyst (FAD) are shown in Table 3.6. The basic and acid strength of this reused catalyst and its textural properties did not change throughout the reuse cycles and regeneration steps.

**Table 3.6** - Textural properties and acid/basic strength of the FAD catalyst used in three FAME synthesis cycles.

Catalyst sample	Specific surface area (m <sup>2</sup> /g)	Pore volume (cm <sup>3</sup> /g)	Average pore diameter (Å)	Basic strength	Acid strength
Fresh	9.0280	0.01055	77.188	10.1 ≤ pKa < 12.2	6.8 ≤ pKa < 7.2
Cycle 1	10.9496	0.01253	82.639	10.1 ≤ pKa < 12.2	6.8 ≤ pKa < 7.2
Cycle 2	10.2876	0.01147	80.365	10.1 ≤ pKa < 12.2	6.8 ≤ pKa < 7.2

From these results, it is reasonable to conclude that after the cycles of reuse of the catalyst, it did not lose its catalytic activity (FAME yield). Indeed, the catalytic activity seems to be slightly increased, although not statistically different between the tests done, which can be explained due to relatively small changes of its textural properties, crystalline active phases (CaCO<sub>3</sub>, Ca(OH)<sub>2</sub> and SiO<sub>2</sub>) and basic and acid strength (surface chemistry) throughout the reuse cycles.

Thus, FAD catalyst has shown good properties for reuse in the process, and that is an advantage, because it is a low cost material, produced from an industrial waste and thus can turn the process more sustainable in terms of natural resources integration.

### 3.4 Conclusions

An efficient fly ash residual catalyst (FAD) was evaluated with mixtures of RPO and WCO to produce FAME using the response surface methodology and an experimental design Box Behnken type for optimizing the response variable (FAME yield). A regression quadratic model without interactions was the one that best fitted the experimental results, predicting the following optimal operating conditions: catalyst loading of 13.57 wt%, methanol/oil molar ratio of 6.7, RPO in the oil mixture of 28.04 wt%, temperature of 55 °C in batch regime over 2 h and 600 rpm of stirring speed. Under these operating conditions maximum FAME yield expected is 78.8 %. In the tested ranges, the most significant variables (95 % confidence level) affecting the FAME yield were the RPO/WCO mass ratio and the reaction temperature (°C), both with p-value <0.0001, followed by the catalyst loading (p-value = 0.0017). On the other hand, the methanol/oil molar ratio was not significant (p-value = 0.1592), indicating that the lowest ratio tested can be used to achieve the higher FAME yield registered.

The selected regression model accurately predicted the experimental results with a  $R^2 = 0.8702$  and  $Adj R^2 = 0.8182$ . Three assays were carried out under the optimal operating conditions, where the average of FAME yield reached was 78.8 % ( $\pm 1.7$  %), near the predicted by the regression model (73.8 %). Thus, the validity of the proposed regression model was demonstrated.

This works showed that FAD catalyst can be used for up to three cycles without loss of catalytic activity. However, the catalyst should be regenerated between each cycle, by washing with isopropyl alcohol and calcined at 700 °C for 3 h. The characterization of the surface, textural and crystalline properties of the catalyst, after use in each FAME synthesis cycle, showed that those properties were not significantly affected. The acid and basic strength remained

constants. In addition, one recommends to evaluate the reuse of FAD above three cycles in order to find the maximum number of cycles that it could be used keeping a high FAME yield and carry out a complementary characterization of the acid and basic catalyst sites with temperature-programmed desorption of  $\text{NH}_3$  and  $\text{CO}_2$  techniques, respectively.

Summing up, exploiting residual feedstocks, this work gives a sustainable and affordable approach to lower the biodiesel production costs and simultaneously, minimizing the environmental burdens traditionally inherent to the management of two wastes streams: WCO and FAD.

Therefore, an awareness should be created so that any material that is deemed a waste could be exploited for usage in this or other applications, thereby implementing the principles of circular economy.

### **Acknowledgments**

Edgar M. Vargas S. expresses his sincere gratitude to the Universidad Jorge Tadeo Lozano (Direction of Investigation, Creation and Extension) for the financial assistance of this work. Márcia C. Neves acknowledges FCT, I.P. for the research contract CEECIND/00383/2017 under the CEEC Individual 2017. The authors thank for the financial support to FCT/MCTES for the financial support to CESAM (UIDP/50017/2020 & UIDB/50017/2020) and CICECO (UIDB/50011/2020 & UIDP/50011/2020) through national funds.

## References

- AENOR-EN 14103. 2011. *Productos Derivados de Aceites y Grasas. Ésteres Metílicos de Ácidos Grasos (FAME). Determinación de Los Contenidos de Éster y de Éster Metílico Del Ácido Linolénico*. España. [www.agilent.com/chem](http://www.agilent.com/chem). (February 15, 2019).
- ASTM. 2010. "Standard Test Method for Kinematic Viscosity of Transparent and Opaque Liquids (and Calculation of Dynamic Viscosity)." *Annual Book of ASTM Standards*: 1–10.
- Avhad, M. R., and J. M. Marchetti. 2015. "A Review on Recent Advancement in Catalytic Materials for Biodiesel Production." *Renewable and Sustainable Energy Reviews* 50: 696–718. <http://dx.doi.org/10.1016/j.rser.2015.05.038>.
- Avramović, Jelena M. et al. 2010. "The Optimization of the Ultrasound-Assisted Base-Catalyzed Sunflower Oil Methanolysis by a Full Factorial Design." *Fuel Processing Technology* 91(11): 1551–57.
- Badday, Ali Sabri, Ahmad Zuhairi Abdullah, and Keat Teong Lee. 2013. "Optimization of Biodiesel Production Process from Jatropha Oil Using Supported Heteropolyacid Catalyst and Assisted by Ultrasonic Energy." *Renewable Energy* 50: 427–32. <http://dx.doi.org/10.1016/j.renene.2012.07.013>.
- Boey, Peng Lim et al. 2011. "Utilization of BA (Boiler Ash) as Catalyst for Transesterification of Palm Olein." *Energy* 36(10): 5791–96. <http://dx.doi.org/10.1016/j.energy.2011.09.005>.
- Boey, Peng Lim, Gaanty Pragas Maniam, and Shafida Abd Hamid. 2009. "Biodiesel Production via Transesterification of Palm Olein Using Waste Mud Crab (*Scylla Serrata*) Shell as a Heterogeneous Catalyst." *Bioresource Technology* 100(24): 6362–68. <http://dx.doi.org/10.1016/j.biortech.2009.07.036>.
- Chakraborty, R., S. Bepari, and A. Banerjee. 2010. "Transesterification of Soybean Oil Catalyzed by Fly Ash and Egg Shell Derived Solid Catalysts." *Chemical Engineering Journal* 165(3): 798–805. <http://dx.doi.org/10.1016/j.cej.2010.10.019>.
- Chatterjee, Amrita, Xijun Hu, and Frank Leung Yuk Lam. 2018. "Catalytic Activity of an Economically Sustainable Fly-Ash-Metal-Organic- Framework Composite towards Biomass Valorization." *Catalysis Today* 314(October 2017): 137–46. <https://doi.org/10.1016/j.cattod.2018.01.018>.
- Chen, Jein Wen et al. 2012. "Carcinogenic Potencies of Polycyclic Aromatic Hydrocarbons for Back-Door Neighbors of Restaurants with Cooking Emissions." *Science of the Total Environment* 417–418: 68–75. <http://dx.doi.org/10.1016/j.scitotenv.2011.12.012>.
- Demirbas, Ayhan. 2009. "Biodiesel from Waste Cooking Oil via Base-Catalytic and Supercritical Methanol Transesterification." *Energy Conversion and Management* 50(4): 923–27. <http://dx.doi.org/10.1016/j.enconman.2008.12.023>.

- Girón, R. P. et al. 2015. "Adsorbents/Catalysts from Forest Biomass Fly Ash. Influence of Alkaline Activating Agent." *Microporous and Mesoporous Materials* 209: 45–53. <http://dx.doi.org/10.1016/j.micromeso.2015.01.051>.
- Hajamini, Zahra, Mohammad Amin Sobati, Shahrokh Shahhosseini, and Barat Ghobadian. 2016. "Waste Fish Oil (WFO) Esterification Catalyzed by Sulfonated Activated Carbon under Ultrasound Irradiation." *Applied Thermal Engineering* 94: 1–10. <http://dx.doi.org/10.1016/j.applthermaleng.2015.10.101>.
- Ho, Wilson Wei Sheng, Hoon Kiat Ng, Suyin Gan, and Sang Huey Tan. 2014. "Evaluation of Palm Oil Mill Fly Ash Supported Calcium Oxide as a Heterogeneous Base Catalyst in Biodiesel Synthesis from Crude Palm Oil." *Energy Conversion and Management* 88: 1167–78. <http://linkinghub.elsevier.com/retrieve/pii/S0196890414002623> (March 7, 2015).
- ICONTEC. 2011. NTC 218. Grasas y Aceites Vegetales y Animales. Determinación Del Índice de Acidez y de La Acidez. Colombia. <https://tienda.icontec.org/wp-content/uploads/pdfs/NTC218.pdf>.
- ICONTEC. 1999. NTC 218. "Grasas Y Aceites Vegetales Y Animales. Determinacion de Índice de Acidez." (571). Colombia. <https://tienda.icontec.org/wp-content/uploads/pdfs/NTC218.pdf>.
- Jacobson, Kathlene, Rajesh Gopinath, Lekha Charan Meher, and Ajay Kumar Dalai. 2008. "Solid Acid Catalyzed Biodiesel Production from Waste Cooking Oil." *Applied Catalysis B: Environmental* 85(1–2): 86–91.
- Kansedo, Jibrail, Keat Teong Lee, and Subhash Bhatia. 2009. "Cerbera Odollam (Sea Mango) Oil as a Promising Non-Edible Feedstock for Biodiesel Production." *Fuel* 88(6): 1148–50. <http://dx.doi.org/10.1016/j.fuel.2008.12.004>.
- Kotwal, M. S. et al. 2009. "Transesterification of Sunflower Oil Catalyzed by Flyash-Based Solid Catalysts." *Fuel* 88(9): 1773–78. <http://dx.doi.org/10.1016/j.fuel.2009.04.004>.
- Lam, Man Kee, and Keat Teong Lee. 2010. "Accelerating Transesterification Reaction with Biodiesel as Co-Solvent: A Case Study for Solid Acid Sulfated Tin Oxide Catalyst." *Fuel* 89(12): 3866–70. <http://dx.doi.org/10.1016/j.fuel.2010.07.005>.
- Leofanti, G et al. 1997. "Catalyst Characterization: Characterization Techniques." *Catalysis Today* 34: 307–27. [https://ac-els-cdn-com.ezproxy.unal.edu.co/S0920586196000569/1-s2.0-S0920586196000569-main.pdf?\\_tid=19d5e4b8-7ff0-4112-8d38-dcc4bfd030cd&acdnat=1550332601\\_264d3d96907b4cb6bcc5cdfbeff93007](https://ac-els-cdn-com.ezproxy.unal.edu.co/S0920586196000569/1-s2.0-S0920586196000569-main.pdf?_tid=19d5e4b8-7ff0-4112-8d38-dcc4bfd030cd&acdnat=1550332601_264d3d96907b4cb6bcc5cdfbeff93007) (February 16, 2019).
- Leung, Dennis Y C, Xuan Wu, and M. K H Leung. 2010. "A Review on Biodiesel Production Using Catalyzed Transesterification." *Applied Energy* 87(4): 1083–95. <http://linkinghub.elsevier.com/retrieve/pii/S0306261909004346> (July 10, 2014).

- Liu, Wei, Ping Yin, Xiguang Liu, and Rongjun Qu. 2014. "Design of an Effective Bifunctional Catalyst Organotriphosphonic Acid-Functionalized Ferric Alginate (ATMP-FA) and Optimization by Box-Behnken Model for Biodiesel Esterification Synthesis of Oleic Acid over ATMP-FA." *Bioresource Technology* 173: 266–71. <http://dx.doi.org/10.1016/j.biortech.2014.09.087>.
- Maneerung, Thawatchai, Sibudjing Kawi, and Chi Hwa Wang. 2015. "Biomass Gasification Bottom Ash as a Source of CaO Catalyst for Biodiesel Production via Transesterification of Palm Oil." *Energy Conversion and Management* 92: 234–43. <http://dx.doi.org/10.1016/j.enconman.2014.12.057>.
- Mansir, Nasar et al. 2018. "Modified Waste Egg Shell Derived Bifunctional Catalyst for Biodiesel Production from High FFA Waste Cooking Oil. A Review." *Renewable and Sustainable Energy Reviews* 82(November 2016): 3645–55.
- Mendonça, Iasmin M. et al. 2019. "New Heterogeneous Catalyst for Biodiesel Production from Waste Tucumã Peels (*Astrocaryum Aculeatum* Meyer): Parameters Optimization Study." *Renewable Energy* 130: 103–10.
- Metawea, Rodaina et al. 2018. "Process Intensification of the Transesterification of Palm Oil to Biodiesel in a Batch Agitated Vessel Provided with Mesh Screen Extended Baffles." *Energy* 158: 111–20.
- Noshadi, I., N. A.S. Amin, and Richard S. Parnas. 2012. "Continuous Production of Biodiesel from Waste Cooking Oil in a Reactive Distillation Column Catalyzed by Solid Heteropolyacid: Optimization Using Response Surface Methodology (RSM)." *Fuel* 94: 156–64. <http://dx.doi.org/10.1016/j.fuel.2011.10.018>.
- Nurfitri, Irma et al. 2013. "Potential of Feedstock and Catalysts from Waste in Biodiesel Preparation: A Review." *Energy Conversion and Management* 74: 395–402. <http://linkinghub.elsevier.com/retrieve/pii/S0196890413002586> (March 13, 2015).
- Rabiah Nizah, M. F. et al. 2014. "Production of Biodiesel from Non-Edible *Jatropha Curcas* Oil via Transesterification Using Bi<sub>2</sub>O<sub>3</sub>-La<sub>2</sub>O<sub>3</sub> Catalyst." *Energy Conversion and Management* 88: 1257–62. <http://dx.doi.org/10.1016/j.enconman.2014.02.072>.
- Rajamma, Rejini et al. 2009. "Characterisation and Use of Biomass Fly Ash in Cement-Based Materials." *Journal of Hazardous Materials* 172(2–3): 1049–60.
- Salamatinia, Babak, Hamed Mootabadi, Subhash Bhatia, and Ahmad Zuhairi Abdullah. 2010. "Optimization of Ultrasonic-Assisted Heterogeneous Biodiesel Production from Palm Oil: A Response Surface Methodology Approach." *Fuel Processing Technology* 91(5): 441–48.
- Sharma, Meeta, Arif Ali Khan, S. K. Puri, and D. K. Tuli. 2012. "Wood Ash as a Potential Heterogeneous Catalyst for Biodiesel Synthesis." *Biomass and Bioenergy* 41: 94–106. <http://dx.doi.org/10.1016/j.biombioe.2012.02.017>.

- Thommes, Matthias et al. 2015. "IUPAC Technical Report Physisorption of Gases, with Special Reference to the Evaluation of Surface Area and Pore Size Distribution (IUPAC Technical Report)." <https://www.3p-instruments.com/wp-content/uploads/2017/04/2015-IUPAC-Technical-Report.pdf> (February 18, 2019).
- Uprety, Bijaya K., Wittavat Chaiwong, Chinomnso Ewelike, and Sudip K. Rakshit. 2016. "Biodiesel Production Using Heterogeneous Catalysts Including Wood Ash and the Importance of Enhancing Byproduct Glycerol Purity." *Energy Conversion and Management* 115: 191–99. <http://dx.doi.org/10.1016/j.enconman.2016.02.032>.
- Vargas, Edgar M., Márcia C. Neves, Luís A.C. Tarelho, and Maria I. Nunes. 2019. "Solid Catalysts Obtained from Wastes for FAME Production Using Mixtures of Refined Palm Oil and Waste Cooking Oils." *Renewable Energy* 136: 873–83.
- Volli, Vikranth, Mihir Kumar Purkait, and Chi Min Shu. 2019. "Preparation and Characterization of Animal Bone Powder Impregnated Fly Ash Catalyst for Transesterification." *Science of the Total Environment* 669: 314–21.
- Wan Omar, Wan Nor Nadyaini, and Nor Aishah Saidina Amin. 2011a. "Biodiesel Production from Waste Cooking Oil over Alkaline Modified Zirconia Catalyst." *Fuel Processing Technology* 92(12): 2397–2405. <http://linkinghub.elsevier.com/retrieve/pii/S0378382011003031> (January 2, 2015).
- Wan Omar, Wan Nor Nadyaini, and Nor Aishah Saidina Amin. 2011b. "Optimization of Heterogeneous Biodiesel Production from Waste Cooking Palm Oil via Response Surface Methodology." *Biomass and Bioenergy* 35(3): 1329–38. <http://dx.doi.org/10.1016/j.biombioe.2010.12.049>.



---

## SECTION D - Optimization of FAME production in continuous fixed-bed reactor

In section D the design and construction of a continuous fixed bed reactor (CFBR) is presented and the study to optimize the FAME production process with methanol at 60 °C, using mixtures of WCO and RPO and pelletized biomass fly ashes as chosen solid catalyst (section B). The effect of three operating variables (residence time, WCO/RPO mass ratio and methanol/oil molar ratio) on FAME concentration was studied, using the experimental Box-Benhken design and the Response Surface Methodology. Some preliminary assays were carried out to identify the time at which the steady state of the continuous fixed bed reactor used in this work was reached. Seventeen experimental runs were required, including five replicates of the central point); all were carried out using a fixed bed depth of 15 cm (bulk density: 2.16 g/mL) and an operating time of 9 h. Furthermore, the solid catalyst was characterized by SEM, EPS, XRD, BET, FT-IR and Hammett indicators. Additionally, the pelletized catalytic stability of the biomass fly ash fixed bed was evaluated through an assay during 32 h of operation, where the FAME concentration was monitored over time. The optimal operating conditions found by the regression model were used in this assay.

- The information presented in this section was adapted from the following published article:

E. M. Vargas, Duvan O. Villamizar, M. C. Neves, and M. I. Nunes, "Pelletized biomass fly ash for FAME production: optimization of a continuous process", *Fuel*, vol. 293, pp. 120425, 2021, doi: <https://doi.org/10.1016/j.fuel.2021.120425>.



## 4 Pelletized biomass fly ash for FAME production: optimization of a continuous process

**Abstract:** Circularity in the resources usage is one of the current challenges in the development of our civilization. At the same time, there is an imperative need for cleaner and competitive energy sources, alternative to those of fossil origin. In this context, the present work aimed to optimize a continuous process for fatty acid methyl esters (FAME) production using residual resources, namely waste cooking oil (WCO) and pelletized biomass fly ash as catalyst. A continuous fixed bed reactor was designed and built. The pelletized catalyst performance was assessed in the reaction system, which was fed with a mixture of refined palm oil (RPO), WCO and methanol at 60 °C. The effect of three operating variables (residence time, WCO/RPO mass ratio and methanol/oil molar ratio) on FAME concentration was studied, using experimental the Box-Benhken design and the Response Surface Methodology (RSM). The maximum FAME concentration achieved was c.a. 89.7 % under the following operating conditions: 124 min of residence time, 74.6 wt% WCO/RPO and 12:1 methanol/oil molar ratio. The catalyst kept stable over the 32 h of continuous operation, without noticeable deactivation. Thus, the pelletization of an industrial biomass fly ash, with bifunctional catalytic properties, allowed its application to the FAME production in a continuous regime, with high performance even when high percentages of WCO were used as feedstock.

**Keywords:** Biomass fly ash; continuous fixed bed reactor; heterogeneous catalysts; FAME; response surface methodology; waste cooking oil.

## 4.1 Introduction

In order to meet the current and growing demand for liquid fuels as well as the increasing concern about climate change, biodiesel has been pointed out as a sustainable solution to partially replace fossil diesel (Suarez et al. 2009). Biodiesel is synthesized through the transesterification and esterification reactions of vegetable oils, animal fats or waste vegetable oil using alcohols and basic and acid catalysts (homogeneous, heterogeneous and enzymatic) (Fang et al. 2011; Mittelbach et al. 1983; Pirez et al. 2012).

Some residual biomass fly ashes have been proven to have catalytic properties suitable for biodiesel production (Vargas et al. 2019a). Uprety et al. (2016) evaluated wood ash from two different sources (birch bark and fly ash from a biomass-based power plant) in the biodiesel production; 88.06 % was the highest yield to FAME observed with birch bark ash. Sharma et al. (2012) studied calcined wood ash and activated wood ash as catalysts for the production of biodiesel using *Jatropha* oil obtaining a conversion in the range of 97-99 %. In both studies the wood ashes contained a high dispersion of  $\text{CaCO}_3$ ,  $\text{CaO}$ ,  $\text{Ca(OH)}_2$  and  $\text{SiO}_2$  (active phase) pointed out as responsible for the observed catalytic performance.

There are several research works (e.g. Vargas et al. (2019a), Teixeira et al. (2019), Miller et al. (2006) and Vargas et al. (2019b)) that have been dedicated to the valorization of residual materials for biodiesel production, aiming to reduce the production costs but also to operationalize the principles of circular economy. Those works (e.g. Tarelho et al. (2015), Jensen et al. (2004)) focused both in the preparation of residual materials with catalytic properties and in the use of residual vegetable oils and fats.

Currently, the biodiesel production at industrial scale comprises three main stages: (i) reaction stage carried out in batch, semi-continuous or continuous reactors, (ii) settling stage for light phase and glycerin separation and (iii) purification stage of the light phase, to obtain a purified biofuel. The reaction stage is carried out at moderate conditions between 50.7 – 405.3 kPa and 30 – 90 °C, using a homogeneous basic catalyst (Evangelista et al. 2012) or acid catalyst when the vegetable oils have high free fatty acids (FFA) content. However, the basic catalysts can

form soaps in the presence of FFA and water, negatively affecting the efficiency of the separation stage (Freedman et al. 1981; Zhang et al. 2003). Other hotspot of the conventional biodiesel production process is the high energy consumption in the separation stage (if centrifuges are used), besides the contamination of large quantities of water during the purification stage contributing for the high water footprint of the process (Vyas et al. 2010).

Nowadays, in some industrial processes, the continuous flow and fixed bed reactors are the most widely used due to their high production capacity and easy process control (Andrigo et al. 1999; Tran et al. 2017). Therefore, this type of reactors can be considered as a good alternative to produce biodiesel at industrial scale. At lab scale, Park et al. (2008) used a continuous fixed bed reactor packed with a solid catalyst of  $WO_3/ZrO$  for oleic acid transesterification; the conditions used were 75 °C, methanol/oil ratio of 20:1 and an operation time of 140 h; the FAME yield achieved was 85 %. Moreover, Da Silva et al. (2014) evaluated the behavior of zinc oxide and aluminum oxide as catalysts in biodiesel production, using soybean oil at 100 °C, a methanol/oil ratio of 20:1 in a continuous reactor with a mass flow of 250 g/h and a residence time of 5 h; the yield to FAME achieved was 75 %. Kutálek et al. (2014) performed rapeseed oil transesterification in a continuous flow reactor and packed bed, using Mg-Al-K and Mg-Al-Na mixed oxide catalyst, with a methanol/oil ratio of 24:1, at 140 °C and residence time of 1.54 h, reaching a yield to FAME of 77 %. Likewise Ren et al. (2012) assessed the behavior of an activated resin for the transesterification of soybean oil in a continuous flow reactor using a methanol/oil ratio of 9:1, at 50 °C and a residence time of 56 min; a yield to FAME of 95.2 % was obtained.

The aim of this work was to assess the catalytic performance of pelletized biomass fly ash in the production of FAME in a continuous fixed bed reactor, using mixture of Refined Palm Oil (RPO) and Waste Cooking Oil (WCO) with methanol as raw materials. An experimental Box-Benhken design and Response Surface Methodology (RSM) was used for the optimization and interpretation of the results obtained. Thus, this work contributes to decrease the environmental burdens (and costs) of the conventional biodiesel process, by using residual materials, in a continuous regime, about which there is some lack of knowledge in the research literature.

## 4.2 Materials and Methods

The Box-Benhken experimental design and Response Surface Methodology (RSM) were used to design the experiments to optimize the FAME production process in a continuous fixed bed reactor and for the data treatment.

Previously, the pelletized solid catalyst (FAD) was prepared and characterized in terms of some of its chemical, physical and structural properties. The raw-material for FAME synthesis consisted of a blends of WCO and RPO in different ratios. The adopted procedures are described in the next sections as well as the analytical methods used and design and construction of continuous reactor.

### 4.2.1 Oil mixtures characterization

Three mixtures were prepared using different percentages of RPO and WCO, namely: M1 (100 wt% RPO), M2 (50 wt% RPO, 50 wt% WCO) and M3 (100 wt% WCO), which were characterized in terms of acid value (NTC 218) (ICONTEC 218 1999), density (NTC 336) (ICONTEC 1998), and saponification number, SN (NTC 335) (ICONTEC 1998). The SN was used to calculate molecular weight (MW) using the Equation 4.1 (Mansir et al. 2018).

$$MW = \frac{56,1 \times 1000 \times 3}{SN} \quad (4.1)$$

The FFA content was calculated from the acid value (AV, mgKOH/g) using the Equation 4.2 (Mansir et al. 2018).

$$FFA = \frac{AV}{2} \quad (4.2)$$

### 4.2.2 Catalysts preparation and characterization

The catalyst pellets were prepared using the protocol described by Da Silva et al. (2014), using biomass fly ash. This ash was collected in a dedusting flue gas equipment (electrostatic

precipitator) of a thermal power-plant using residual eucalyptus biomass as fuel, located in the Centre Region of Portugal.

The particle size analysis of the fly ash (powder) showed the following size distribution (ASTM series): 66.4 wt% has a particle size in the 200-230 mesh with diameters ranging between 75  $\mu\text{m}$  and 63  $\mu\text{m}$ , respectively; 33.6 wt% has a particle size smaller than 230 mesh. A mixture of fly ash (60.94 wt%), soluble starch (1.2 wt%) and distilled water (37.86 wt%) were used for the catalyst pellet manufacturing. The resulting aqueous paste was extruded using a syringe with 2 mm internal diameter tip, obtaining pellets 1 to 1.5 cm in length, which were dried in an oven at 120 °C for 12 h.

Figure 4.1 shows pictures of biomass fly ash powder used in the pellets (Figure 4.1 a) and the pellets ready (Figure 4.1 b) to be used for the FAME production.

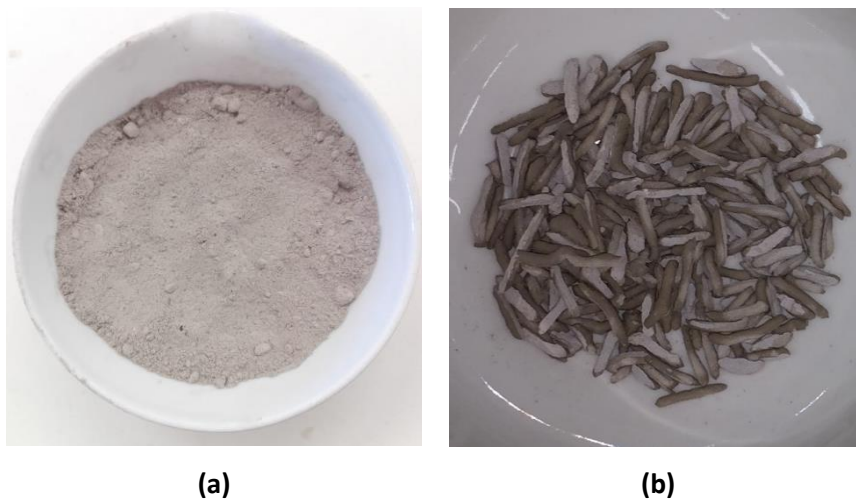


**Figure 4.1-** Biomass fly ash catalyst: (a) powder (before pelletization), (b) pelletized.

The pelletized biomass fly ash catalyst was further characterized in terms of: (i) crystallographic structures using X-Ray Diffraction (XRD, PAN Analytical Empyrean X-ray diffractometer equipped with Cu-K $\alpha$  radiation source  $\lambda= 1.54178 \text{ \AA}$  at 45 kV/ 40 mA); (ii) surface area, pore size and pore volume was carried out by nitrogen adsorption studies at 77 K using a surface area analyzer Micromeritics Gemini V- 2380); (iii) surface morphology using surface scanning electron microscopy (SEM, using Hitachi SU-70 microscope operating at 15 kV); (iv) functional

surface species by infrared Fourier transform (FTIR, Agilent CARY 630 with a wave number range of 400 to 4000  $\text{cm}^{-1}$ ); (v) superficial elemental atomic concentration by means of X-ray photoelectronic spectroscopy (XPS, using a PHOIBOS 150 2D-DLD equipment, with a monochromatic Al K-radiation source -FOCUS 500- operated at 100 W) and (vi) basic and acid strength by using Hammett indicators following the protocol described by Vargas et al. (2019a) (for basic strength: neutral red,  $\text{pK}_a = 6.8$ ; bromothymol blue,  $\text{pK}_a = 7.2$ ; phenolphthalein,  $\text{pK}_a = 9.3$ ; indigo carmine,  $\text{pK}_a = 12.2$ ; and 2,4-dinitroaniline,  $\text{pK}_a = 15.0$ ; indicators for acid strength: bromothymol blue,  $\text{pK}_a = 7.2$ ; neutral red,  $\text{pK}_a = 6.8$ ; bromocresol purple,  $\text{pK}_a = 6.1$ ; bromocresol green,  $\text{pK}_a = 4.7$ ; and bromophenol blue,  $\text{pK}_a = 3.8$ ).

### **4.2.3 Experimental setup**

Figure 4.2 and Figure 4.3 show the experimental setup assembled for this work. It had three main zones: (1) feed, (2) reaction and (3) separation. In the feed zone there was a closed glass container with a capacity of 1 L where the reagents (methanol and oil mixture) were mixed and heated (heating plate). This mixture was pumped from the V-100 to the bottom of the continuous fixed bed reactor (Figure 4.2. Reaction zone) using a peristaltic pump (Masterflex and model: EW-77122) and a rotameter (Gilmond) was used to measure the flowrate.



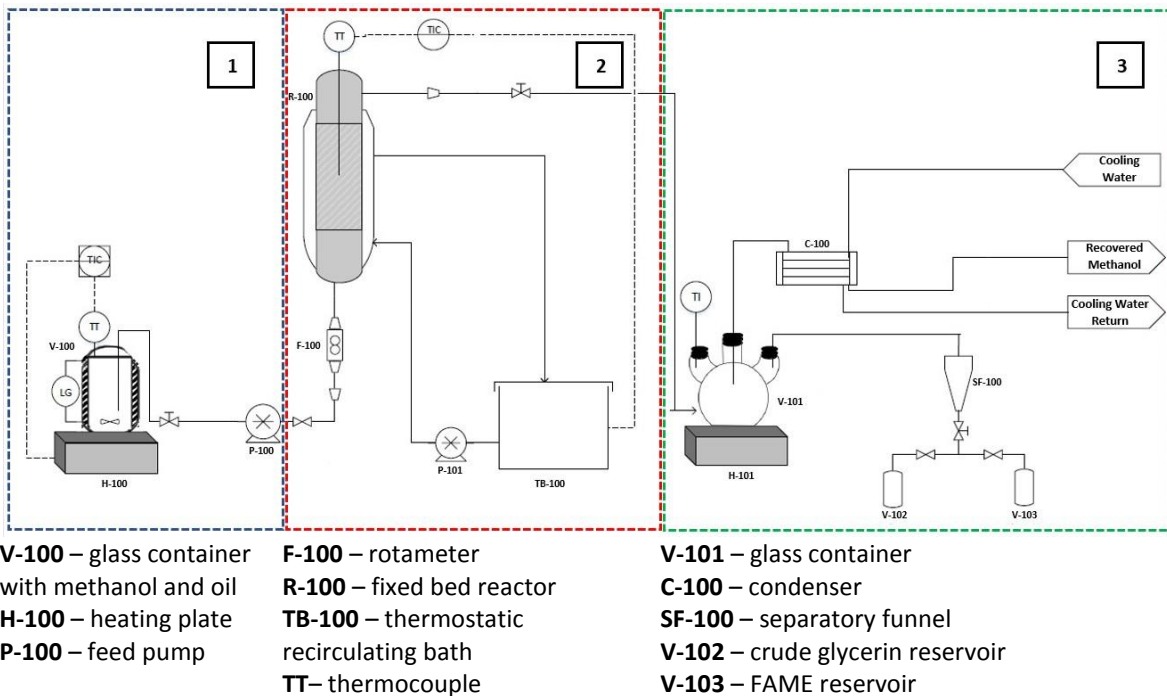


**Figure 4.2** - Experimental setup diagram used in this work (1. Feed zone, 2. Reaction zone, 3. Separation zone).

For each oil mixture tested, a pump calibration was carried out to guarantee the residence time (RT) set for each experiment. The operating flowrates used in this work ranged between 0.28 mL/min and 0.85 mL/min which were used together with the packing density and the fixed bed void fraction to calculate the residence time of the reactor in each experiment (Chattopadhyay and Ramkrishna 2013). The reactor was a glass tube with an internal diameter of 21.9 mm and 320 mm height, with two stainless-steel mesh to support the catalyst.

The temperature inside the reactor was controlled by a heating jacket connected to a thermostatic bath (Lauda Alpha A6). In order to ensure a uniform temperature inside the reactor there was a thermocouple type K (Watlow AW) with three measuring points along the catalytic fixed bed.

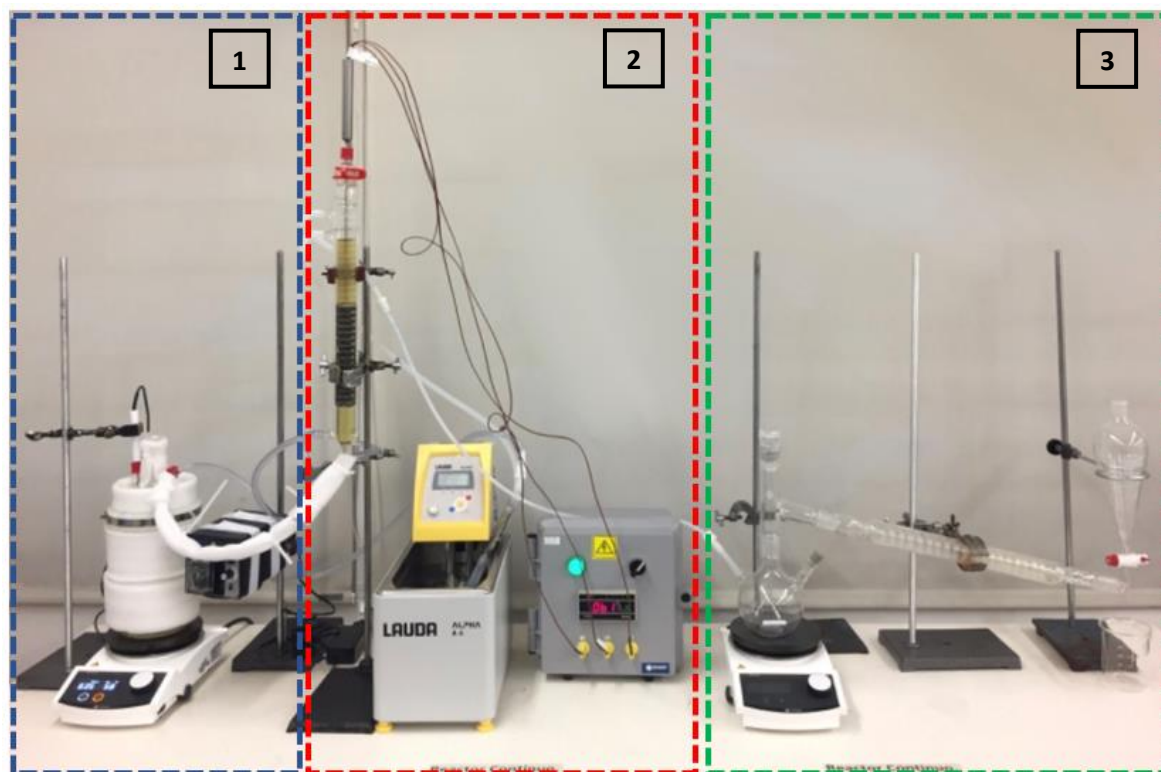


**Figure 4.3** - Assembly of the fixed bed reaction system for continuous FAME production.

Downstream of the reactor there was the separation step (Figure 4.2. Separation zone), where the reactor's outflow was separated into 3 fractions: methanol, crude glycerin and FAME. The devices used for the separation were a glass container (V-101), a condenser and separatory funnel. Firstly, the excess methanol was separated by heating the mixture of V-101 and recovered the alcohol by condensation (C-100). Then, the remaining mixture (in V-101) was transferred to a separatory funnel in order to separate the crude glycerin from FAME (light phase). These two products were then stored in different reservoirs (V-102 and V-103). The sampling was performed from FAME's reservoir for chromatographic (GC) analysis.

#### 4.2.4 FAME content

After the separation step, the collected samples were characterized in terms of FAME content with a SHIMADZU G-C 2014 gas chromatograph (GC) equipped with a flame ionization detector (FID), a capillary column SGE BP-20 (60 m x 0.25 mm ID x 0.25  $\mu$ m) and using helium as a carrier gas with a flow rate of 16.7 mL/min and a pressure of 2.5 atm. The injector (AOC-20i) was

operated at 200 °C and an injection volume of 2.0 µL in Split mode. Methyl heptadecanoate was used as an internal standard and the samples were solubilized in hexane grade HPLC. The samples to be analyzed were firstly dehydrated (using anhydrous sodium sulfate) and filtered (using Thermo Scientific Nalgene membranes of 0,2 µm). Then, one mixed 500 µL of the phase rich in esters (i.e., the solution resulting from the previous step) in hexane (10 mg / 10 mL), 200 µL of methyl heptadecanoate solution in hexane (10 mg / 10 mL) and 800 µL of hexane. The FAME concentration was calculated using Equation 4.3 (AENOR-EN 14103 2011).

$$C = \frac{\sum A - A_{EI}}{A_{EI}} \times \frac{W_{EI}}{W} \quad (4.3)$$

Where  $C$  is the concentration of FAME in the purified final mixture (w/w),  $\sum A$  is the total peak areas of the methyl ester from  $C_{14}$  until  $C_{24:1}$ ,  $A_{EI}$  is the peak area corresponding to methyl heptadecanoate,  $W_{EI}$  is the mass (mg) of methyl heptadecanoate used and is the mass (mg) of the sample used in the analysis.

#### 4.2.5 Preliminary assays for steady state identification

Some preliminary assays were carried out to identify the time at which the steady state of the continuous fixed bed reactor used in this work was reached. The range of resident time, WCO/RPO mass ratio and methanol/oil molar ratio tested in these assays were chosen based on data reported by different authors and shown in Table 4.1. These assays were carried out at temperature  $T = 60$  °C with a catalytic bed depth of 15 cm (bulk density of 2.16 g/mL) around 14 h of continuous operation. No replicates of these assays were performed.

**Table 4.1** - Operating conditions of continuous flow reactors to produce FAME.

<b>Oil</b>	<b>Catalyst</b>	<b>T (°C)</b>	<b>RT (min)</b>	<b>Methanol/oil (mol/mol)</b>	<b>Reference</b>
Sunflower	Calcium oxide	60	120	12:1	(Miladinović et al. 2020)
WCO	Sodium hydroxide	60	75	6:1 to 12:1	(Avellaneda and Salvadó 2011)
Soybean	Resin D261 activated	50	56	9:1	(Ren et al. 2012)
Cottonseed	Sodium silicate calcined	55	180	12:1	(Gui et al. 2016)
Soybean	Sodium silicate	60	65	9:1	(Luo et al. 2017)

The results obtained in these assays are shown in Figure 4.4, where it is possible to identify the steady state achievement at approximately 6h of operating time. Furthermore, it is observed that a 3:1 molar ratio methanol/oil produces the lower content of FAME whereas the 12:1 molar ratio produces the higher one, and does not have a significant difference with respect to 18:1 for the same RT. Therefore, the range from 6:1 to 12:1 (mol/mol) for methanol/oil was selected in the optimization study (see next section). Regarding the residence times tested (60, 120 and 180 min), they were maintained in the process' optimization study given the high concentrations of FAME obtained in these preliminary assays.

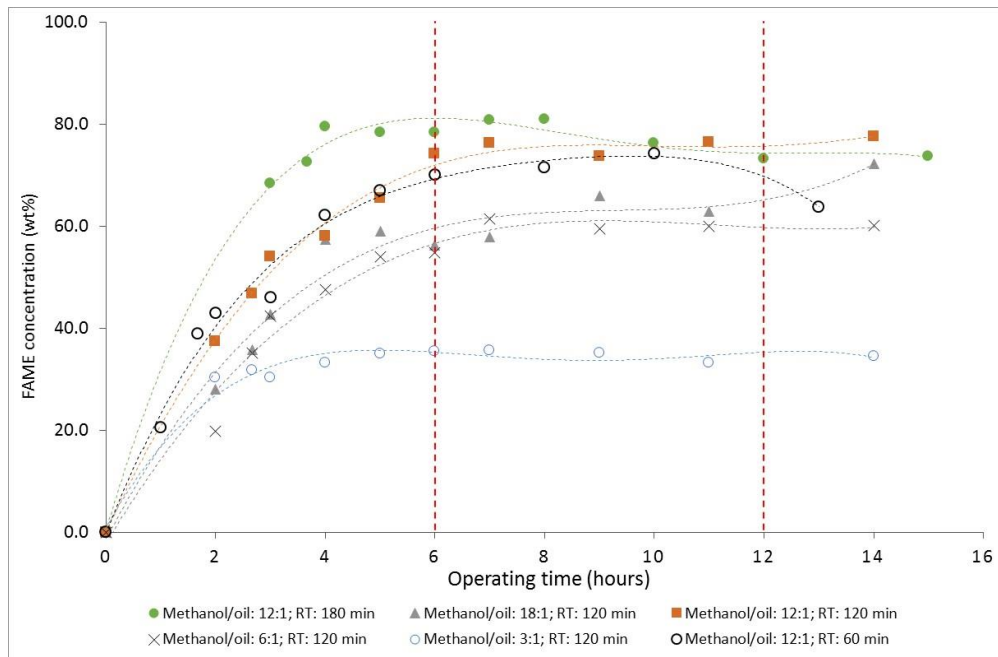


**Figure 4.4** - Preliminary assays to identify the steady state of the continuous fixed bed reactor.

In short, for the residence time ranging between 60 and 180 min, 7, 8 and 9 h were set as sampling times in the next experimental design, since the steady state is assured.

#### 4.2.6 Experimental design for optimization of the FAME production

Software Design - Expert 11.1.0 was used to perform the processing and analysis of experimental data. The experimental Box-Benkhken design is a spherical and rotating design (Mishra et al. 2008), which consists of the center point and midpoints of the edges. It is represented as a shape consisting of three interlaced  $2^2$  factorial designs (Aslan and Cebeci 2007) and a center point. Likewise, the RSM creates correlations, evaluates the effects of various factors and their interactions to obtain the system response (Liu et al. 2014; Salamatinia et al. 2010).

The influence on FAME concentration (response variable) of three factors – residence time, WCO/RPO mass ratio and methanol/oil molar ratio – was investigated. Table 4.2 presents the experimental range and factor levels tested in this work.

**Table 4.2** - Factor and levels of process variables used in the Box – Behnken experimental design.

Real variables	Coded variables	Level		
		Low (-1)	Medium (0)	High (+1)
Residence time (min)	<b>A</b>	60	120	180
WCO/RPO (wt%)	<b>B</b>	0 (M1)	50 (M2)	100 (M3)
Methanol/oil (mol/mol)	<b>C</b>	6	9	12

All experiments were carried out using a fixed bed depth of 15 cm (bulk density: 2.16 g/mL), temperature of 60 °C and an operating time of 9 h. As stated before, sampling of purified FAME (from reservoir V-102, Figure 4.2) was performed at 7, 8 and 9 h for GC characterization. The average of these three points is taken as the value of the FAME concentration (experimental).

Seventeen experimental assays were conducted, including five repetitions of the center point. The correlation in the form of a quadratic polynomial equation was developed to predict the response (FAME concentration) based on independent variables (or factors) and their interactions according to Equation 4.4.

$$Y = \beta_0 + \sum_{i=1}^k \beta_i x_i + \sum_{i=1}^k \beta_{ii} x_i^2 + \sum_{i=1}^k \sum_{j=i+1}^k \beta_{ij} x_i x_j + \varepsilon \quad (4.4)$$

Where  $Y$  is the predicted response for the process, i.e., the dependent variable;  $\beta_0$  is the intercept coefficient (offset);  $\beta_i$  are the linear terms;  $\beta_{ii}$  are the quadratic terms;  $\beta_{ij}$  are the interaction terms;  $x_i$  and  $x_j$  are the independent variables; and  $\varepsilon$  is the error (Hajamini et al. 2016).

The inference in the regression model was made through an analysis of variance (ANOVA), for a 95 % confidence level, where statistically significant factors in the response variable were identified, and an analysis of the model determination coefficients,  $R^2$  and  $R^2$  adjusted (Adj  $R^2$ ), were used to evaluate the degree of adjustment of the regression model to the experimental data.

Validation of the assumptions of the regression model was performed through a residual analysis (normality and residual plots). This analysis was based on standardized residues.

Once the best regression model was selected and validated, optimal reactor operating conditions were identified using RSM. Then, for model validity purposes, three runs were performed using the optimal conditions, which allowed to determine the deviations between the data predicted by the model and the experimental ones. Additionally, the catalytic stability of the biomass fly ash fixed bed was evaluated through an assay during 32 h of operation, where the FAME concentration was monitored over time. The optimal operating conditions found by the regression model were used in this assay.

### 4.3 Results and discussion

#### 4.3.1 Oil mixtures characterization

The properties of the oil mixtures prepared for this study are shown in the Table 4.3.

**Table 4.3** - Properties of the oil mixtures used.

	<b>M1</b>	<b>M2</b>	<b>M3</b>
<b>%WCO</b>	0	50	100
<b>%RPO</b>	100	50	0
Density (g/mL)	0.896 ± 0.005	0.905 ± 0.006	0.910 ± 0.005
AV (mg KOH/g)	0.052 ± 0.008	4.254 ± 0.062	7.328 ± 0.152
FFA (wt%)	0.026 ± 0.008	2.127 ± 0.032	3.664 ± 0.069
MW (g/mol)	826.444 ± 0.252	837.189 ± 1.586	847.935 ± 2.681

The properties of M1 (RPO) are similar to those reported by Kansedo et al. (2009), Núñez et al. (2019) and Singh and Dipti (2010). Regarding the properties of the oil mixture M3, Wan Omar et al. (2011a) and Lam et al. (2010) found results similar for both FFA (wt%) and AV (mg KOH/g). Seeing the WCO has an FFA content less than 15 wt% it can be classified as yellow fat (Avhad and Marchetti 2015).

### 4.3.2 Catalysts characterization

The solid catalyst prepared was characterized for some textural properties such as specific surface area, crystalline structure, surface functional groups, but also their basic and acid strength, etc. The results are shown and discussed in the next sections.

#### 4.3.2.1 XRD analysis

The XRD diffractogram of the biomass fly ash catalyst is shown in Figure 4.5 where there are the diffraction peaks corresponding to sylvite phase (potassium chloride, KCl, ICDDPDF4+00-041-1476) detected at  $2\theta = 28.4^\circ$ ,  $40.7^\circ$  and  $50.2^\circ$ , calcite phase (calcium carbonate,  $\text{CaCO}_3$ , ICDDPDF4+01-080-9776) detected at  $2\theta = 23.2^\circ$ ,  $29.3^\circ$ ,  $36.0^\circ$ ,  $39.1^\circ$ ,  $43.4^\circ$ ,  $47.7^\circ$ ,  $48.7^\circ$  and  $57.7^\circ$ , portlandite phase (Calcium hydroxide,  $\text{Ca}(\text{OH})_2$ , ICDDPDF4+01-083-4600) detected at  $2\theta = 47.7^\circ$  and  $64.9^\circ$  and quartz phase (silicon dioxide,  $\text{SiO}_2$ , ICDDPDF4+04-006-1757) detected at  $2\theta = 21.0^\circ$  and  $26.7^\circ$ . Similar results were reported by Miladinović et al. (2020) for walnut ash; these authors found compounds of  $\text{CaO}$ ,  $\text{Ca}(\text{OH})_2$  and  $\text{SiO}_2$ . Indeed, the combustion of biomass residues generates compounds of  $\text{CaO}$ ,  $\text{Ca}(\text{OH})_2$  and  $\text{CaCO}_3$  as described by Osman et al. (2018) and Luque et al. (2012). These alkaline species (which order of basicity is: oxide > hydroxide > carbonate form) and the sylvite species (Betiku et al. 2016; Nath et al. 2019) are able to catalyse the reaction of FAME production (Yoosuk et al. 2011).

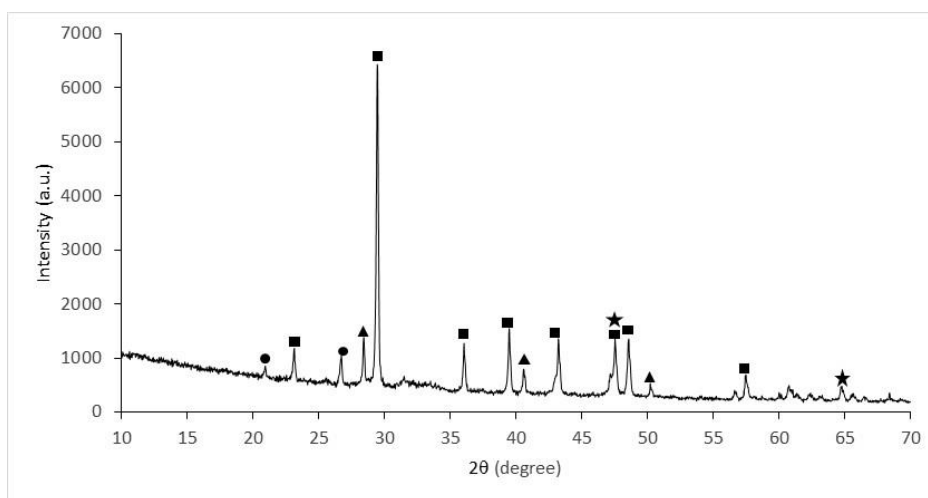


**Figure 4.5** - XRD Diffractogram of biomass fly ash catalyst (●  $\text{SiO}_2$ , ■  $\text{CaCO}_3$ , ▲ KCl, ★  $\text{Ca}(\text{OH})_2$ ).



The absence of CaO and the presence of Ca(OH)<sub>2</sub> and CaCO<sub>3</sub> in the pelletized biomass fly ash (Figure 4.5) can be explained by hydration and carbonation reactions that occurred during the preparation of this catalyst from powder ash. Indeed, the CaO existing in the powder ash (characterized in a previous work (Vargas et al. 2019b)) must have been converted to Ca(OH)<sub>2</sub> and CaCO<sub>3</sub> due to the contact with water and atmospheric air.

#### 4.3.2.2 Hammett indicators and BET surface area analyses

Biomass fly ash used in this work has an intermediate basic strength ( $10.1 \leq \text{pKa} < 12.2$ ), due to the high basicity of the metal-oxygen groups (Lewis bases) present in the calcium compounds and alkaline metal (K and Na) on its surface (see Sections 4.3.2.1 and 4.3.2.5) and a low acid strength ( $6.8 \leq \text{pKa} < 7.2$ ) (Pavlović et al. 2020).

This ash has a surface area (BET) of 4.8568 m<sup>2</sup>/g, a pore volume of 0.009691 cm<sup>3</sup>/g and an average pore diameter of 74.853 Å, which is according to the reported data by Chakraborty et al. (2010). Given the pore diameter, this material has favorable characteristics for the absorption and desorption of triglyceride molecules, diglycerides, monoglycerides, glycerin and FAME, since it is greater than 58 Å (Jacobson et al. 2008).

Figure 4.6 shows nitrogen absorption-desorption isotherm the type IV for the catalyst assessed, which is in agreement with the classification proposed by the International Union of Pure and Applied Chemistry (Thommes et al. 2015). The isotherms' behavior is characteristic of mesoporous catalysts and low surface area.

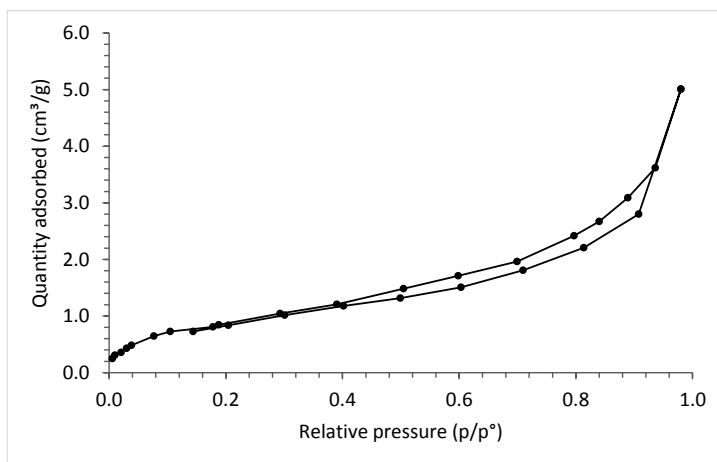


**Figure 4.6** - Absorption and desorption isotherms of biomass fly ash.

#### 4.3.2.3 SEM analysis

Figure 4.7 shows the SEM images for the biomass fly ash catalyst.

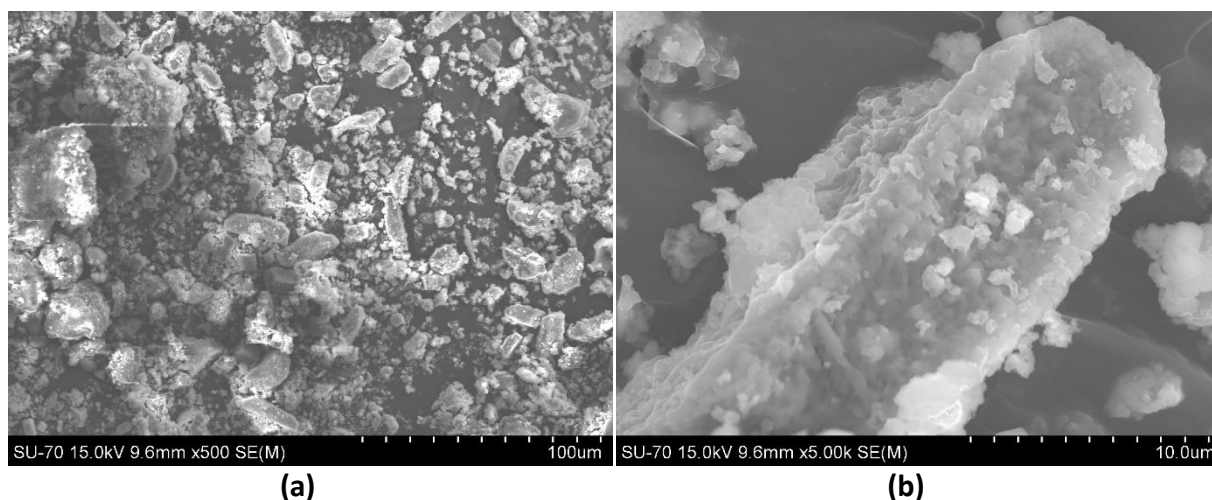


**Figure 4.7** - SEM images of biomass fly ash using a magnification of 500X (a) and 5000X (b).

In Figure 4.7 a, the particles have irregular shapes of different sizes, this morphology is like that found by Wang et al. (2008) for wood ashes. On the other hand, in Figure 4.7 b, the catalyst particles have a diameter near 100 nm, which is similar to the eucalyptus fly ashes characterized by Rajamma et al. (2009).

#### 4.3.2.4 FTIR analysis

The FTIR spectrum of the biomass fly ash catalyst used in this work is shown in Figure 4.8. A major absorption broadband is observed at  $1401\text{ cm}^{-1}$  and minor absorption bands at 712, 872, 2855 and  $2922\text{ cm}^{-1}$ , corresponding to asymmetric stretching and vibration modes in the carbonate group ( $\text{CO}_3^{2-}$ ). This result confirms the presence of  $\text{CaCO}_3$  in this ash already detected by XRD.

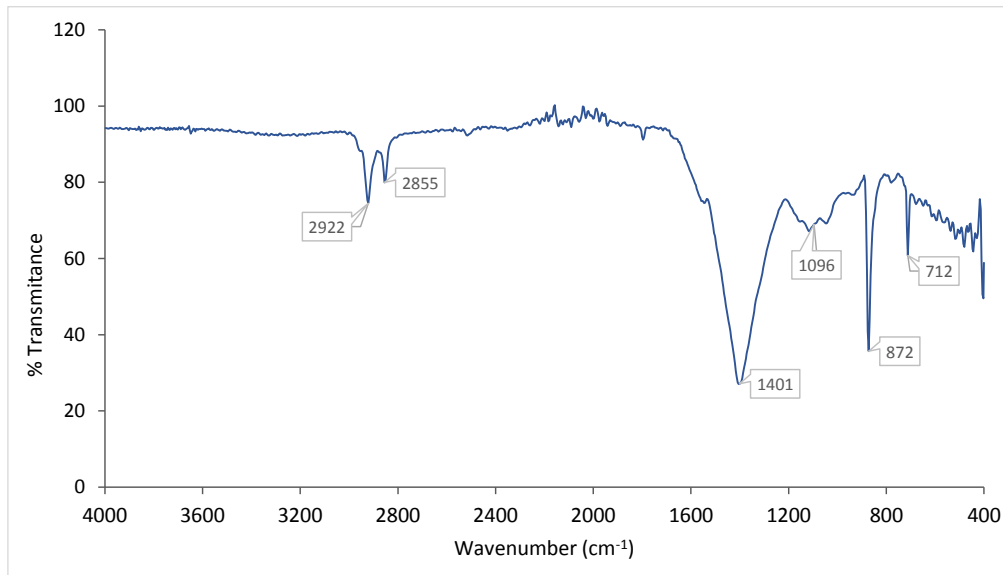


**Figure 4.8** - FTIR spectrum of biomass fly ash catalyst.

Groups  $\text{PO}_4^{3-}$  and Si-O (phosphates and silicon oxides) show wide absorption bands in the region of  $1096 \text{ cm}^{-1}$ ; similar bands were found by Maneerung et al. (2015) and Liang et al. (2020) in residues of fly ash from gasification of woody biomass and fly ash of rice husk respectively.

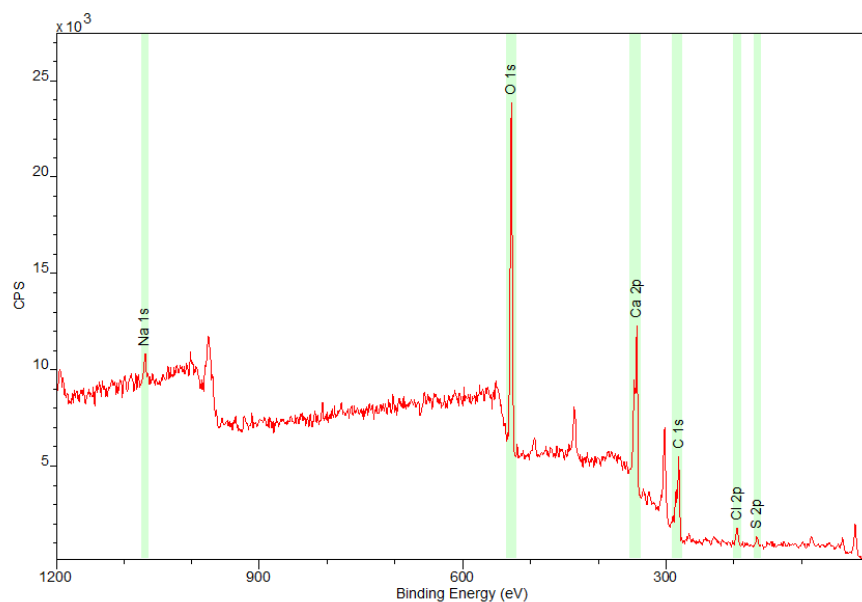
#### 4.3.2.5 XPS analysis

The biomass fly ash catalyst wide energy spectrum is shown in Figure 4.9. An intense peak of O1s can be seen at 528.68 eV, and peaks at 1069.06, 343.65, 281.65, 194.88 and 166.60 eV for Na1s, Ca2p, C1s, Cl2p and S2p, respectively. Yang et al. (2019) found similar binding energy peaks in the spectrum for carbon ash samples.

Table 4.4 shows the wide scanning result of surface (layer up to 10 nm) chemical composition of biomass fly ash. Elements O and C are presented in higher atomic concentrations on the surface of the catalyst.

**Table 4.4** - Summary of XPS analysis done on the surface of biomass fly ash catalyst.

Sample	Atomic concentration (%)										
	C	O	Ca	Mg	Cl	Na	Si	Al	K	S	P
Biomass fly ash	31.16	35.48	13.95	5.05	2.18	0.75	0.81	0.68	7.62	1.56	0.76


**Figure 4.9** - The XPS wide energy spectrum of biomass fly ash catalyst.

A significant amount of alkaline metals (Na and K) but mainly alkaline earth metals (Mg and Ca) was registered, which give the basic character to this solid material. It was also recorded the presence of Cl, Si, Al, S and P; some of these elements (e.g. Si and Al) give an acidic character to the catalyst (Pavlović et al. 2020). Similar atomic concentrations were found by Rajamma et al. (2009) for C, O, Ca and Na in fly ash of eucalyptus biomass of 38.7 %, 29.0 %, 12.1 % and 1.0 %, respectively.

#### 4.3.3 Optimization of FAME production process: regression model and statistical analysis

The experimental results and those predicted by the regression model (Equation 4.5) for each set of operating conditions (see Table 4.2) are shown in Table 4.5.

**Table 4.5** - Experimental and predicted results of RSM.

Run	Real variables			FAME concentration (wt%)	
	RT (min)	WCO/RPO (wt%)	Methanol/oil (mol/mol)	Experimental	Predicted*
1	60	50	12	84.9	84.7
2	120	100	12	85.3	83.3
3	180	0	9	72.4	70.2
4	120	0	6	59.8	61.8
5	180	50	12	92.0	92.1
6	180	50	6	75.0	75.3
7	120	50	9	85.11	84.9
8	120	50	9	84.5	84.9
9	60	0	9	52.8	50.9
10	120	100	6	62.2	60.1
11	180	100	9	61.1	63.0
12	120	50	9	84.8	84.9
13	120	50	9	84.7	84.9
14	120	0	12	75.8	77.9
15	60	100	9	59.4	61.7
16	60	50	6	62.2	62.1
17	120	50	9	85.5	84.9

\*Predicted by the regression model

The ANOVA results for the quadratic polynomial model are shown in Table 4.6, where one can see that the model has a good fit with an  $R^2 = 0.9859$  and  $Adj R^2 = 0.9678$ . The  $R^2$  value indicates that the model predicts 98.6 % of the response variability. However the lack of fit is significant ( $p$ -value 0.0006), which is undesirable. The lack-of-fit test is used as support test for adequacy of the fitting model. A significant lack of fit means that the variation of the repeats around their mean values is lower than the variation of the design points around their predicted values

(Miladinović et al. 2016). Nonetheless, in Figure 4.10 c one observe that predicted and experimental values are similar, therefore the lack of fit may be due to the existence of a systematic variation (experimental values) that cannot be explained by the regression model (Miladinović et al. 2016). Moreover, as will be discussed later, the experimental FAME concentration registered under the optimal operating conditions, obtained from the model, was close to the one predicted by the model.

**Table 4.6** - ANOVA table of the regression model.

Source of variations	Sum of squares	Degrees of freedom	Mean square	F - value	p – value
Model	2442.88	9	271.43	54.51	< 0.0001
Residual	34.85	7	4.98		
Lack of fit	34.23	3	11.41	73.78	0.0006
Pure error	0.6187	4	0.1547		
Total	2477.73	16			
	R <sup>2</sup> = 0.9859	Adj	Pred	C.V. <sup>a</sup> = 2.99 %	S.D. <sup>b</sup> = 2.23
		R <sup>2</sup> = 0.9678	R <sup>2</sup> = 0.7785		

<sup>a</sup> C.V.= coefficient of variation.

<sup>b</sup> S.D.= standard deviation.

The high F-value (54.51) and the low p-value (<0.0001) of the model means that it is statistically significant. The "Pred R<sup>2</sup>" and the "Adj R<sup>2</sup>" values are consistent since their difference is less than 0.2 (note reported by Design Expert software); which confirm that the fitting regression model satisfactorily predicts the effect of the three factors evaluated on FAME concentration. Equation 4.5 represents the fitting quadratic polynomial model (coded variables).

$$Y = 84.93 + 5.16 x_A + 0.9093 x_B + 9.82 x_C - 4.49 x_A \times x_B - 1.45 x_A \times x_C + 1.78 x_B \times x_C - 7.78 x_A^2 - 15.64 x_B^2 + 1.49 x_C^2 \quad (4.5)$$

Where  $Y$  is the response variable (FAME concentration, wt%),  $x_A$  (residence time, min),  $x_B$  (WCO/RPO, wt%) and  $x_C$  (methanol/oil, molar ratio) are the factors studied. The positive sign of a coefficient means synergistic effect while the negative sign shows an opposite effect on variables that influence the FAME concentration (Liu et al. 2014).

The statistical significance of each regression coefficient of the model in the response variable was evaluated and the results are shown in the Table 4.7. The terms  $x_A$ ,  $x_C$ ,  $x_A \times x_B$ ,  $x_A^2$  and  $x_B^2$  are significant since the respective p-values are lower 0.05 (Avramović et al. 2010). Besides that, the influence of square value of residence time ( $x_A^2$ ) and WCO/RPO ( $x_B^2$ ) have a significant negative effect (on the FAME concentration) of -7.87 (p-value = 0.0002) and -15.64 (p-value < 0.0001), respectively. The linear term of the molar methanol/oil ratio ( $x_C$ ) has greatest positive effect of 9.82 (p-value < 0.0001) on the FAME concentration. The interaction terms  $x_A \times x_C$  (p-value = 0.2355) and  $x_B \times x_C$  (p-value = 0.1546) are not statistically significant. On the other hand,  $x_A \times x_B$  (p-value = 0.005) is statistically significant, which means that there is interaction between the variables RT and WCO/RPO ratio (wt%). In other words, the influence of WCO/RPO ratio (wt%) on the FAME concentration depends on the RT, which could be due to viscosity effects on resistance to mass transfer (the higher WCO/RPO ratio (wt%), the higher viscosity (Vargas et al. 2019a)) and to the reversibility of esterification and transesterification reactions.

**Table 4.7** - Regression coefficients (coded factors) for the fitting quadratic polynomial model.

Model parameters	Estimate coefficient	Standard error	p - value
Intercept	84.93	0.99	
$x_A$	5.16	0.79	0.0003
$x_B$	0.9093	0.79	0.2869
$x_C$	9.82	0.79	< 0.0001
$x_A \times x_B$	-4.49	1.12	0.0050
$x_A \times x_C$	-1.45	1.12	0.2355
$x_B \times x_C$	1.78	1.12	0.1546
$x_A^2$	-7.87	1.09	0.0002
$x_B^2$	-15.64	1.09	< 0.0001
$x_C^2$	1.49	1.09	0.2136

In summary, all the variables studied have a statistically significant effect on FAME concentration, but not in the same way. Concerning the residence time both linear and

quadratic terms are significant, on the other hand, only the quadratic term of the WCO/RPO ratio (wt%) affects (negatively) the response variable. With regard to the molar ratio methanol/oil only the linear term is statistically significant. There is no interaction between the independent variables, except for the residence time and WCO/RPO ratio (wt%).

The residual plots shown in Figure 4.10 were used to validate the model assumptions. Figure 4.10 a shows a normal probability plot of residues, which corresponds to the difference between the experimental response and the predicted by the model. The data are along a straight line and without the distribution presenting S-shape, so it can be concluded that the residues follow a normal distribution (Hajamini et al. 2016; Jaliliannosrati et al. 2013).

The graph of the residuals vs. the predicted values is illustrated in Figure 4.10 b and shows the data randomly distributed with equal number of points above and below the central horizontal line and between two horizontal lines at a threshold of  $\pm 3.00$  (three standard deviations) (Noshadi et al. 2012).

The experimental values of FAME concentration vs. the values predicted by the model are shown in Figure 4.10 c, which corroborates the tuning effectiveness of the developed regression model. In short, this analysis confirms the accuracy and reliability of the proposed regression model.



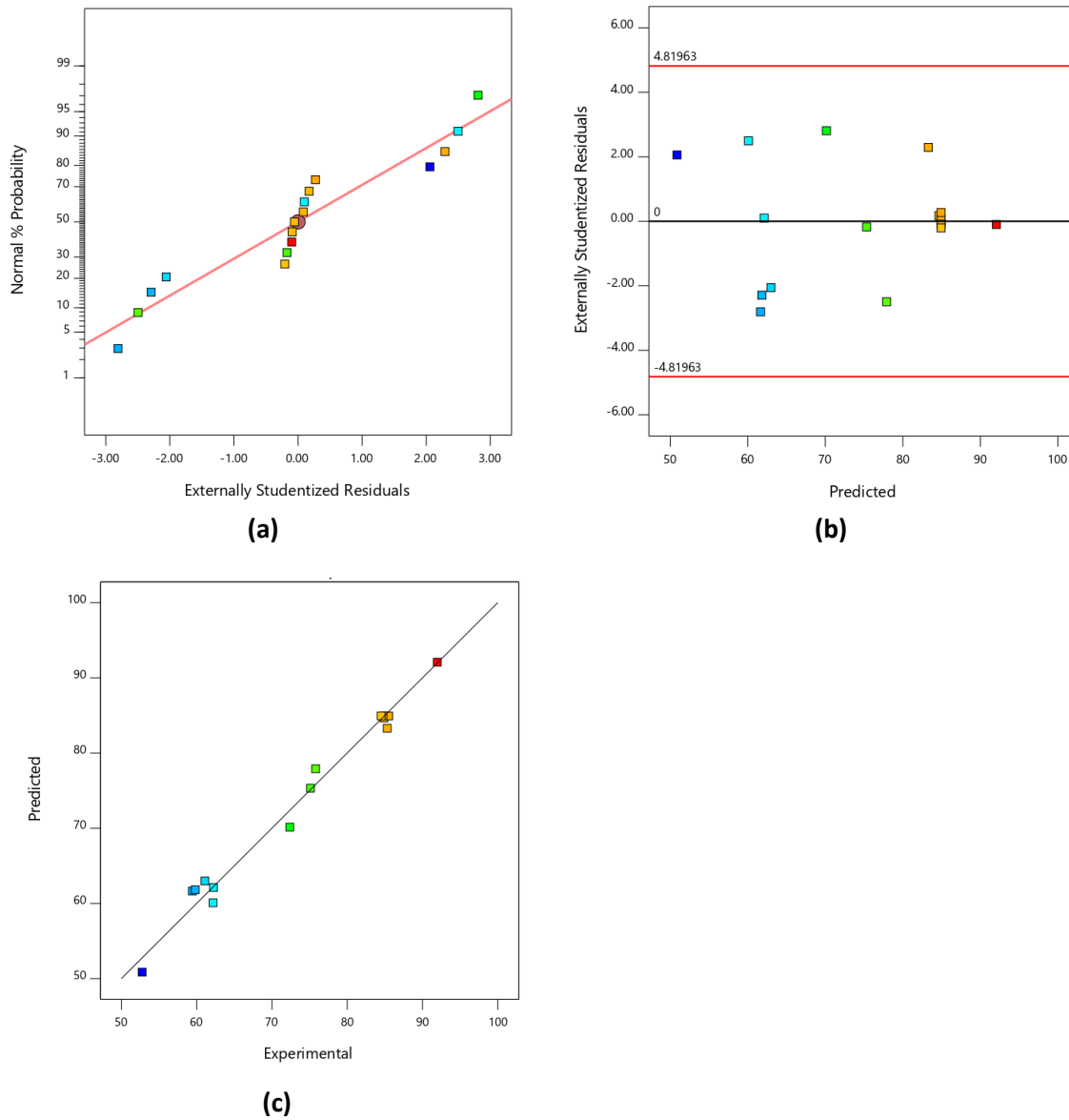


**Figure 4.10** - (a) Residual normal probability plot, (b) Residual versus predicted response plot, (c) Predicted versus experimental values plot.

Figure 4.11 shows the response surface graphs for three evaluated variables.

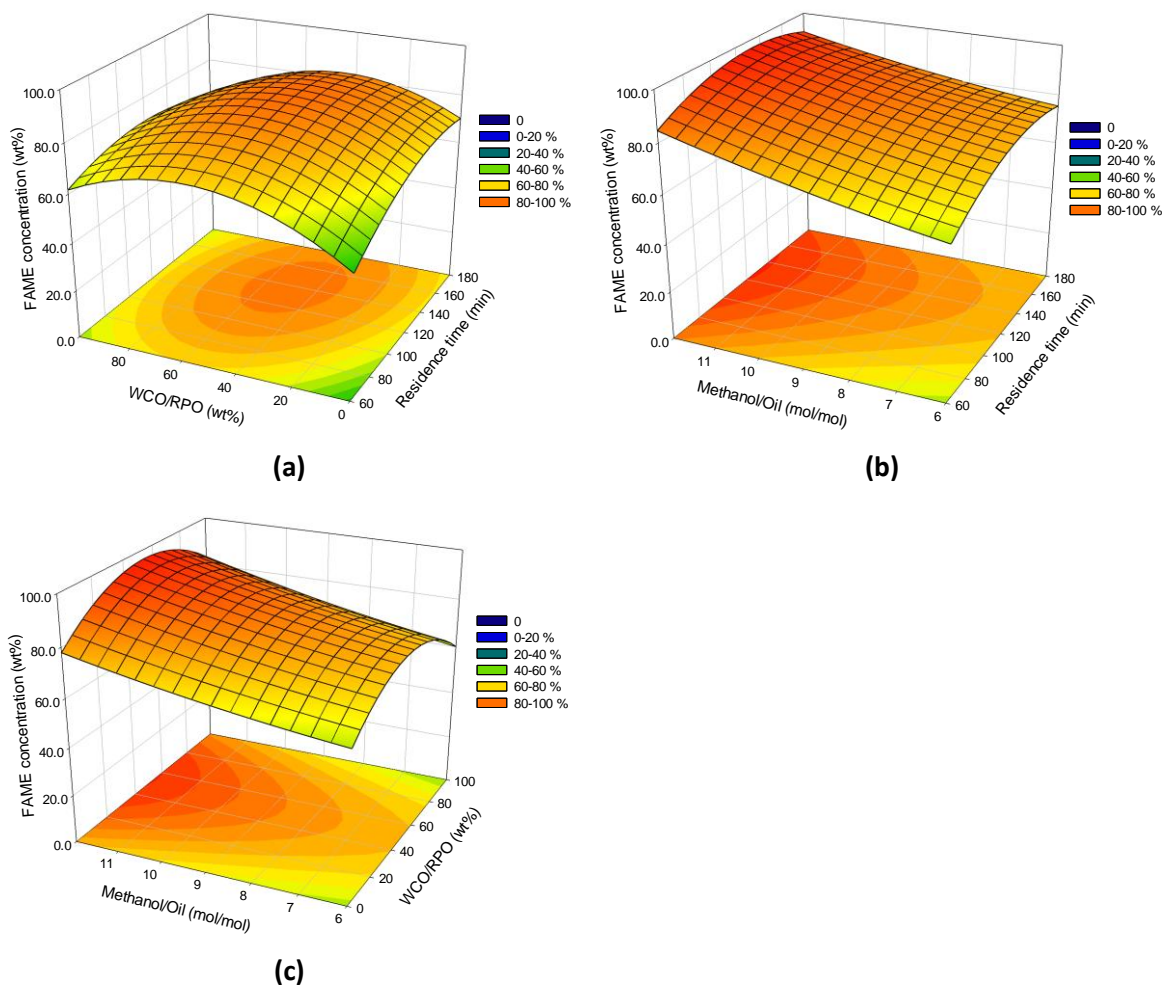


**Figure 4.11** - FAME concentration response surface graphics based on: (a) Residence time and WCO/RPO ratio (wt%) at molar methanol/oil ratio of 9 mol/mol; (b) Time of residence and molar methanol/oil ratio at WCO/RPO ratio of 50 wt%; (c) Molar methanol/oil ratio and WCO/RPO ratio (wt%) at time of residence of 120 min.

Residence time up to 120 min favors significantly the FAME concentration (see Figure 4.11 a&b); for RT greater than 120 min, the FAME concentration does not rise, regardless of the WCO/RPO (wt%) used (Figure 4.11 a) and, depending on methanol/oil molar ratio (Figure 4.11 b), may even slightly decrease. The reversibility of (global) reaction of FAME production may be one of the reasons for this. Gui et al. (2016) observed similar trends in a residence time range between 60 and 180 min using sunflower oil and charred sodium silicate as catalyst.

Concerning the effect of WCO/RPO (wt%), Figure 4.11 a&c show that for the range between 50 and 80 wt% the highest FAME concentrations are achieved. This means that till certain percentages in the oil mixture, the WCO promotes higher FAME concentrations which, in turn, is a promising outcome for the economic and environmental sustainability of the process (Vargas et al. 2019b). Moreover, Figure 4.11 b&c show the great influence of the methanol/oil molar ratio on the response variable; 12:1 value reached the highest FAME concentration around 92 %. Similar results were found by Ni and Meunier (2007), who observed the higher FAME concentrations for methanol/oil ratio of 12:1; above this ratio did not present a noticeable increase on FAME concentration.

The high concentrations of FAME registered in this work can be due to the majority presence of crystalline phases of calcium carbonate, calcium hydroxide and alkaline metals that bring basic character to the catalyst (Yoosuk et al. 2011), which was observed by XRD and Hammett's indicators. Thus, even in the absence of the most basic form of calcium (CaO), the species present ( $\text{Ca(OH)}_2$  and  $\text{CaCO}_3$ ) and KCl have been shown to provide sufficient basicity to catalyze efficiently the transesterification reaction. In addition, high concentrations of Ca (13.95 %), K (7.62 %) and Mg (5.05 %) were found on its surface and pore diameters of 74.853 Å in the XPS and BET, respectively, which are suitable for transesterification reactions.

The bifunctional character of the powder fly ash used to prepare the pelletized catalyst was verified in a previous work (Vargas et al. 2019a). This catalyst feature can also explain the high concentrations of FAME observed with oil mixtures with high percentages of WCO, i.e. with high acid values. Actually, despite of its low acid strength, this catalyst seems to be able to also catalyze the esterification reaction. According to some authors (Rabiah Nizah et al. 2014; Wan Omar et al. 2011b) the balance of acid and basic catalyst sites plays an important role in the bifunctional performance of the catalysts.

### **Optimal operating condition**

An important objective of this research was to find the optimal operating conditions to achieve the maximum FAME concentration, combining the various independent variables studied using a regression model. The model showed two possible combinations of variables to achieve

the highest FAME concentration: (i) residence time of 124 min, WCO/RPO of 74.6 wt% and molar methanol/oil ratio of 12:1, reaching a FAME concentration of 93.8 %; and (ii) residence time of 135 min, WCO/RPO of 57.2 wt% and molar methanol/oil ratio of 12:1 reaching a FAME concentration of 96.4 %.

The first set of operating conditions was chosen, since, it has the largest amount of WCO and the least residence time, which results in a decrease in costs in raw materials and operating times compared to the second set.

Aiming to check the optimal operating conditions found by the regression model, three experiments were performed under the selected conditions shown in Table 4.8.

**Table 4.8** - Experimental data on optimal operating conditions.

Run	FAME concentration (wt%)			
	5 h	6 h	7 h	Average $\pm$ S.D.
1	90.2	89.9	89.2	89.7 $\pm$ 0.5
2	88.8	88.5	91.4	89.5 $\pm$ 1.5
3	90.5	89.9	88.9	89.8 $\pm$ 0.7

Experimental FAME concentration = 89.7 wt%

Predicted FAME concentration = 93.8 wt%

% error = 4.6 %

The average experimental FAME concentration was 89.7 % ( $\pm$  0.8%), which is close to the predicted by the regression model (93.81 %); with a 4.6% error ( $\pm$  0.05%) confirming the fit of the found model.

#### 4.3.4 Catalytic stability of the pelletized biomass ash

Figure 4.12 shows the results of the experiment, carried out under optimal operating conditions, to assess the catalytic stability of the fixed bed over 32 h of continuous operation. After steady state is reached, FAME concentration remains at *c.a.* 88 % until (at least) around 20 h. However, about 30 h there is a slight decrease ( $\approx$  5.6%) in the FAME concentration, which

may indicate some loss of catalytic activity in the fixed bed. Other authors such as Ren et al. (2012) and Da Silva et al. (2014) also checked the catalyst stability of other catalysts used for FAME production. The first authors observed a 74.4 % loss of catalytic activity of D261 resin after 8 h of operation, on the other hand, Da Silva et al. (2014) reported a quite small loss of activity (3%) for a zinc oxide catalyst after 120 h of operation. In a perspective of scaling up the process, the results of this work regarding the biomass fly ash pelletized catalyst performance are promising and encouraging.

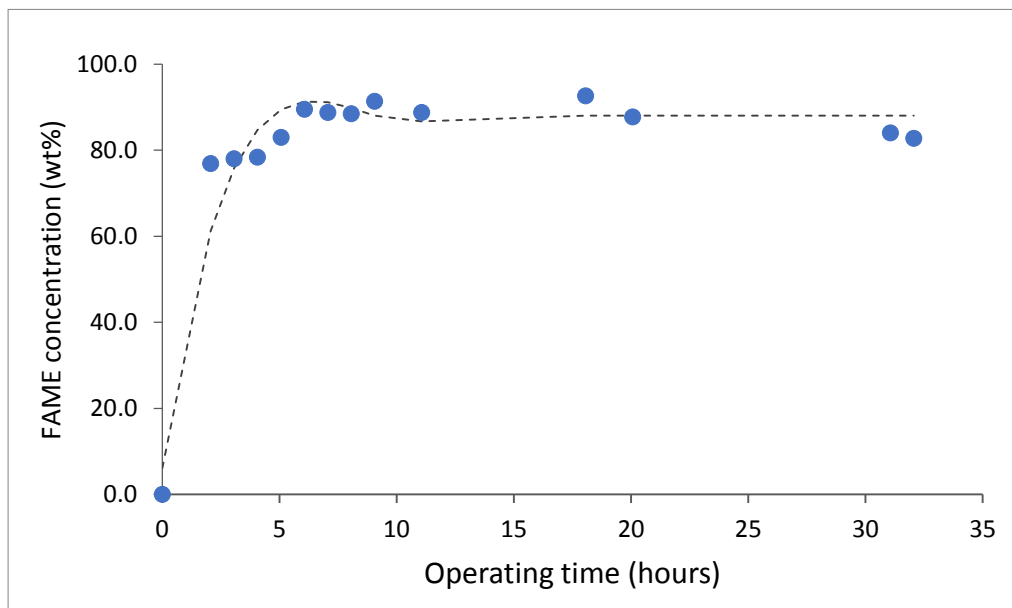


**Figure 4.12** - FAME concentration of the catalyst over 32 h of continuous operation.

#### 4.4 Conclusions

The continuous fixed bed reaction system designed and built for this work allowed to evaluate the catalytic activity and stability of the pelletized residual catalyst in a simple and repeatable way.

The evaluation of a pelletized residual catalyst of fly ash to produce FAME was performed, using RPO and WCO mixtures and using RSM and an experimental Box Behnken design to optimize the response variable (FAME concentration). A quadratic regression model was well

fitted to the experimental results ( $p$ -value  $< 0.0001$ ), predicting as optimal conditions a residence time of 124 min, a WCO of 74.6 wt% and a molar methanol/oil ratio of 12:1 to obtain a FAME concentration of 93.8 %. Thus, the biomass fly ash has shown to have a bifunctional character, i.e., capable of catalyzing the transesterification and esterification reactions, as high concentrations of FAME have been registered for high WCO/RPO ratios.

In the tested range, the most statistically significant variable (with a 95 % confidence level) which affected the FAME concentration was the methanol/oil ratio with a  $p$ -value  $< 0.0001$ , followed by the residence time ( $p$ -value = 0.0003).

High WCO/RPO percentages up to 74.6 % can be used to achieve high FAME concentration. Thus, significant quantities of WCO can be valorized in the FAME production process.

The selected regression model had a good adjustment of the experimental results found with an  $R^2 = 0.9859$  and  $\text{Adj } R^2 = 0.9678$ ; Furthermore, the precision and reliability of the regression model were confirmed.

Three tests were conducted under optimal operating conditions, where average experimental FAME concentration was 89.7 % ( $\pm 0.8\%$ ), which is close to the predicted value by the model (93.8 %). The error found between statistical correlation and experimental data was 4.6 % ( $\pm 0.05$  %). In addition, it was demonstrated that the pelletized residual catalyst can be used for up to 32 h of operation without significant loss of its catalytic activity. In future work, it would be important to extend the operating time until find a significant drop in catalytic activity. In addition, foreseeing a future commercialization, the FAME properties must be characterized in order to assess whether it meets the ASTM D-6751, EN 14214 or other standards.

This work is contributing to enhance knowledge on continuous process of biodiesel production based on residual materials, and also to increase its competitiveness in relation to the conventional process, widely installed at industrial scale.

In short, it is important to make the most of residual raw materials such as biomass fly ash or WCO, as they represent a contribution on strengthening the circular economy by making good

use of these wastes for the energy generation (biodiesel). Thus, this research offers a sustainable and affordable approach by minimizing the environmental impact and costs generated by biodiesel production.

### Acknowledgments

The authors thank to the Universidad Jorge Tadeo Lozano (Direction of Investigation, Creation and Extension) for the financial assistance of this work. The authors thanks to FCT/MCTES for the financial support to CESAM (UIDP/50017/2020 & UIDB/50017/2020), through national funds. This work was also developed within the scope of CICECO (UIDB/50011/2020 & UIDP/50011/2020), financed by national funds through the FCT/MCTES and when appropriate co-financed by ERDF under the PT2020 Partnership Agreement. Márcia C. Neves acknowledges FCT, I.P. for the research contract CEECIND/00383/2017 under the CEEC Individual 2017.

### References

- AENOR-EN 14103. 2011. *Productos Derivados de Aceites y Grasas. Ésteres Metílicos de Ácidos Grasos (FAME). Determinación de Los Contenidos de Éster y de Éster Metílico Del Ácido Linoléico*. España. [www.agilent.com/chem](http://www.agilent.com/chem). (February 15, 2019).
- Andrigo, P, R Bagatin, and G Pagani. 1999. "Fixed Bed Reactors (Chapter).Pdf." *Catalysis Today* 52: 197–221.
- Aslan, N., and Y. Cebeci. 2007. "Application of Box-Behnken Design and Response Surface Methodology for Modeling of Some Turkish Coals." *Fuel* 86(1–2): 90–97.
- Avellaneda, Fredy, and Joan Salvadó. 2011. "Continuous Transesterification of Biodiesel in a Helicoidal Reactor Using Recycled Oil." *Fuel Processing Technology* 92(1): 83–91.
- Avhad, M. R., and J. M. Marchetti. 2015. "A Review on Recent Advancement in Catalytic Materials for Biodiesel Production." *Renewable and Sustainable Energy Reviews* 50: 696–718. <http://dx.doi.org/10.1016/j.rser.2015.05.038>.
- Avramović, Jelena M. et al. 2010. "The Optimization of the Ultrasound-Assisted Base-Catalyzed Sunflower Oil Methanolysis by a Full Factorial Design." *Fuel Processing Technology* 91(11): 1551–57.
- Betiku, Eriola, Aramide Mistura Akintunde, and Tunde Victor Ojumu. 2016. "Banana Peels as a Biobase Catalyst for Fatty Acid Methyl Esters Production Using Napoleon's Plume (Bauhinia Monandra) Seed Oil: A Process Parameters Optimization Study." *Energy* 103:

797–806. <http://dx.doi.org/10.1016/j.energy.2016.02.138>.

- Chakraborty, R., S. Bepari, and A. Banerjee. 2010. "Transesterification of Soybean Oil Catalyzed by Fly Ash and Egg Shell Derived Solid Catalysts." *Chemical Engineering Journal* 165(3): 798–805. <http://dx.doi.org/10.1016/j.cej.2010.10.019>.
- Chattopadhyay, Soham, and Ramkrishna Sen. 2013. "Development of a Novel Integrated Continuous Reactor System for Biocatalytic Production of Biodiesel." *Bioresource Technology* 147: 395–400. <http://dx.doi.org/10.1016/j.biortech.2013.08.023>.
- Evangelista-Flores, A. Alcantar-Gonzalez, F. S. Ramirez de Arellano Aburto, N. Cohen Barki, A. Robledo-Perez, J. M. Cruz-Gomez 2012). "Diseño de Un Proceso Continuo de Producción de Biodiesel." *Revista Mexicana de Ingeniería Química* 11(1): 23–43. <https://www.redalyc.org/articulo.oa?id=62031508011>
- Fang, Dong, Jinming Yang, and Changmei Jiao. 2011. "Dicationic Ionic Liquids as Environmentally Benign Catalysts for Biodiesel Synthesis." *ACS Catalysis* 1(1): 42–47.
- Freedman, B., E.H. Pryde, and T.L. Mounts. 1981. "Hour Screening Test for Alternate Fuels in Energy Notes for , Variables Affecting the Yields of Fatty Esters from Transesterified Vegetable Oils 1." *American Society of Agricultural Engineers* 2(10): 385–90.
- Gui, Xia, Sichen Chen, and Zhi Yun. 2016. "Continuous Production of Biodiesel from Cottonseed Oil and Methanol Using a Column Reactor Packed with Calcined Sodium Silicate Base Catalyst." *Chinese Journal of Chemical Engineering* 24(4): 499–505. <http://dx.doi.org/10.1016/j.cjche.2015.11.006>.
- Hajamini, Zahra, Mohammad Amin Sobati, Shahrokh Shahhosseini, and Barat Ghobadian. 2016. "Waste Fish Oil (WFO) Esterification Catalyzed by Sulfonated Activated Carbon under Ultrasound Irradiation." *Applied Thermal Engineering* 94: 1–10. <http://dx.doi.org/10.1016/j.applthermaleng.2015.10.101>.
- ICONTEC. 2011. NTC 218. Grasas y Aceites Vegetales y Animales. Determinación Del Índice de Acidez y de La Acidez. Colombia. <https://tienda.icontec.org/wp-content/uploads/pdfs/NTC218.pdf>.
- ICONTEC. 1999. NTC 218. "Grasas Y Aceites Vegetales Y Animales. Determinacion de Índice de Acidez." (571). Colombia. <https://tienda.icontec.org/wp-content/uploads/pdfs/NTC218.pdf>.
- Jacobson, Kathlene, Rajesh Gopinath, Lekha Charan Meher, and Ajay Kumar Dalai. 2008. "Solid Acid Catalyzed Biodiesel Production from Waste Cooking Oil." *Applied Catalysis B: Environmental* 85(1–2): 86–91.
- Jaliliannosrati, Hamidreza, Nor Aishah Saidina Amin, Amin Talebian-Kiakalaieh, and Iman Noshadi. 2013. "Microwave Assisted Biodiesel Production from *Jatropha Curcas* L. Seed by Two-Step in Situ Process: Optimization Using Response Surface Methodology." *Bioresource Technology* 136: 565–73. <http://dx.doi.org/10.1016/j.biortech.2013.02.078>.



- Jensen, R. R., S. S. Brake, and J. M. Mattox. 2004. "Trace Element Uptake in Plants Grown on Fly Ash Amended Soils." *Toxicological and Environmental Chemistry* 86(1–4): 217–28.
- Kansedo, Jibrail, Keat Teong Lee, and Subhash Bhatia. 2009. "Cerbera Odollam (Sea Mango) Oil as a Promising Non-Edible Feedstock for Biodiesel Production." *Fuel* 88(6): 1148–50. <http://dx.doi.org/10.1016/j.fuel.2008.12.004>.
- Kutálek, Petr, Libor Čapek, Lucie Smoláková, and David Kubička. 2014. "Aspects of Mg-Al Mixed Oxide Activity in Transesterification of Rapeseed Oil in a Fixed-Bed Reactor." *Fuel Processing Technology* 122: 176–81.
- Lam, Man Kee, and Keat Teong Lee. 2010. "Accelerating Transesterification Reaction with Biodiesel as Co-Solvent: A Case Study for Solid Acid Sulfated Tin Oxide Catalyst." *Fuel* 89(12): 3866–70. <http://dx.doi.org/10.1016/j.fuel.2010.07.005>.
- Liang, Guangbing et al. 2020. "Production of Biosilica Nanoparticles from Biomass Power Plant Fly Ash." *Waste Management* 105: 8–17. <https://doi.org/10.1016/j.wasman.2020.01.033>.
- Liu, Wei, Ping Yin, Xiguang Liu, and Rongjun Qu. 2014. "Design of an Effective Bifunctional Catalyst Organotriphosphonic Acid-Functionalized Ferric Alginate (ATMP-FA) and Optimization by Box-Behnken Model for Biodiesel Esterification Synthesis of Oleic Acid over ATMP-FA." *Bioresource Technology* 173: 266–71. <http://dx.doi.org/10.1016/j.biortech.2014.09.087>.
- Luo, Qingliang et al. 2017. "Continuous Transesterification to Produce Biodiesel under HTCC/Na<sub>2</sub>SiO<sub>3</sub>/NWF Composite Catalytic Membrane in Flow-through Membrane Reactor." *Fuel* 197: 51–57.
- Luque, Rafael et al. 2012. "Carbonaceous Residues from Biomass Gasification as Catalysts for Biodiesel Production." *Journal of Natural Gas Chemistry* 21(3): 246–50.
- Maneerung, Thawatchai, Sibudjing Kawi, and Chi Hwa Wang. 2015. "Biomass Gasification Bottom Ash as a Source of CaO Catalyst for Biodiesel Production via Transesterification of Palm Oil." *Energy Conversion and Management* 92: 234–43. <http://dx.doi.org/10.1016/j.enconman.2014.12.057>.
- Mansir, Nasar et al. 2018. "Modified Waste Egg Shell Derived Bifunctional Catalyst for Biodiesel Production from High FFA Waste Cooking Oil. A Review." *Renewable and Sustainable Energy Reviews* 82(November 2016): 3645–55.
- Miladinović, Marija R. et al. 2016. "Modeling and Optimization of Sunflower Oil Methanolysis over Quicklime Bits in a Packed Bed Tubular Reactor Using the Response Surface Methodology." *Energy Conversion and Management* 130: 25–33.
- Miladinović, Marija R. et al. 2020. "Valorization of Walnut Shell Ash as a Catalyst for Biodiesel Production." *Renewable Energy* 147: 1033–43.

- Miller, B., D. Dugwell, and R. Kandiyoti. 2006. "The Fate of Trace Elements during the Co-Combustion of Wood-Bark with Waste." *Energy and Fuels* 20(2): 520–31.
- Mishra, Abha, Sunil Kumar, and Sudhir Kumar. 2008. "Application of Box-Benken Experimental Design for Optimization of Laccase Production by *Coriolus Versicolor* MTCC138 in Solid-State Fermentation." *Journal of Scientific and Industrial Research* 67(12): 1098–1107.
- Mittelbach, Martin, Manfred Wörgetter, Josef Pernkopf, and Hans Junek. 1983. "Diesel Fuel Derived from Vegetable Oils: Preparation and Use of Rape Oil Methyl Ester." *Energy in Agriculture* 2(C): 369–84.
- Nath, Biswajit, Bipul Das, Pranjal Kalita, and Sanjay Basumatary. 2019. "Waste to Value Addition: Utilization of Waste Brassica Nigra Plant Derived Novel Green Heterogeneous Base Catalyst for Effective Synthesis of Biodiesel." *Journal of Cleaner Production* 239: 118112. <https://doi.org/10.1016/j.jclepro.2019.118112>.
- Ni, J., and F. C. Meunier. 2007. "Esterification of Free Fatty Acids in Sunflower Oil over Solid Acid Catalysts Using Batch and Fixed Bed-Reactors." *Applied Catalysis A: General* 333(1): 122–30.
- Noshadi, I., N. A.S. Amin, and Richard S. Parnas. 2012. "Continuous Production of Biodiesel from Waste Cooking Oil in a Reactive Distillation Column Catalyzed by Solid Heteropolyacid: Optimization Using Response Surface Methodology (RSM)." *Fuel* 94: 156–64. <http://dx.doi.org/10.1016/j.fuel.2011.10.018>.
- Ñústez-Castaño, Stephanie Alexa, Duvan Oswaldo Villamizar-Castro, and Edgar Mauricio Vargas-Solano. 2019. "Evaluation of Dolomite as Catalyst in the Transesterification Reaction Using Palm Oil (RBD)." *DYNA (Colombia)* 86(209): 180–87.
- Osman, Ahmed I., Abdelkader T. Ahmed, Christopher R. Johnston, and David W. Rooney. 2018. "Physicochemical Characterization of Miscanthus and Its Application in Heavy Metals Removal from Wastewaters." *Environmental Progress and Sustainable Energy* 37(3): 1058–67.
- Park, Young Moo et al. 2008. "The Heterogeneous Catalyst System for the Continuous Conversion of Free Fatty Acids in Used Vegetable Oils for the Production of Biodiesel." *Catalysis Today* 131(1–4): 238–43.
- Pavlović, Stefan M. et al. 2020. "A CaO/Zeolite-Based Catalyst Obtained from Waste Chicken Eggshell and Coal Fly Ash for Biodiesel Production." *Fuel* 267(September 2019): 117171. <https://doi.org/10.1016/j.fuel.2020.117171>.
- Pirez, Cyril et al. 2012. "Tunable KIT-6 Mesoporous Sulfonic Acid Catalysts for Fatty Acid Esterification." *ACS Catalysis* 2(8): 1607–14.
- Rabiah Nizah, M. F. et al. 2014. "Production of Biodiesel from Non-Edible *Jatropha Curcas* Oil via Transesterification Using Bi<sub>2</sub>O<sub>3</sub>-La<sub>2</sub>O<sub>3</sub> Catalyst." *Energy Conversion and Management* 88: 1257–62. <http://dx.doi.org/10.1016/j.enconman.2014.02.072>.

- Rajamma, Rejini et al. 2009. "Characterisation and Use of Biomass Fly Ash in Cement-Based Materials." *Journal of Hazardous Materials* 172(2–3): 1049–60.
- Ren, Yanbiao et al. 2012. "Continuous Biodiesel Production in a Fixed Bed Reactor Packed with Anion-Exchange Resin as Heterogeneous Catalyst." *Bioresource Technology* 113: 19–22. <http://dx.doi.org/10.1016/j.biortech.2011.10.103>.
- Salamatinia, Babak, Hamed Mootabadi, Subhash Bhatia, and Ahmad Zuhairi Abdullah. 2010. "Optimization of Ultrasonic-Assisted Heterogeneous Biodiesel Production from Palm Oil: A Response Surface Methodology Approach." *Fuel Processing Technology* 91(5): 441–48.
- Sharma, Meeta, Arif Ali Khan, S. K. Puri, and D. K. Tuli. 2012. "Wood Ash as a Potential Heterogeneous Catalyst for Biodiesel Synthesis." *Biomass and Bioenergy* 41: 94–106. <http://dx.doi.org/10.1016/j.biombioe.2012.02.017>.
- da Silva, Fábio M. et al. 2014. "Continuous Biodiesel Production Using a Fixed-Bed Lewis-Based Catalytic System." *Chemical Engineering Research and Design* 92(8): 1463–69. <http://dx.doi.org/10.1016/j.cherd.2014.04.024>.
- Singh, S. P., and Dipti Singh. 2010. "Biodiesel Production through the Use of Different Sources and Characterization of Oils and Their Esters as the Substitute of Diesel: A Review." *Renewable and Sustainable Energy Reviews* 14(1): 200–216.
- Suarez, Paulo A.Z., Andre L.F. Santos, Juliana P. Rodrigues, and Melquizedeque B. Alves. 2009. "Biocombustíveis a Partir de Oleos e Gorduras: Desafios Tecnológicos Para Viabilizá-los." *Quimica Nova* 32(3): 768–75.
- Tarelho, L. A.C. et al. 2015. "Characteristics of Distinct Ash Flows in a Biomass Thermal Power Plant with Bubbling Fluidised Bed Combustor." *Energy* 90: 387–402. <http://dx.doi.org/10.1016/j.energy.2015.07.036>.
- Teixeira, E. R. et al. 2019. "Recycling of Biomass and Coal Fly Ash as Cement Replacement Material and Its Effect on Hydration and Carbonation of Concrete." *Waste Management* 94: 39–48. <https://doi.org/10.1016/j.wasman.2019.05.044>.
- Thommes, Matthias et al. 2015. "IUPAC Technical Report Physisorption of Gases, with Special Reference to the Evaluation of Surface Area and Pore Size Distribution (IUPAC Technical Report)." <https://www.3p-instruments.com/wp-content/uploads/2017/04/2015-IUPAC-Technical-Report.pdf> (February 18, 2019).
- Tran, Dang Thuan, Jo Shu Chang, and Duu Jong Lee. 2017. "Recent Insights into Continuous-Flow Biodiesel Production via Catalytic and Non-Catalytic Transesterification Processes." *Applied Energy* 185: 376–409. <http://dx.doi.org/10.1016/j.apenergy.2016.11.006>.
- Uprety, Bijaya K., Wittavat Chaiwong, Chinomnso Ewelike, and Sudip K. Rakshit. 2016. "Biodiesel Production Using Heterogeneous Catalysts Including Wood Ash and the Importance of Enhancing Byproduct Glycerol Purity." *Energy Conversion and Management* 115: 191–99. <http://dx.doi.org/10.1016/j.enconman.2016.02.032>.

- Vargas, E. M., J. L. Ospina, L. A.C. Tarelho, and M. I. Nunes. 2019b. "FAME Production from Residual Materials: Optimization of the Process by Box–Behnken Model." *Energy Reports* 6: 347–52. <https://doi.org/10.1016/j.egy.2019.08.071>.
- Vargas, Edgar M., Márcia C. Neves, Luís A.C. Tarelho, and Maria I. Nunes. 2019a. "Solid Catalysts Obtained from Wastes for FAME Production Using Mixtures of Refined Palm Oil and Waste Cooking Oils." *Renewable Energy* 136: 873–83.
- Vyas, Amish P., Jaswant L. Verma, and N. Subrahmanyam. 2010. "A Review on FAME Production Processes." *Fuel* 89(1): 1–9. <http://dx.doi.org/10.1016/j.fuel.2009.08.014>.
- Wan Omar, Wan Nor Nadyaini, and Nor Aishah Saidina Amin. 2011a. "Biodiesel Production from Waste Cooking Oil over Alkaline Modified Zirconia Catalyst." *Fuel Processing Technology* 92(12): 2397–2405. <http://linkinghub.elsevier.com/retrieve/pii/S0378382011003031> (January 2, 2015).
- Wan Omar, Wan Nor Nadyaini, and Nor Aishah Saidina Amin. 2011b. "Optimization of Heterogeneous Biodiesel Production from Waste Cooking Palm Oil via Response Surface Methodology." *Biomass and Bioenergy* 35(3): 1329–38. <http://dx.doi.org/10.1016/j.biombioe.2010.12.049>.
- Wang, Shuangzhen, Larry Baxter, and Fernando Fonseca. 2008. "Biomass Fly Ash in Concrete: SEM, EDX and ESEM Analysis." *Fuel* 87(3): 372–79.
- Yang, Lu et al. 2019. "Effect of the Intensification of Preconditioning on the Separation of Unburned Carbon from Coal Fly Ash." *Fuel* 242(June 2018): 174–83.
- Yoosuk, Boonyawan, Parncheewa Udomsap, and Buppa Puttasawat. 2011. "Hydration–Dehydration Technique for Property and Activity Improvement of Calcined Natural Dolomite in Heterogeneous Biodiesel Production: Structural Transformation Aspect." *Applied Catalysis A: General* 395(1–2): 87–94. <http://linkinghub.elsevier.com/retrieve/pii/S0926860X11000421> (May 29, 2015).
- Zhang, Y., M. A. Dubé, D. D. McLean, and M. Kates. 2003. "Biodiesel Production from Waste Cooking Oil: 1. Process Design and Technological Assessment." *Bioresource Technology* 89(1): 1–16.

---

## **SECTION E – Final remarks**

Section E presents the main conclusions that can be drawn from this study, as well as some limitations. It is also provided a list of suggestions for future works that can be developed in the research field of this thesis.



## 5 Final remarks

### 5.1 General conclusions

This research work prepared, from waste materials, efficient bifunctional solid catalysts to produce FAME from mixtures of low cost vegetable oils (WCO and RPO) with methanol. Among four materials used, the fly ash of biomass dried exhibited the best performance in the catalysis of both esterification and transesterification reactions. In this work it was also optimized the production process of FAME in both batch reactor and in a continuous fixed bed reactor, using biomass fly ash as (bifunctional) catalyst. Thus, through the use of waste materials it may be possible to reduce the production costs of biodiesel and simultaneously prolong the life-cycle of the materials in the economy, i.e., promoting a circular economy. Therefore, an awareness should be created so that any material that is deemed a waste could be exploited for usage in this or other applications.

It is important to mention that in the several experimental works performed in this thesis, exhaustive characterization of the final product was not carried out, in order, for example, to check if it meets any of the standards for the commercialization of this biofuel (biodiesel). Thus, throughout this dissertation it was decided to designate the final product as FAME and not biodiesel, since the "biodiesel" label is reserved for the FAME product that meets a marketing standard. However, the word biodiesel appears in the title of the thesis, and not the acronym FAME, as it is the word of greatest public domain.

Concerning the main conclusions that can be drawn from these studies, they are summarized in the following paragraphs.

Efficient heterogeneous catalysts were successfully prepared from solid waste materials for FAME production by transesterification and esterification, using mixtures of refined palm oil and waste cooking oil in different ratios and methanol (in batch reactor). The results

demonstrated that all the solid materials prepared and evaluated had different catalytic performances. The best catalyst for catalyzing simultaneous both transesterification and esterification reactions, i.e., having a bifunctional character (the balance of acid and basic catalyst), was biomass fly ash dried (FAD), achieving yields and conversions above 95 % for a blend of up to 25 wt% of WCO at 60 °C, 9:1 (mol/mol) of methanol to oil, 10 %wt catalyst loading and over 180 min. The catalysts produced from dolomite rock (Dolomite C and dolomite CSC) showed good performances of catalytic activity for transesterification (high yields to FAME up to 87.8 %) and esterification (high conversion of FFA up to 100 %) reactions, respectively. In fact, the sulfonation of Dolomite C was aimed at increasing its acid strength to improve the catalytic activity for the esterification reaction. However, this treatment strongly affected its ability towards the transesterification reaction, practically canceling it (yield to FAME less than 3.4 %). While for the catalysts prepared from eggshells, the sulfonation improved its ability for catalyzing the transesterification reaction, however the maximum values attained did not exceed 70 % of FAME yield. On the other hand, this treatment worsened the performance of this catalyst in FFA conversion (average conversion up to 62.7 %). Regarding the catalysts produced from PET, the results showed that they are good candidates for catalyzing the esterification reaction of high acid value feedstocks reaching FAME yield up to 88.9 %.

It is important to highlight that biomass fly ash dried (FAD) can be used as a catalyst as it collected in the electrostatic precipitator equipment (directly and immediately), as its moisture content is very low, with subsequent economic benefits.

The FAD underwent an optimization process using the RSM and a Box Behnken type experimental design; testing it with methanol and mixtures of RPO and WCO in a batch reactor. The solid catalyst showed a maximum FAME yield of 73.8 %, which can be achieved by using 13.57 wt% of catalyst loading, 6.7 methanol/oil molar ratio, 28.04 wt% of RPO/WCO mass ratio and 55 °C for the reaction temperature (optimal operating conditions found). In the tested range, the most significant variables were the RPO/WCO mass ratio and the reaction temperature, followed by the catalyst loading. On the other hand, the methanol/oil molar ratio



---

was not significant; furthermore, biomass fly ash in powder can be used for up to three cycles (batch mode) without loss of catalytic activity. However, the catalyst should be regenerated between each cycle, by washing with isopropyl alcohol and calcined at 700 °C for 3 h. The characterization of the surface, textural and crystalline properties of the catalyst, after use in each FAME synthesis cycle, showed that those properties were not significantly affected. The acid and basic strength remained constants.

Testing the FAD catalyst in a continuous reaction system is novel when using a fixed bed reactor. Therefore, the powdered catalyst (FAD) was pelletized and a fixed-bed continuous reaction system designed and constructed to perform a set of assays for the optimization of FAME production. The regression model predicted as optimal conditions: a residence time of 124 min, a WCO of 74.6 wt% and a molar methanol/oil ratio of 12:1 to obtain a FAME concentration of 93.8 %. Thus, the pelletized FAD showed to have again a bifunctional character, that is, capable of catalyzing the transesterification and esterification reactions, since high concentrations of FAME have been registered for high WCO/RPO ratios.

In the tested range, the most statistically significant variable (with a 95 % confidence level) which affected the FAME concentration was the methanol/oil ratio followed by the residence time. Moreover, high WCO/RPO percentages up to 74.6 % can be used to achieve high FAME concentration. Thus, significant quantities of WCO can be valorized in the FAME production process. It is important to mention that three assays were conducted under optimal operating conditions, where average experimental FAME concentration was 89.7 % ( $\pm 0.8\%$ ), which is close to the predicted value by the model (93.8 %). The error found between statistical correlation and experimental data was 4.6 % ( $\pm 0.05\%$ ). In addition, it was demonstrated that the pelletized residual catalyst can be used for up to 32 h of operation without significant loss of its catalytic activity.

Note: in principle, the drying step of the raw biomass fly ashes to prepare it for pelletization could be skipped. In this work it was not done because one wanted to have the same (initial) pretreatment procedure for all studies.

In this work it was found that biomass fly ash can be used as a solid catalyst in the production of FAME just as it comes out of electrostatic precipitators, without the need of further treatment, reaching high yields and with bifunctional characteristics. This means that it is possible to carry out a transesterification and esterification reaction simultaneously in only one stage, innovating over the conventional production process that uses two stages. In addition, the pelleted biomass fly ash, with the characteristics of those used in this work, allows to achieve high yields to FAME in both batch and continuous reactor. The production of FAME in a continuous fixed-bed reactor using pelletized biomass fly ashes is a novelty of this work.

In short, it is important to make the most of residual raw materials such as biomass fly ash or WCO, as they represent a contribution on strengthening the circular economy by making good use of these wastes for the energy generation (biodiesel). In this context, this research work offers an approach that could allow minimizing the environmental impact and costs generated by biodiesel production.

## **5.2 Future works**

Based on the analysis carried out in the present study, some proposals for future studies are suggested:

- Complement characterization of the acidity and basicity on the surface of the evaluated solid catalyst (biomass fly ash) using techniques such as temperature-programmed desorption with  $\text{NH}_3$  and  $\text{CO}_2$ . This characterization would assist the interpretation of the results obtained regarding the catalytic performance of the material.
- Carry out a characterization of the final products (FAME) obtained with the raw materials and catalysts used in order to know their properties and compare them with the specifications given by the ASTM D-6751 standard (or other).

- It would be convenient to increase the operating time in the evaluation of the stability of the pelletized catalyst in the continuous fixed-bed reactor, until a significant drop in the catalytic activity is found.
- Carry out a kinetic study of the solid biomass fly ash catalyst in the continuous fixed bed reactor to find a representative kinetic model. Then, proceed to scale-up the process, for example to a pilot scale, designing the continuous fixed-bed reactor to perform assays with the solid pelleted fly ash catalyst to obtain data in conditions that are more real and close to industrial ones.
- Carry out a preliminary cost study for the production of FAME using several WCO incorporation rates (i.e., several scenarios) and using the biomass fly ash catalyst. A life cycle assessment study is also recommended in order to estimate the potential environmental benefits of recovering these new raw (waste) materials in the FAME production process.



## Annexes

In the four articles published in co-authorship, the contribution of the author of this thesis was:

- i. Conceptualization of the research work supported by an exhaustive and detailed review of scientific literature;
- ii. Design of research methodologies (both experimental and statistical) to achieve the objectives set out;
- iii. Execution of the following experimental activities : preparation of the catalysts, runs of the chemical reactions in the laboratory reactors, gas chromatography for the quantification of the products, design and construction of the continuous fixed-bed reaction system, characterization of solid catalysts by FTIR and Hammett indicators, physical-chemical characterization of oily raw materials;
- iv. Validation and formal analysis of the experimental and statistical results obtained;
- v. Both financial and laboratory resources (for de activities of previous point iii);
- vi. Writing of article draft and review (in the process of submission to the scientific journal).